Investigating the effects of altered Rad51 expression on the DSB repair pathway choice and the conservation of RecA homologs in *Saccharomyces cerevisiae*

Submitted September 2022, in partial fulfilment of the conditions for the award of the degree ***Master of Research***

Mahari Rodrigo, BSc

Student ID- 14333738

Supervised by Dr Stephen Gray and Prof Thorsten Allers

Word Count- 23773

School of Life Sciences
University of Nottingham

Contents

Abstract

S. cerevisiae has been used as model Eukaryotic system because many of its genes are homologous to those in higher Eukaryotes and due to it's ease of culturing. As a result, many reporter strains have been developed to investigate a range of cellular processes but, to generate deletion mutants in reporter strains, individual genes must be amplified from their respective strains in the Yeast Deletion Collection (YDO) and transformed individually into reporter strains. However, the bacterial Cas9 system may provide an alternative. Cas9 is an endonuclease which catalyses the formation of double strand breaks (DSBs), at specific loci. DSBs can be repaired by two major pathways, Non-Homologous End Joining (NHEJ), which is considered to be error prone or Homologous Recombination (HR), which is relatively error free. By targeting Cas9 to the desired genes, mutations can be created, provided the DSBs induced by Cas9 are repaired by NHEJ. In order to alter the DSB repair pathway choice, and force the cell to repair DSBs by NHEJ, the expression of Rad51, a recombinase involved in HR, was altered. Rad51 was placed under the control of a capped degron, a meiosis only promoter, P^{DMC1} and a mitosis only promoter, P^{CLB2}. The sporulation efficiency and growth of the strains was assayed to determine whether they were comparable to wildtype, and therefore, could be used alongside reporter strains. While the strains generated may not be suitable, selection of a different target, such as proteins involved in resection or different promoters may yield the desired results. Cas9 may also have uses in identifying and sequencing novel recombinants, previous work in the Gray lab has identified ectopic recombinants whose partner locus is unknown. By adapting the sequencing tool Fusion Detection from Gene Enrichment (FUDGE) to detect novel recombinants forming from the *HIS4::LEU2* and *leu2::hisG* hotspots, at abundances below the threshold of detection by pulsed field gel electrophoresis. In addition, in order to investigate the conservation of protein binding domains across the Rec A homologs, Rad51 was replaced by several RecA homologs from across the Tree of Life. These strains were then driven through meiosis to determine whether the RecA homologs could compensate for Rad51. Interestingly, RadA, from *Haloferax volcanii* showed a partial compensation phenotype, when the sporulation efficiency was assayed, however no viable spores were generated.

Abbreviations

BIR	Break Induced Replication
Cas	CRISPR Associated
CRISPR	Clustered Regularly Interspaced Short Palindromic Repeats
crRNA	CRISPR RNA
DDR	DNA Damage Response
DSB	Double Strand Break
D loop	Displacement Loop
EJ	End Joining
gDNA	Genomic DNA
gRNA	Guide RNA
HR	Homologous recombination
KAc	Potassium Acetate
LB	Lysogeny Broth
LiAc	Lithium Acetate
MDEJ	Microhomology Directed End joining
NaAc	Sodium Acetate
NHEJ	Non-Homologous End Joining
PCR	Polymerase Chain Reaction
PIKKs	phosphatidylinositol 3-kinase–like protein kinases
SDW	Sterile Distilled Water
SDSA	Synthesis Dependent Strand Annealing
SSA	Single Strand Annealing
ssDNA	Single stranded DNA
TCE	Trichloroethylene
tracrRNA	Trans-activating crRNA
YKO	Yeast Knockout
YPD	Yeast Peptone Dextrose
YPA	Yeast Peptone Acetate

Chapter 1 Introduction

I Meiosis in *S. cerevisiae*

Meiosis is a reductional division resulting in the production of haploid gametes, after two rounds of DNA segregation and cell division[1]. During the metaphase of the first division of meiosis, Metaphase I, the pairs of homologous chromosomes line up at the midline of the cell, with the orientation of each parental copy at random. During the second division, Anaphase II, the sister chromatids are split, creating the four haploid nuclei of the daughter cells (Figure 1). In *S. cerevisiae* the product of meiosis is four non-identical spores[2]. *S. cerevisiae* has emerged as an ideal system to study the effects of crossing over during meiosis as it is possible to easily access all four spores generated through meiosis[3].To allow the generation of haploid spores, in wildtype *S. cerevisiae*, only diploid cells, cells expressing both the a and α mating types, can enter meiosis[4]. Entry into meiosis is triggered by inoculation into nutrient deficient media, containing a non-fermentable carbon source. Nutrient starvation induces the transcription of the master meiotic regulator Ime1, within two hours[5]. Ime1 then induces the transcription of the early meiosis genes, including a meiosis specific recombinase Dmc1, via Ume6[5] and Ime2, which promotes entry into pre-meiotic S phase[1].

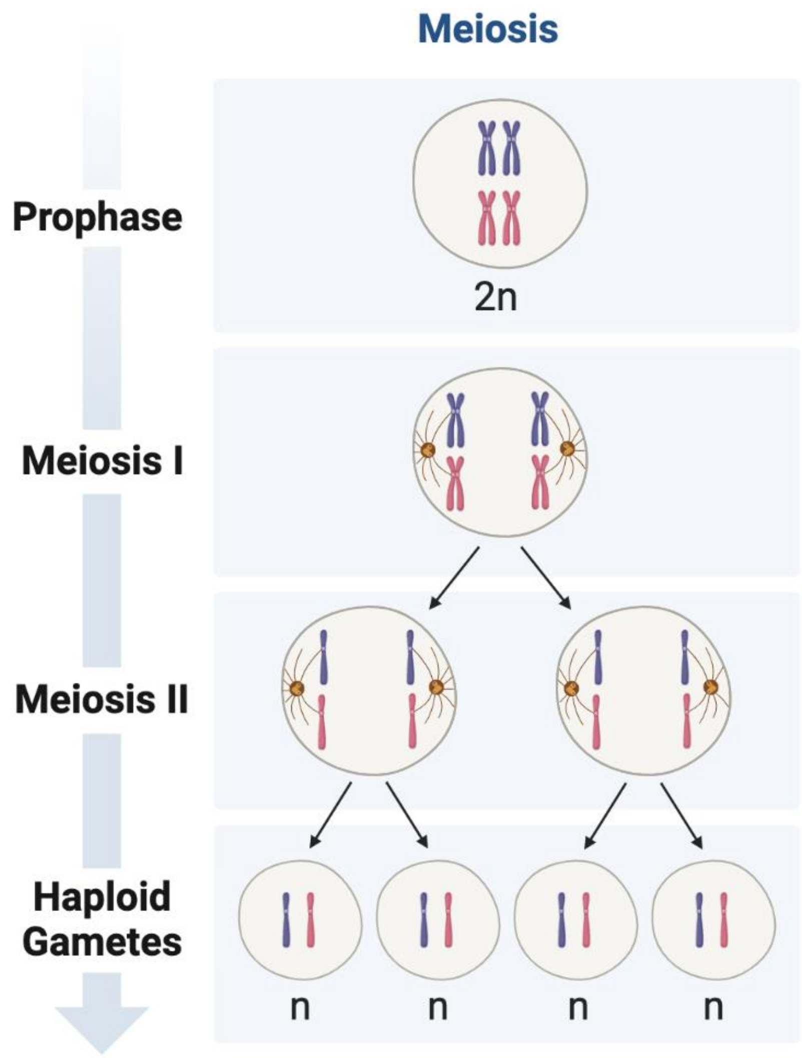

Figure 1 Meiosis consists of two rounds of division, resulting in gametes with a single copy of each chromosome**.** Not represented are the crossover events which create chiasmata, physical linkages between the homologous chromosomes, ensuring they align at metaphase 1. Figure created by author using BioRender.

In order to generate heterogenous daughter cells, meiosis differs from mitosis in three key aspects: the persistence of cohesion on sister chromatids, recombination events resulting in the formation of chiasmata, and the random orientation of homologous chromosomes at anaphase I. During pre-meiotic S phase, sister chromatid cohesion is established, and maintained until anaphase II, to allow segregation of the homologs during anaphase I, and prevent the premature separation of sister chromatid before the second meiotic division[1], therefore generating heterogenous haploid spores[2]. This is due to the incorporation of meiosis specific Spo13 at the centromeric cohesin[6].

Spo13 inhibits the cleavage of the cohesion subunit Rec8 by the separase Esp1, preventing the separation of the sister chromatids prior to anaphase II[7, 8]. During anaphase I the homologous chromosomes are drawn to opposite poles, as opposed to the sister chromatids as seen in mitosis[9]. To enable correct segregation of the homologous chromosomes at anaphase I, the homologous pairs of chromosomes exchange genetic material during meiotic prophase I, forming physical linkages, or chiasmata, between the homologs [10]. In order to form these chiasmata, intentional DSBs are created, generated by Spo11[11], at the leptotene phase of meiotic prophase[12]. Two Spo11 proteins are required to generate each DSB and remain covalently linked to the 5' DNA ends. Sae2 and the MRX complex then release the Spo11 proteins, and the DNA they are bound to by endonucleolytic cleavage[13]. The DNA ends are then processed to form ssDNA, and, as in outside of meiosis, RPA binds the ssDNA, removing any secondary structure. The ssDNA is then bound by Rad51 5' of the break, stabilising the Dmc1 polymerising at the 3' of the ssDNA. The filament can then search for homologous sequences, with the Hop2 -Mnd1 complex stabilising interactions between ssDNA bound by Dmc1 and the dsDNA[11]. During meiosis, both Rad51 and Dmc1 are required for proper crossover formation and resolution[14, 15]. However, while both recombinases are present, the majority of DSBs are repaired using the homologous chromosome as opposed to the sister chromatid, in a 4: 1 ratio[16]. This is due to the downregulation of Rad52 strand exchange activity due to the expression of Hed1, and the phosphorylation of Rad54 by Mek1, both of which prevent the formation of the Rad51- Rad54 complex, which is responsible for stimulating strand exchange and chromatin remodelling[16, 17].

II Repair of Double Strand Breaks

DNA double strand breaks (DSBs) can be caused by both exogenous sources, such as radiation or by the metabolism of the cell, and, if left unrepaired, can be fatal to the cell[18]. This is because these lesions can lead to genomic instability and if incorrectly repaired, result in gross chromosomal rearrangements. However, because this type of damage is highly dangerous, the cell has several pathways to repair this form of DNA damage. As *Saccharomyces cerevisiae* is the model system studied, this thesis will only focus on DNA DSB repair in *S. cerevisiae*, other organisms will only be mentioned where relevant. *S. cerevisiae* are able to utilise three main pathways to repair DSBs; End Joining (EJ), Homologous Recombination (HR), and Single Strand Annealing (SSA), which is a less common pathway which relies on annealing repeating sequences after resection[19, 20]. EJ can be further subdivided into two pathways; Non-Homologous End Joining (NHEJ) or Microhomology Directed End joining (MDEJ)[21]. While HR can be subdivided into three distinct pathways; Double Strand Break Repair pathway (DSBR), which involves the formation of a double Holliday junction, Synthesis Dependent Strand Annealing (SDSA) and Break Induced Replication (BIR). The shared commonality between these pathways is the generation of a ssDNA molecule which then invades a DNA duplex, encoding a homologous sequence[22]. This 'strand invasion event' forms a structure known as a Displacement loop or D loop.

III DSB Repair pathway selection

While in humans the main pathway for DSB repair is NHEJ, in *S. cerevisiae*, HR is the more common pathway[23], due to the higher coding density of their genomes as opposed to NHEJ being favoured in mammals due to the large intergenic spaces of their genomes. In addition to this, the larger genome size of higher eukaryotes would decrease the chance of successfully and accurately identifying the correct donor, increasing the likelihood of ectopic recombination and, decreasing the accuracy of HR[24].

DNA lesions activate the DNA damage response (DDR). The DSB is recognised, triggering a kinase cascade. Initially, the kinases Tel1 and Mec1, which are members of the phosphatidylinositol 3-kinase–like protein kinase (PIKKs) family are activated[25], once activated, Mec1 phosphorylates the kinases Chk1 and Rad53, which then act to co-ordinate the DNA damage response, including activating checkpoints, such as the Rad17 and Rad24 checkpoint complexes[26, 27]. Repair pathway selection is dependent on several factors, including ploidy and cell cycle stage[28]. *S. cerevisiae* can exist in either a haploid or diploid state. In the haploid state, before the S phase of the cell cycle, in the instance of a DSB needing repair, a homologous template is not present in the cell for use for HR repair. Therefore, in haploid cells, NHEJ is the primary pathway for DNA repair in the G1 phase of the cell cycle. However in diploid cells, where the homolog is present throughout the cell cycle, the products of both mating type alleles, a1 and α2 form a transcriptional repressor, a1-α2[29].
a1-α2 acts to suppress NHEJ through transcriptional repression of the genes *NEJ1*, which is the gene responsible for NHEJ activation[30], and *LIF1*, which encodes the protein Lif1 which interacts with Dnl4, through upstream repressors[31].
The cell cycle is also responsible for DSB repair pathway selection through the regulation of resection. During the G1 phase of the cell cycle, Cdk1, the main cyclin dependent kinase in *S. cerevisiae,* is inhibited by the cyclin dependent kinase inhibitors, Sic1 and Far1[32].

Low levels of Cdk1 limit end resection of DSBs, as Cdk1 must activate Sae2 by phosphorylating it's Serine 267 residue in order for resection to occur, lack of phosphorylated Sae2 commits the cell NHEJ repair[33].

IV Homologous Recombination

Homologous recombination is a DNA repair pathway that uses a homologous sequence as a template for DNA repair. In *S. cerevisiae* HR is carried out by proteins of the Rad52 epistasis group[34], and involves three key steps; resection, presynaptic filament formation, strand invasion. The defining step of recombination is the formation of the D-loop by strand invasion, which is catalysed by Rad51, a recombinase. While the separate pathways of HR are differentiated in the final resolution stage[35].

Initially, the DSB is bound by the MRX complex formed of Mre11, Rad50 and Xrs2, and Sae2, which begin resection of the DSB.
The MRX complex is recruited via the interaction between Xrs2 and Tel1. Xrs2 is responsible for the nuclear localisation of Mre11. Rad50 is a member of the ABC ATPase superfamily and contains a Walker A motif at it's amino terminus, and a Walker B motif at it's carboxy terminus. The Walker A and B are ATP binding motifs, which associate with each other, allowing the intervening amino acids to form a coiled-coil, while the ATPase domain formed by the Walker motifs binds Mre11. The coiled coil domains tether the opposite ends of the DSB together, while end resection is completed by Exo1 and the helicase Sgs1 forming 3' ssDNA tails[20, 36]. The ssDNA is then coated by RPA. RPA acts to remove secondary structure from ssDNA, allowing the formation of a Rad51 filament on the DNA[35]. Rad51 is required for the next step of HR; pre-synaptic filament formation, during which, Rad51 binds to the ssDNA, and prepares to catalyse strand exchange. However Rad51 Rad52 and the Rad55/57 complex to displace RPA[37]. Rad52 recruits Rad51[38] to ssDNA coated by RPA and, along with the Rad55/57 complex, promotes formation of the nucleoprotein filaments[22]. Once the recombinase has polymerised on the ssDNA, this forms the pre-synaptic complex. this single stranded region can then be used as a template to search for homologous sequences. Once the repair template has been found Rad51 can then catalyse strand invasion of the dsDNA at a homologous locus, by the ssDNA tail. This strand invasion event forms a Displacement loop (D-loop), these D loops can then either be resolved by DSBR or Synthesis Dependent Strand Annealing (SDSA)[39]. SDSA involves a short stretch of DNA synthesis followed by displacement of the invading strand. The displaced strand then reanneals back to its original partner and

generates only non-crossover products, once fill-in synthesis and ligation of the backbone nick have been completed[40]. On the other hand, DSBR involves the extension of the invading 3' end and second end capture, generating a double Holliday junction. The Holliday junctions are then resolved to form either crossover or non-crossover products depending on whether the DNA molecules are cleaved symmetrically or non-symmetrically (Figure 2).

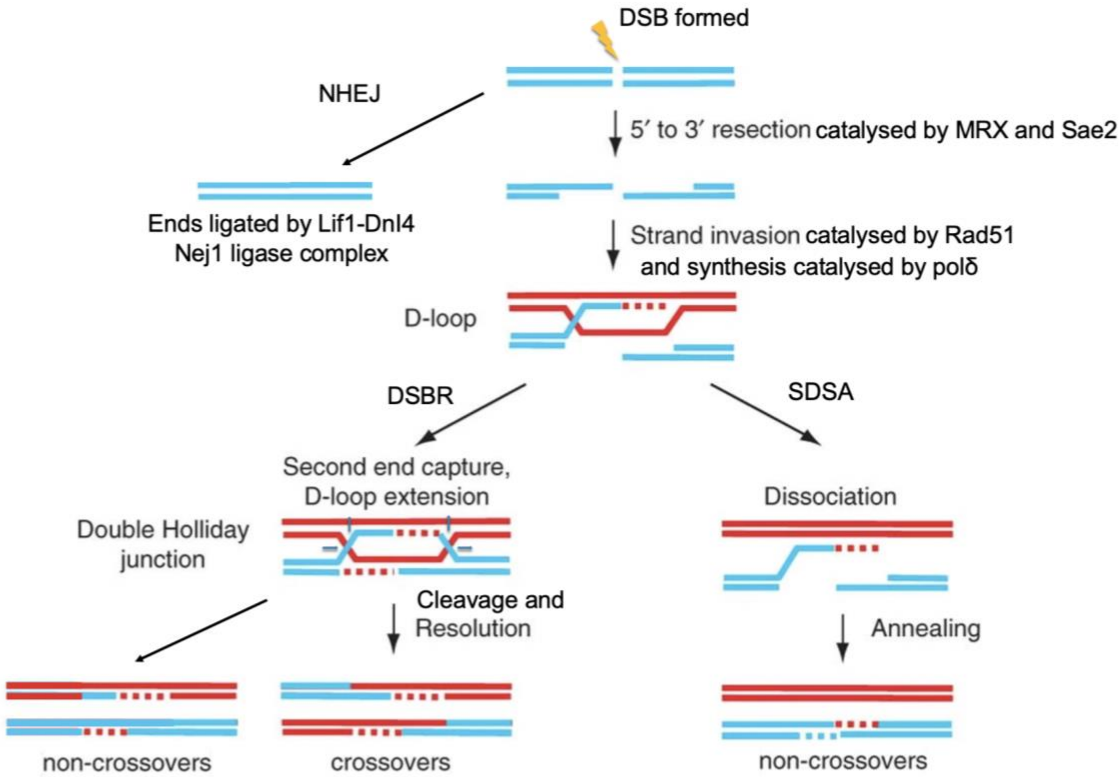

Figure 2 Summary of DSB Repair pathways. Once a break is formed, the ends are either ligated, in NHEJ, by the Lif1-Dnl4-Nej1 ligase complex or resected by Sae2, in DSBR and SDSA. Rad51 polymerises on the ssDNA formed by resection and catalyses strand exchange. This is followed by DNA synthesis. The newly synthesised strand can then dissociate and reanneal to it's original partner strand forming non-crossover products, this is the SDSA pathway. Alternatively, a double Holliday junction can be formed by second end capture. Following this, the formation of crossover and non-crossover products depend on the axis of cleavage at the resolution stage of the double Holliday junction. Figure adapted from[39]. This figure does not depict Break Induced Replication (BIR) as this repair mechanism is used for single ended DSBs, however the strand invasion step is catalysed by Rad51. The strand invasion and formation of a D loop is then followed by a round of replication. The newly synthesised DNA is then used as a template for a second round of synthesis, this

asynchronous replication results in conservative synthesis of the DNA [41].

V Non-Homologous End Joining

NHEJ is the favoured pathway of DNA repair in haploid *S. cerevisiae* cells, during the G1 phase of the cell cycle [42]. During this period, end resection is repressed, allowing the progression of NHEJ. While NHEJ is considered an error prone pathway, in reality NHEJ can repair 'clean' DSBs, such as those generated by restriction enzymes, in an error-free manner, however insertions or deletions may occur at 'dirty' DSBs, which may require processing before ligation, e.g. to remove covalently attached groups[43, 44]. When the DSB is repaired by NHEJ, the DNA ends are protected by the Ku heterodimer, which consists of Yku70 and Yku80[45]. The Ku dimer is conserved across Eukaryotes and forms a scaffold onto which the subsequent proteins required for the catalysis of NHEJ can interact with the DNA. This is due to the dimers forming a β barrel ring which interacts with the sugar phosphate backbone and fits into the major and minor grooves of the DNA helix[46]. The ring formed by Ku dimerisation encases two turns of the DNA double helix and suppresses HR, by preventing DNA end resection[47]. The MRX protein complex, which is also involved in HR, tethers the ends of the break together[24, 48]. It is unclear whether the Ku dimer binds the DSB initially, recruiting the MRX complex, once bound or whether the MRX complex binds the DSB directly, however what is clear is that the MRX complex is required for efficient NHEJ[47]. The action of Ku binding is key to committing the DSB to repair by NHEJ. Dnl4 and Lif1 are then recruited by the MRX complex and interact with the YKu heterodimer. Dnl4 is an ATP dependent DNA ligase which catalyses the ligation of the DNA ends[49], while the Lif1 homodimer acts as a regulatory cofactor, which stabilises Dnl4[24, 28]. Nej1 is also involved in NHEJ and is essential for end ligation[50]. Dnl4 then ligates the ends of the break. Two Dnl4 molecules are required, one to ligate each strand, the strand ligation reaction probably occurs sequentially due to the size of Dnl4 and the proximity of the two strands, however, once one strand is ligated, the break is stabilised so the delay in second end ligation is not of concern.

VI RecA Homologs with the Tree of Life

RecA homologs are recombinases involved in HR, and their ATP dependent strand exchange activity is required for the formation of the of the D loop. These proteins were initially identified by their homology to RecA, the first member of the family to be discovered, in *E. coli*. The key region of homology which allowed the identification of these proteins was a highly conserved region of around 230 amino acids, known as the Core ATPase Domain (CAD) which all RecA recombinase family members share [51] (Figure 3).

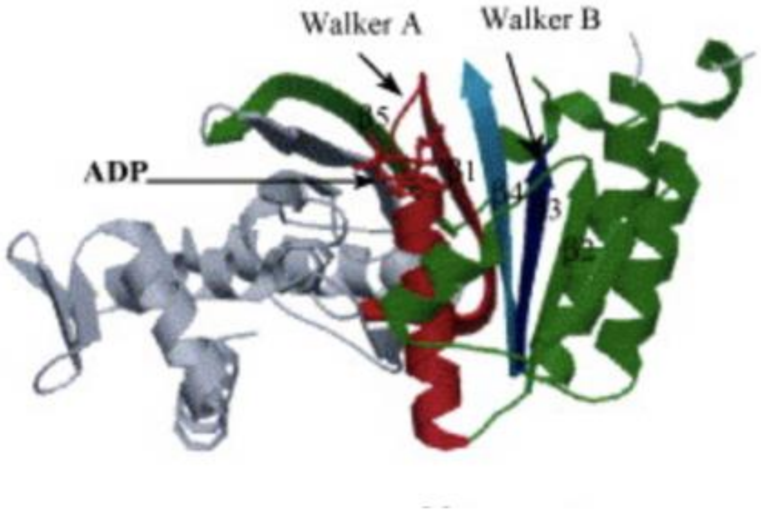

Figure 3 Model of RecA bound to ADP with the CAD highlighted. The CAD is common to all RecA homologs and allows ATP binding and catalysis of strand exchange. The Walker A domain is highlighted in red, and the Walker B domain is in blue. Figure taken from [52].

Within this region there are several conserved domains including the Walker A and B domains, which allow the proteins to bind and hydrolyse ATP[53]. RecA recombinases all act in an ATP dependent manner to bind and under-wind DNA, extending DNA 1.5 times, compared to B form DNA[38], which enables the homology search via base flipping[54]. ATP binding and hydrolysis results in a confirmational change which is only required for the formation of filaments on the DNA and the alignment of the homologous sequences, not the homology search or strand exchange[55]. The CAD also contains two disordered loops; L1 and L2, which bind ssDNA and contribute to the homology tolerance of the RecA homolog[51]. Adjacent to the CAD, all RecA homologs contain a polymerisation motif. This motif contains a hydrophobic phenylalanine residue which inserts into a hydrophobic pocket of the ATPase domain of the adjacent monomer[56]. Enabling the formation of polymers or filaments, as seen in the Eukaryotic RecA homologs, or the toroidal rings of RadA
These molecules form helical filaments on ssDNA, when bound to ATP, with each monomer spanning 3-4 DNA bases[54] (Figure 4). These filaments, when bound to ssDNA are known as the presynaptic filament

and are activated by binding to DNA. Once activated it is able to locate and bind a homologous molecule of dsDNA, forming a heteroduplex DNA molecule. The filament then catalyses strand exchange, and the D loop is formed[51].

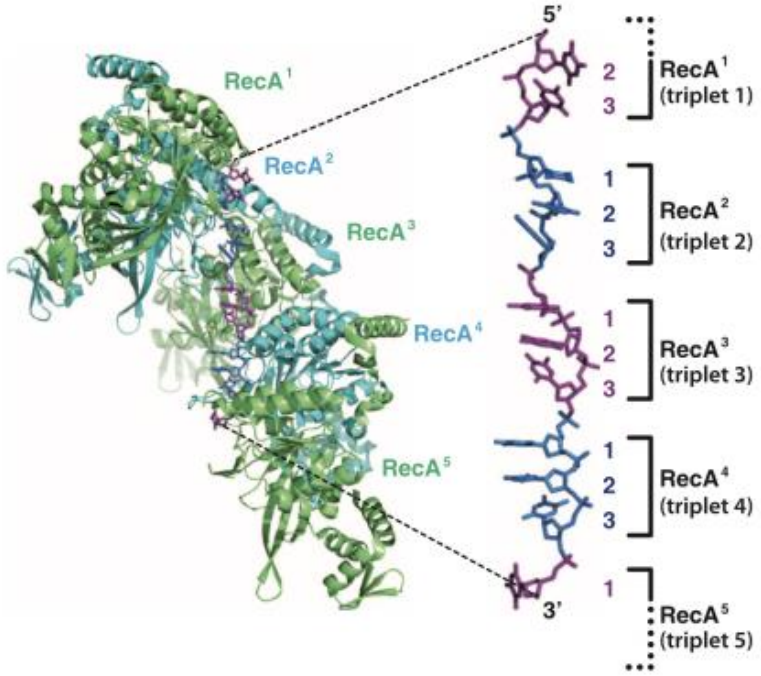

Figure 4 Rec A filament model demonstrating how each monomer spans 3 base pairs. The DNA passes through the centre of the filament, allowing the stabilisation of strand exchange intermediates. Figure taken from [57].

While the level of sequence homology between RecA and the eukaryotic RecA homologs is high, RecA has an additional C terminal domain, not seen in the eukaryotic RecA homologues, which appears to be required for inter-filament interactions. The lysine residues at positions 286 and 302 also appear to have a role in binding to double stranded DNA[58], as the RecA molecule appears to have a cleft, which can accommodate double stranded DNA helix, to facilitate strand exchange (Figure 5). In addition to this, the eukaryotic and archaeal RecA homologs have an extended N-terminal domain. The N terminus may be responsible for the dsDNA binding activity of the eukaryotic RecA homologs, similar to the C terminal domain of RecA[59, 60].

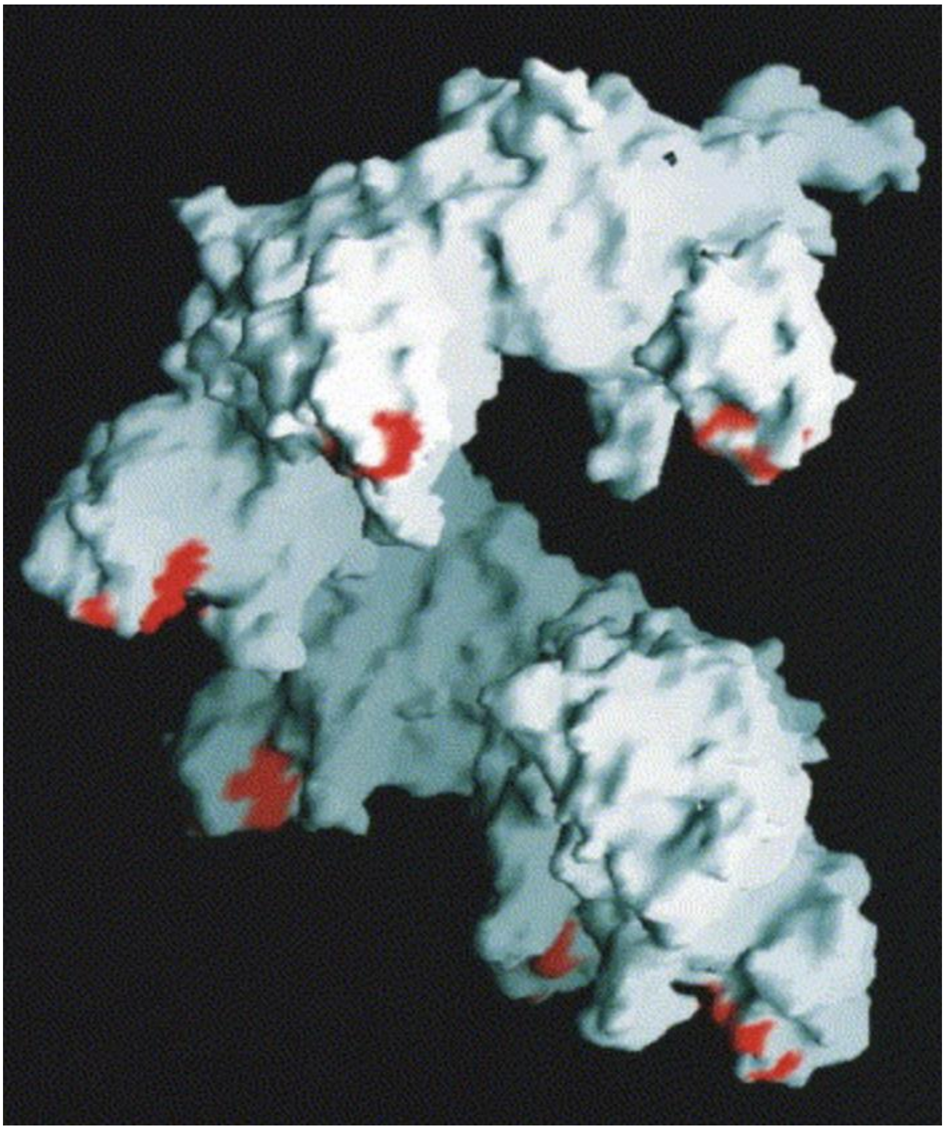

Figure 5 Molecular surface model with the C-terminal DNA binding sites highlighted. Model depicts 6 monomers, i.e. one turn of the filament, and highlights residues; Tryptophan- 290, Isoleucine-298, Glycine-301, Lysine- 302, Alanine- 303 and Asparagine-304. Molecular model was generated with GRASP [61]. Figure taken from [62].

i Rad51

The Rad51 of *S. cerevisiae* (scRad51) has a 69% sequence identity with mouse Rad51[63] and forms a filament with three -fold symmetry, not sixfold symmetry, despite each turn of the filament being composed of 6 protomers, due to two distinct interfaces[56]. One interface is formed by Histidine 352 in close proximity to ATPase site while the second interface is formed by a patch of three positively charged residues; Arginine 188, Lysine 361 and, Lysine 371, which similar to loop 2 in RecA, forms a low affinity DNA binding site required for strand exchange[11]. Loop 1 binding appears to be independent from loop 2 binding and may only be required to catalyse stand exchange.

Filament assembly occurs via the interaction between the β strand of the interdomain linker and the central sheet of the adjacent monomer. This brings the nucleotide binding pocket into close contact with ATPase domain of the adjacent monomer, allowing the coordinated hydrolysis of ATP along the filament [54]. This interaction between the N terminus of one monomer and the ATPase domain of the next is mediated by two tyrosine residues: Tyrosine 112 at the N terminus and Tyrosine 253 at the ATPase domain[64].
These interactions are also present in the *M. musculus* homolog of Rad51 (mRad51) is a 339 amino acid protein which is expressed at high levels in the thymus, spleen, testis and ovary, it is also expressed at lower, but still elevated, levels in the brain, compared to other organs such as the liver and heart[65]. The high expression in the sexual organs is expected, as Rad51 is required during meiosis. Like the other RecA homologs, mRad51 contains the central CAD, which allows it to catalyse strand invasion. mRad51 also has an extended N terminal region characteristic of eukaryotic and archaeal RecA homologs, allowing it to bind dsDNA and stabilise strand invasion. mRad51 is almost identical to *Homo sapien* Rad51, differing by only four amino acids, demonstrating how close these proteins are on an evolutionary scale.

ii Dmc1

Dmc1 is a Meiosis specific recombinase in *S. cerevisiae*, due to its role in Meiosis, Dmc1 favours inter-homolog recombination and to facilitate this Dmc1 has a higher tolerance for mismatches than Rad51. Rad51 is active during vegetative growth and meiosis, while Dmc1 is meiosis specific[66]. Both form nucleoprotein filaments on ssDNA and catalyse homology search and the formation of a D-loop. However, Rad51 favours inter-sister chromatid exchange, while Dmc1 favours exchange between homologous chromosomes[66]. However, during meiosis, Dmc1 still requires Rad51 for function, as Rad51 mutants accumulates DSBs during meiosis[38].On the other hand, Dmc1 mutants are unable to complete meiosis and arrest in late meiotic prophase[67, 68], after triggering the meiotic recombination checkpoint[69].
Most eukaryotes have at least two RecA homologues, Rad51 and Dmc1, believed to have been generated by a gene duplication event as they share 45% amino acid sequence homology in *S. cerevisiae*[39]. This gene duplication event is thought to have occurred after divergence from archaea, but before plants diverged from the rest of the eukaryotes[53]. However, this sequence divergence is why Dmc1 can catalyse exchange between non-identical sequences, it is more tolerant to mismatches, due to the greater flexibility of the protein in Loop 1 and

2, allowing it to stabilise distortions in the DNA backbone, caused by mismatches[70].

iii Interactions between Rad51 and Dmc1

During *S. cerevisiae* meiosis, once the DSBs have been formed and the ends resected to prepare for homolog search and crossover formation. Rad51 and Dmc1 bind to the ssDNA on both sides of the DSB[71], Rad51 polymerises on the ssDNA further from the break, while Dmc1 polymerises closer to the break site[72]. However Rad51 indirectly mediates the activity of Dmc1 during meiosis, enabling the formation of Dmc1 foci during meiosis[73]. Studies have shown that this interaction is mediated through the heterodimer Mei5-Sae3, however Rad51 appears to be essential to the formation of Dmc1 foci, as when Mei5 and Sae3 are present, in a Rad51 mutant phenotype, the Dmc1 foci are faint, compared to wildtype[11]. In addition, Rad51 has been shown to increase the speed of Dmc1 nucleation on ssDNA[74]. However Rad51 is not essential for sporulation as *rad51* strains report a sporulation efficiency of around 39%[68].

iv RecA

In bacteria homologous recombination involves the recombinase RecA and occurs between a linear double stranded donor and a supercoiled recipient [59]. RecA is the eponymous member of the RecA family of recombinases, which are found across all three domains of life[75]. RecA is a 352 amino acid protein, whose structure is highly conserved across bacteria. Like all other RecA recombinases it contains the Core ATPase Domain, which in RecA, extends from residues 34 to 240[59]. This core region is characterised by a central β sheet, sandwiched by two α helices. The Walker A motif spans one strand of the β and the adjacent α helix, and is involved in the binding and hydrolysis of ATP, while the Walker B motif is formed of one strand of the β and is required for magnesium ion co-ordination[52] (Figure 3).

RecA contains two DNA binding sites; the high affinity binding site is involved in the presynaptic phase, which is required for the initial filament formation on ssDNA, while the low affinity binding site is required for the formation of the DNA triplex and homology search[73]. The low affinity binding site is present in the extended C terminal region of RecA, and forms a cleft, containing two highly conserved lysine residues, within a conserved patch of positively charged residues, [62] which accommodate the DNA backbone [58]. Once a DSB is recognised, it is resected, by either RecJ or RecQ[35], RecA then begins to load onto the ssDNA exposed by the resection. RecA polymerisation onto DNA occurs in two phases; the rate limiting nucleation of RecA onto ssDNA, followed by the elongation of the filament, which is enabled due to locally high concentrations of RecA[76]. The extension of the filament activates the SOS response, which is mediated and regulated by RecA[77]. The SOS response involves a wide range of repair mechanisms and is repressed by LexA. Once activated by binding to ssDNA, RecA can release the repression of LexA, allowing DSB repair to commence [78]. RecA can then act as a recombinase, searching for homologous sequences and accommodating both the dsDNA and ssDNA to allow for base pairing and displacement of one of the dsDNA strands[62]. ATP hydrolysis then induces the dissociation of RecA from the DNA[76]. Alongside it's strand exchange ability, RecA also possesses a DNA annealing activity, which in *S. cerevisiae* is catalysed by Rad52. RecA has been shown to partially compensate in *rad52* strains in *S. cerevisiae* after MMS treatment, which raises the question of whether it's strand exchange activity could compensate for Rad51[79].

v RadA

RadA is the archaeal form of RecA, however it shares greater sequence similarity with the eukaryotic RecA homologs than bacterial RecA, 40% sequence similarity compared to 20% sequence similarity, respectively[75]. Like the eukaryotic Rad51 and Dmc1, RadA consists of two domains; a Central ATPase Domain and an Extended N terminal domain. Notably, it is lacking the C terminal domain characteristic of bacterial RecA. The central domain contains the RecA- like fold, which is required for ssDNA binding and ATP binding and hydrolysis. This domain contains the Walker A and B motifs and the L1 and L2 ssDNA binding loops[80]. On the other hand, the N terminal domain is involved in inter-filament and intermonomer interactions[51, 81]. Additionally, the N terminal domain of RadA may be involved in DNA binding, along with L1, which is known to interact with ssDNA. Studies in *Sulfolobus solfataricus* have identified five conserved positively charged residues would form a continuous surface on the exterior of the filament. This positively charged region is made up of three arginine residues in L1, and two lysine residues within the N terminal domain. These domains in proximity may allow the formation of heteroduplex DNA and strand exchange [82].

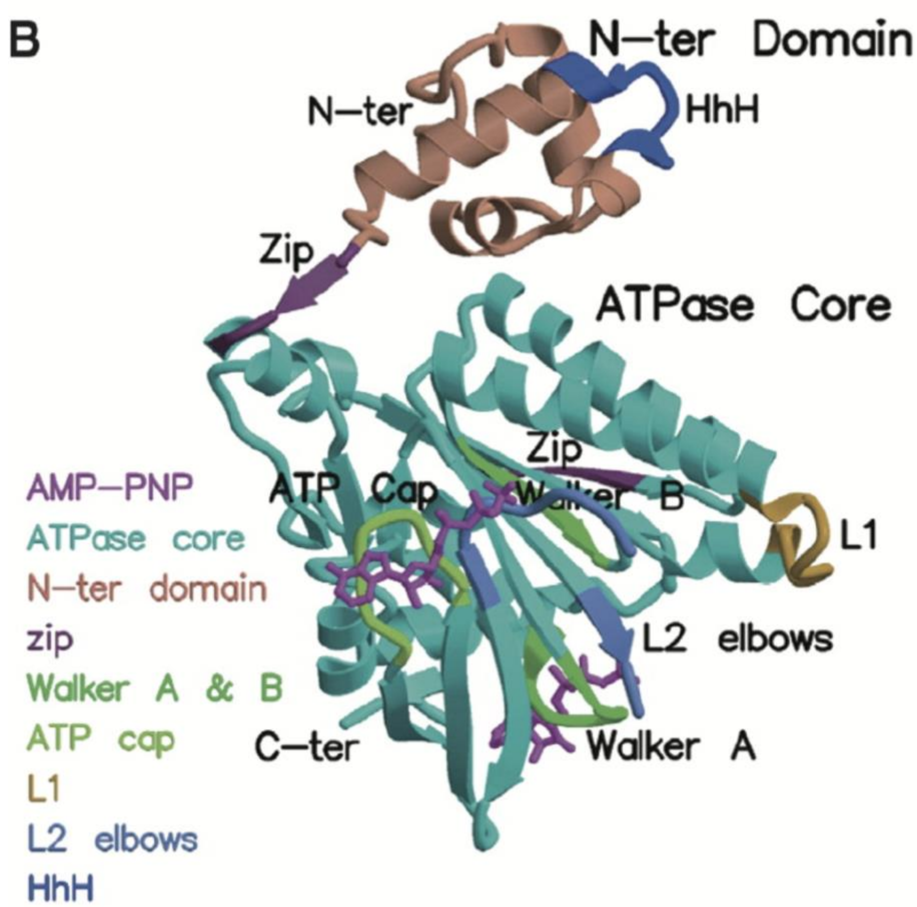

Figure 6 Model of RadA from *Methanococcus voltae* illustrating the relative positions of the different domains of RadA*.* *M voltae* is a methanogenic archaeon, however, it's RadA is also formed of the two domain structure characteristic of eukaryotic and archaeal RecA homologs. Figure taken from [80].

VII Project Aims

Cas9 is a nuclease that forms part of the Type II Clustered Regularly Interspaced Short Palindromic Repeats (CRISPR) system. The CRISPR system originated as a prokaryotic adaptive immune system, which protected the organism from phage infection[83]. Upon infection, viral DNA is digested into short fragments and incorporated into CRISPR arrays, separated by direct repeats. This array is flanked by sequences encoding the Cas9 proteins[83]. Once the short fragments are transcribed, generating a CRISPR RNA (crRNA), they can bind to a Cas9 protein, along with a the trans-activating RNA (tracrRNA)[84] . This Cas9-crRNA-tracr-RNA complex catalyses the formation of a DSB at the target site, guided by the crRNA. For use in gene editing systems, these RNAs have been fused into a single guideRNA (gRNA) for convenience. This system has been shown to be functional in mammalian cells and can be used to generate DSBs, which are then repaired by NHEJ, to cause deleterious mutations or, when a template with the desired sequence is either present in the cell or provided, by HR, to alter the genetic sequence[85]. Due to the success of CRISPR Cas9 editing in mammalian cells it would be a useful tool to use to generate mutations in *S. cerevisiae*, as the current method of gene deletion requires the amplification and transformation of individual gene deletion cassettes from the Yeast Knockout (YKO) collection into the desired experimental strain. However, the HR repair pathway is much more active in *S. cerevisiae* cells, leading to precise break repair. The aim of this project was to determine whether selective downregulation of Rad51 would force the cell to repair breaks by NHEJ, this system could then be transformed into a reporter strain of choice, along with Cas9 under a promoter of choice and CRISPR guide library targeting the desired genes, thereby allowing the generation of deleterious mutants in any reporter strain.

Cas9 has also been used to develop tools to identify fusion genes, known as Fusion Detection by Gene Enrichment (FUDGE), which uses the active Cas9 protein. This tool could be adapted to sequence across known recombination hotspots and identify the unknown partner locus involved in recombination. Previous work from the Gray lab has identified novel ectopic recombinants derived from the *HIS4::LEU2* and *leu2::hisG* hotspots. FUDGE could be adapted to identify the other side of these recombinants and other recombinants that form at levels below the threshold of pulsed field gel imaging.

Additionally, due to their vital function, RecA homologs are highly conserved across the Tree of Life. In order to determine the extent of protein binding domain conservation, Rad51 will be replaced by several RecA homologs, these strains will be driven through meiosis, in order to determine whether the homologs can compensate for Rad51.

Chapter 2 Materials and Methods

I Chemicals and Media

	Composition
1x TAE	04M Tris Acetate (pH 8.3) 0.01M EDTA
Agarose gel	1% Agarose 1x TAE
S. cerevisiae	
YPD	1% Yeast Extract 2% Peptone 2% Dextrose 0.5mM Adenine Sulphate 0.8mM Uracil
YPD Plates	1% Yeast Extract 2% Peptone 2% Dextrose 0.5mM Adenine Sulphate 0.8mM Uracil 15 $g.L^{-1}$ Bacto agar
YPA	1% Yeast Extract 2% Peptone 1% KAc
20 x AUL	1.82 g. L^{-1} Adenine 1.79 g. L^{-1} Uracil 2.62 g. L^{-1} Leucine
100 x AAHLTU	1 mg. ml^{-1} Adenine 1 mg. ml^{-1} Arginine 1 mg. ml^{-1} Histidine 1 mg. ml^{-1} Tryptophan 3 mg. ml^{-1} Leucine
Hygromycin	200 μg. mL^{-1}
Spheroplasting Buffer	1M Sorbitol 100mM Tris. HCl pH 7.8 100mM EDTA 1% 2-Mercaptoethanol 0.25mg. ml^{-1}
Lysis Buffer	3% SDS 0.1M EDTA 1 mg. μl^{-1} Proteinase K
RNAse A	10mg. ml^{-1}

E. coli	
Ampicillin	100 μg. ml^{-1}
Kanamycin	50 μg. ml^{-1}
LB	10 g/L tryptone 5 g/L (w/v) yeast extract 10 g/L NaCl NaOH to pH 7
SOC media	5 g/L yeast extract 20 g/L tryptone 10 mM NaCl 2.5 mM KCl 20 mM MgSO4 20 mM D-glucose NaOH to pH 7.5
SDS PAGE	
Resolving gel (12%)	12% Bis/Acrylamide 5 ml 1M Tris pH 8.8 + TCE 10% SDS 10% APS TEMED SDW
Stacking gel	Stacking mix (Tris.HCl, SDS) 10% APS TEMED SDW
Zymolyase	100mg/ml

II General Methods

i Primer preparation

Primers were ordered from IDT and resuspended according to manufacturer instructions, giving a final concentration of 100nM.

ii Agarose gel electrophoresis

Agarose gels were prepared by adding the required mass of Agarose powder and then made up to the required volume with 1x TAE, all gels are 1% agarose unless stated otherwise. The solution was then boiled and left to cool. Ethidium bromide was then added, at 8μl per 100ml to yield a final concentration of 0.008%. The gel was then poured and left to set, before the samples were loaded and run in 1xTAE running buffer.

iii PCR

Primers were diluted to 10nM from the stock solution and added to the PCR mixture. The Primers and DNA were added, along with SDW to dilute x2 Q5, to either a final volume of 50μl for a fragment generation reaction or 25 μl for a screening reaction. Volumes listed in Table 1.

Table 1 Volumes used for PCR reactions. Screening reactions were reactions only used to verify products by gel electrophoresis, hence the smaller reaction volume.

Liquid	Amplification Reaction (μl)	Screening Reaction (μl)
DNA	1	1
Q5 MasterMix x2	25	12.5
Primers (10nM)	1	1
Water	23	10.5
Final Volume	50	25

Table 2 Template for general PCR protocol. X= Annealing time, either calculated using NEB Tm calculator or given in Gibson Assembly summary. Y= Amplification time, calculated using 1Kb per minute for Q5 polymerase.

Stage	Temperature (°C)	Time	Repetition
Initial Denaturation	98	1 min	
Denaturation	98	30s	X 30
Annealing	X	30s	
Amplification	72	Y	
Final Amplification	72	Y	

iv PCR clean-up

The Machery-Nagel PCR clean-up kit was used according to the manufacturer's instructions. First Buffer NT1 was added to the PCR reaction mixture in a 2:1 ratio, to adjust the DNA binding condition. The sample was then loaded into the Nucleospin column and centrifuged at 13,000 rpm for 30 seconds(s) to bind the DNA to the column. The flow through was discarded and the column was washed using 700 μl of NT3 Buffer. Once NT3 was added, the column was centrifuged for 30 s at 13,000 rpm and the flow through was discarded. The column was then dried by centrifuging at 13,000 rpm for 1 minute and the flow through was discarded. The column was then placed in a 1.5 mL Eppendorf and 15-30 μl of Elution buffer was added to the column and incubated for 1 min at room temperature. The DNA was then eluted by centrifuging for 1 minute at 13,000 rpm. The column was then discarded.

v Gibson assembly

Gibson assembly can be used to ligate fragments generated by restriction digest or PCR. The fragments are amplified using primers designed with homologous sequences, the sequences are then resected during the Gibson assembly reaction, exposing the single stranded sequences which can then anneal together. Once the complementary sequences are annealed the backbone is ligated and the plasmid is fully assembled. This method of assembly allows for the ligation of plasmids from up to 15 fragments. The NEBuilder tool was used to design the primers for PCR amplification of the fragments required, the primers contained regions of overlap, which would allow annealing during the Gibson assembly. The primers were diluted to 100nM as per manufacturer's instructions and used in PCR, as detailed in PCR protocol. Once generated, the backbone and inserts were nanodropped to determine their concentrations in ng.μl^{-1}. This was then converted to pmol.µl-1 using the formula $\mathrm{pmol} = \frac{(\text{weight in ng})\ \text{x}\ 1000}{(\text{basepairs x 650 daltons})}$. Using these concentrations, the fragments were assembled in a 1:2 backbone to insert ratio if there were 2-3 fragments with 0.02 to 0.5 pmoles of DNA added to the mixture overall. If there was greater than three inserts the fragments were added in a 1:1 ratio of backbone: insert with 0.2 -1.0 pmol of total DNA in the mixture. X2 Gibson assembly MasterMix was then added and the volume made up to 20µl with SDW. The samples were then incubated at 50°C for 60 minutes and then stored on ice for transformation.

Table 3 Gibson assembly reaction mixture.

	Volume (µl)
Fragments	X
X2 Gibson Assembly MasterMix	10
Water	10- X
Final volume	20

vi Preparing glycerol stocks

Glycerol stocks were made using either *E. coli* or *S. cerevisiae* overnight cultures. 100% Glycerol was diluted with SDW to a final concentration of 50% Glycerol and autoclaved. 50% Glycerol was then mixed with overnight culture in a 1:1 ratio, i.e., 750µl overnight culture to 750µl 50% glycerol in 2ml screw top cryotubes. These were then stored in the -80°C freezer

III E. coli

i Plasmid isolation

The plasmid was isolated from *E. coli* using the Machery-Nagel Nucleospin Plasmid Protocol: Isolation of High Copy Plasmid DNA from *E. coli.* Overnight *E. coli* culture pelleted, and supernatant discarded. The cells were resuspended and lysed using 250µl of A1 buffer and resuspended in 250µl of A2 buffer was added and mixed by inversion the tubes were then incubated for 5 minutes at room temperature. 300µl of Buffer A3 was added and mixed by inversion. The tubes were then centrifuged at 13000 rpm for 5 minutes. The DNA was then bound to the column, the supernatant was added to the column and centrifuged for 1 minute at 13000rpm. The flow through was discarded and 500 µl of Wash buffer AW was added This was then centrifuged and the flow through discarded. 600µl of Buffer A4 was then added and centrifuged, the flow through was discarded. The membrane was then dried by centrifuging for 2 minutes, the flowthrough was discarded.

ii Bacterial transformation

Chemically competent *E. coli* cells underwent a heat-shock transformation. An aliquot of competent cells was removed from -80°C storage and defrosted on ice. The plasmid mixture and labelled 1.5 ml Eppendorf's were also cooled, allowing the reaction mixture to be assembled on ice to prevent loss of competency. Once defrosted, 10μl of the competent cells was mixed with the desired volume of plasmid and incubated on ice for 20 minutes. The mixtures were then heat-shocked at 42°C for 42 seconds using a waterbath and then incubated on ice for a further 5 minutes. 100μl of SOC LB was then added to the mixture and incubated for 1 hour to allow time for transformation. The cells were then plated onto the required LB + selection plates, usually Ampicillin or Kanamycin plates, and incubated at 37°C overnight.

iii Colony PCR

Desired bacterial strain is retrieved from the -80°C and streaked out and incubated overnight at 37°C on LB agar plates. Single colonies are selected from the plate and inoculated into 20μl of SDW, this is then boiled at 100°C for 10 minutes to lyse the cells. This mixture can then added to the PCR reaction in the required volume as and used as template DNA.

IV S. cerevisiae

i AUL x20

The required mass of Adenine, Uracil and Leucine powders were made up with SDW to a x20 solution. This was then gently warmed and stirred to dissolve the powder and filter sterilised.

ii AAHLTU X100

The required masses of Adenine, Arginine, Histidine, Tryptophan, Uracil and Leucine powders were made up with SDW to a x100 solution. This was then gently warmed and stirred to dissolve the powder and filter sterilised and stored at 4°C.

iii YPD + AUL broth

Liquid media was made by first dissolving the YPD powder in the 20x AUL solution, while stirring. SDW was then added to the desired volume. The bottles were then autoclaved, and any selection drugs were added once the media was around 60-45°C or, comfortable hand holding temperature, and stored at room temperature. Any selection drugs were added once cool and the broth was stored at 4°C.

iv YPD + AUL plates

Plates were made as above, but with the addition of Bacto agar, the mixture was then stirred to dissolve the YPD powder and the Bacto agar and then autoclaved. Any required selection drugs were then added once the media was around 60-45C and the plates were poured and labelled, then stored at 4°C until required.

Dissection plates must be poured on a flat surface. Once autoclaved, leave to cool until comfortable to handle, then measure 25ml of YPD+ AUL agar into a falcon tube, pour into plate and leave to set.

v Yeast transformation

Method from [86], adapted by S Gray. The yeast strains required were woken up from the -80°C, streaked onto YPD+AUL plates and incubated at 30°C. Once large enough, single colonies were inoculated into 20ml YPD+AUL broth and grown overnight at 30°C and 250 rpm. Cells are then re-inoculated into fresh YPD+AUL, and incubated at 30°C for 3-5 hours, allowing the cells to re-enter and grow in the log growth phase. Once incubated, the cells are spun down for 5 minutes at 4,000 rpm. The supernatant is then removed, and the cells are re-suspended in 20ml of SDW to wash the cells. The cells are then spun again at 4,000 rpm at 5 minutes, the supernatant is removed, and they are resuspended in 1ml of 100mM Lithium Acetate and transferred into a 1.5 ml Eppendorf and spun down and re-suspended in 500μl of LiAc. 50μl aliquots were transferred into 1.5ml Eppendorfs for each transformation. (If more than 10 transformations were done, the cells were resuspended in larger volume to allow 50μl per transformation). Once transferred the cells were then spun down at 7,000rpm, to avoid rupturing the cells, for 30 seconds and the supernatant was removed, and the transformation mix and DNA was added. The tube was then vortexed to resuspend the cell pellet in the transformation mix and then incubated at 30 °C for 20 minutes and 42°C for another 20 minutes. The cells were then spun down at 7,000rpm and the supernatant was removed. The cells were resuspended in YPD+AUL and incubated for up to 1 hour at 30°C and 250rpm. The cells were then spun down and resuspended in 100μl of water and plated onto selection plates.

Table 4 Transformation mix composition. The ssDNA was derived from Salmon Sperm (Sigma D1626-250MG) which was dissolved in 1x TAE and sonicated until dissolved. This is then aliquoted and boiled at 95°C for 5 minutes and then chilled and stored at -20°C. Before each transformation the ssDNA is defrosted and re-boiled for 5 minutes at 95°C, before being added to the transformation mix. 10μl of transformation cassette DNA was used in the transformation mix.

Table 4 Make up of the transformation mix. 10μl of DNA was used.

	Volume (μl)
50% PEG 3350	240
1M LiAc	36
10mg/ml ssDNA	10
DNA	X
Water	74 – X
Total	360

vi gDNA preparation

Overnight cultures were centrifuged and resuspended in spheroplasting solution, and incubated, to digest the cell walls. Lysis buffer was then added and incubated to digest the cellular proteins. Phenol chloroform: Isoamyl Alcohol was then added, and the samples centrifuged to separate the DNA from the cellular debris. The DNA was removed and precipitated using 3M Sodium Acetate and 70% Ethanol. The DNA was then centrifuged and transferred to 100% Ethanol. RNAase A was then added to remove the RNA and the DNA was re-precipitated and suspended using 3M Sodium Acetate and 100% Ethanol. The DNA was then dissolved in 1x TE and stored at -20°C.

vii Mating Strains

Strains to be crossed were streaked out to form individual colonies and grown up for two days at 30°C. Equal amounts of a single colony of each strain was added to 10μl of SDW on parafilm and mixed by pipette. The mixture was then spotted onto a YPD AUL plate and left to dry. Once dry, the plates were incubated in the 30°C incubator overnight. If diploids were required, the mating patches were then streaked out for single colonies and grown up for two days, diploid colonies were then selected. If diploids are not required, the mating patch can then be added to Potassium Acetate (KAc) for sporulation.

viii Sporulation

Mating patches were added to 2ml KAc and mixed until single cells dispersed (no cell clumps). These were then left to sporulate in the 30°C at 250rpm.

ix Tetrad Dissection

Cultures were checked for sporulation by adding 10μl of sporulation culture to a slide and adding a coverslip. Observe under a microscope, if tetrads observed, the cultures are ready for dissection. Spin down 1ml of sporulation culture and re-suspend in 500ml of water. Then add 5μl Zymolyase and incubate at 37°C for 30 minutes. While incubating, dry out dissection plates. When the cells are ready, draw a line across the left of the dissection plate, this will help with orientation during the dissection. Place the plate on the dissection microscope and use the needle to select and separate the individual spores of the tetrads.

x Sporulation Efficiency

Diploids were streaked out from the -80°C onto YPD plates and grown up for two days at 30°C. These cells were then inoculated into YPD and grown overnight at 30°C. The cultures were then pelleted and washed with SDW, to remove any growth medium, and then resuspended in KAc to induce sporulation and incubated for 72 hours at 30°C. Sporulation efficiency was determined from 3 independent diploids of each strain and at least 300 cells were counted from each sample.

xi Meiotic time course

Diploids were streaked from -80°C and grown up at 30°C for two days. Single diploid colonies were selected and inoculated into 20ml of YPD and incubated in a shaking incubator at 250 rpm overnight at 30°C. 5ml of overnight YPD culture was added to 200ml of YPA, and incubated in a shaking incubator at 250 rpm and 30°C. This must be done 13.5 hours before transfer to sporulation media. KAc (200ml x n) and ddH2O (100ml x n) were placed in the 30°C incubator to warm overnight. The cultures were separated into 4 50ml Falcon tubes and were pelleted by spinning at 4,000 rpm for 5 minutes, and then washed once using 25ml of ddH2O per falcon tube, then spun down and resuspended in 25ml KAc. An extra 25mlof KAc was then added after. The 4 falcon tubes were then poured into a 1l conical flask and placed in the 30°C incubator at 250 rpm. T0 was then taken immediately after, 20ml of culture was taken every hour until T8. The flask was then left overnight and the remaining 20ml was the final timepoint. The samples taken were immediately prepared Dapi staining and Western Blot. For Dapi staining, 100ul of unprocessed culture was added to 500ul of 100% methanol and stored at either 4°C for short term storage or -20°C for longer storage. For Western blotting, the remaining culture was spun down and resuspended in 1ml ddH2O. Half of the sample was added to a 2ml tube, then spun down and the supernatant removed. This was stored at -20°C until required. The remaining half was added to a 1.5ml Eppendorf tube. This was also spun down, the supernatant removed and stored at -20°C.

xii SDS PAGE Gel

Glassware was cleaned using 70% Ethanol bath and the casting clips were placed on, ensuring that the bottom of both glass pieces was flush with the flat surface. Water was then poured into the casting mould to check for leaks. For Rad51 a 12.5% Acrylamide gel was used, due the S. cerevisiae Rad51 protein having a molecular mass of approximately 42kDa. The SDS-PAGE resolving gel mix was then made up, adding the APS and TEMED last, as they cause polymerization so the gel must be poured quickly once added. Once the gel was poured a layer of 100% Isopropanol was poured onto the top of the gel to allow gel to set flat. Once the resolving gel set, the Isopropanol was poured off and the gel was rinsed with ddH2O and dried. The stacking gel mix was then made up and poured on top of the resolving gel, the comb was then inserted and the gel was then left to set. The set gel was then placed in gel running container and submerged in buffer, the comb was then removed. The samples were then loaded and run at 100V until appropriate separation had occurred.

xiii Protein preparation for Western Blotting

10% TCA was made up as required and chilled on ice. The pelleted cell samples, in the 2ml tubes, reserved from the meiotic time course were defrosted, the supernatant was discarded and 300µl of 10% TCA was then added to the 2ml tube. One scoop, equal to the volume of TCA, of cold silica beads were then added to the tube and the tube was vortexed to break open the *S. cerevisiae* cells. The supernatant, containing the cellular contents, were transferred to a new 1.5ml Eppendorf tube and spun down for 1 minute at 13,000rpm. The supernatant was then removed and discarded. The pellets were then fully resuspended in 300µl of STE and boiled at 95°C for 5 minutes. The sample was then cooled and spun down for 1 minute at

13,000rpm. The supernatant was then transferred to a new tube and either stored at –20°C for later use or run on a gel. To run the sample on a gel, 950µl of 2x Loading Buffer was combined with 5% BME in a 1.5ml tube. Then equivalent volumes of 2x Loading buffer + 5% BME and protein supernatant was mixed and, the sample was loaded on a gel.

xiv Western Blot

The filter paper was equilibrated in 1x Transfer buffer. The PVDF membrane was then Activated in 100% Ethanol, by pouring Ethanol all over the membrane and then pouring it off. The membrane was the also equilibrated in 1x transfer buffer for at least 10 minutes. It is key to ensure the membrane is completely covered with no bubbles, which prevent equilibration. Once the gel was run the running container was then disassembled and the gel was then transferred to a UV gel imager and placed on a layer of water to prevent the gel from drying out. The ladder was then cut from the gel and reserved for re-assembly before transfer. The gel imager was used to UV activate the TCE and Image the gel, ensuring no bands are saturated. The transfer cassette was created by sandwiching: Filter paper, Membrane, Gel (with the ladder), and Filter paper. Bubbles between the gel and the membrane were removed by rolling a roller over blotting paper, whilst holding gel in place. The gel was then transferred using the BioRad Trans-Blot Turbo Transfer system and the appropriate program. The cassette was then disassembled and transferred for western blotting. The membrane was then blocked in 5ml EveryBlot blocking buffer for 5 minutes on shaker/rotator at room temperature. The primary antibody was then added in 5ml EveryBlot blocking buffer and incubated for 1 hour on a shaker/rotator at room temperature. The membrane was then washed 5 times every 5 minutes in 1x TBST. The secondary was then added, usually in a 1:5,000 ratio in 5ml EveryBlot blocking buffer. This was then incubated for 1 hour on a shaker/rotator at room temperature. The membrane was then washed 6 times every 5 minutes in 1x TBST. The membrane was then developed, using equal volumes of ECL (Pierce 32106) and incubated for 1 minute.

xv Growth Assay

Colonies were streaked out from the -80°C onto YPD plates and grown up for 2 days. Individual colonies were then selected from the plate and inoculated into 20ml YPD AUL media and grown up overnight at 30C and 250 rpm. The cultures were then re-inoculated into 20mL of fresh YPD to the starting OD_{600} of 0.05. The cultures were then incubated at 30°C and 250 rpm. OD_{600} readings were taken every 90 minutes using a spectrophotometer. The spectrophotometer was blanked between each reading using uninoculated YPD.

V Plasmids

PSG Number	Name	Selection Marker	Content	Comments
11	pFA6a-3HA-Kan	Kanamycin	6xHis-3xHA-ADH1 Terminator- kanMX-Ori-AmpR-AmpR promoter	
19	pBRA66	Ampicillin	hphMX6-p^{GAL1}-Cas9-3xFLAG-f1 Ori-gRNA scaffold-Ori-AmpR-AmpR promoter	
70	pFA6a-Floxed(HphMX)		pFA6a-HphMX (PSG10) with loxP sites flanking HYG marker (loxP-HYG-loxP)	Used as the backbone for both Rad51 replacement and altered expression of Rad51 plasmids
201	pADH1- dCas9-MXi1-GFP	Ampicillin	pADH1- dCas9-MXi1-GFP	
292	pADH1- TEV	Kanamycin	pYTK096-pADH1-3HA-p14-TEV	
304	pIME2- TEV	Kanamycin	pYTK096-pIME2-3HA-p14-TEV	
319	pYTK096	Kanamycin	URA3 5' Homology-sfGFP-P^{URA3}-URA3-URA3 3' Homology-KanR	Contains BsmBI site for insertion, resulting in loss of GFP and NotI sites flanking regions of URA3 upstream and downstream homology
	pCLB2-Rad51 (1)	Ampicillin	Rad51 upstream homology-P^{CLB2}-3xHA-RAD51-hphMX6-Rad51 Downstream homology-Ori- AmpR-AmpR promoter	

	pCLB2-Rad51 (2)	Ampicillin	Rad51 upstream homology-P^{CLB2}-3xHA-RAD51-hphMX6-Rad51 Downstream homology-Ori- AmpR-AmpR promoter	
	pDMC1-Rad51 (1)	Ampicillin	Rad51 upstream homology-P^{DMC1}-3xHA-RAD51-hphMX6-Rad51 Downstream homology-Ori- AmpR-AmpR promoter	
	Degron-Rad51 (1)	Ampicillin	Rad51 upstream homology-Degron-3xHA-RAD51-hphMX6-Rad51 Downstream homology-Ori- AmpR-AmpR promoter	
	Degron-Rad52 (2)	Ampicillin	Rad51 upstream homology-Degron-3xHA-RAD51-hphMX6-Rad51 Downstream homology-Ori- AmpR-AmpR promoter	
	RadA replacement (1)	Ampicillin	Rad51 upstream homology-HvRadA-hphMX6-Rad51 Downstream homology-Ori- AmpR-AmpR promoter	
	RadA replacement (2)	Ampicillin	Rad51 upstream homology-HvRadA-hphMX6-Rad51 Downstream homology-Ori- AmpR-AmpR promoter	
	mRad51 replacement (1)	Ampicillin	Rad51 upstream homology-mouseRAD51-hphMX6-Rad51 Downstream homology-Ori-AmpR-AmpR promoter	
	mRad51 replacement (2)	Ampicillin	Rad51 upstream homology-mouseRAD51-hphMX6-Rad51 Downstream homology-Ori-AmpR-AmpR promoter	
	RecA replacement (1)	Ampicillin	Rad51 upstream homology-EcRecA-hphMX6-Rad51 Downstream homology-Ori- AmpR-AmpR promoter	

	RecA replacement (55.1)	Ampicillin	Rad51 upstream homology-EcRecA-hphMX6-Rad51 Downstream homology-Ori- AmpR-AmpR promoter	
	Tagged Rad51 (1)	Ampicillin	Rad51 upstream homology-6xHis-3xHA-RAD51-hphMX6-Rad51 Downstream homology-Ori- AmpR-AmpR promoter	
	Tagged Rad51 (2)	Ampicillin	Rad51 upstream homology-6xHis-3xHA-RAD51-hphMX6-Rad51 Downstream homology-Ori- AmpR-AmpR promoter	
	pADH1- Cas9	Ampicillin	hphMX6-pADH1-Cas9-GFP-gRNA scaffold-Ori- AmpR	cRNA inserted by ligation following Bpl1 digest, resulting in loss of GFP
	ADE2 cRNA1	Ampicillin	hphMX6-pADH1-Cas9-GFP-ADE2 cRNA1-Ori-AmpR	Transformation cassette generated by NotI digest
	ADE2 cRNA1	Ampicillin	hphMX6-pADH1-Cas9-GFP-ADE2 cRNA1-Ori-AmpR	
	ADE2 cRNA2	Ampicillin	hphMX6-pADH1-Cas9-GFP-ADE2 cRNA2-Ori-AmpR	
	ADE2 cRNA2	Ampicillin	hphMX6-pADH1-Cas9-GFP-ADE2 cRNA2-Ori-AmpR	
	ADE2 cRNA3	Ampicillin	hphMX6-pADH1-Cas9-GFP-ADE2 cRNA3-Ori-AmpR	
	ADE2 cRNA3	Ampicillin	hphMX6-pADH1-Cas9-GFP-ADE2 cRNA3-Ori-AmpR	

VI Primers

Primer Number	Primer Name	Primer Sequence	Comments
657	LEU2- Final Reverse	CCTCCATTTCGTTCACTTTGGG	Used to amplify the 66a6 bp fragment used for the Cas9 cleavage assay
658	LEU2 +998	ACCCACTCTTGCTACTACCTCT	
659	LEU2 +1743	ATTGCCGATGAAGATGCCGA	
660	LEU2 +1957	CGCCAACTTTTTCTGCGACA	
661	LEU2 +2774	AGGACGCTCCAGAGGAATCT	
662	LEU2 +3251	TTCCACAACAACACGCTCCT	
663	LEU2 + 4145	GTGGGCTAAAGAACGCGAAC	
664	LEU2+4352	ACTGCTTTTGTTTGGCTTGCT	
665	LEU2+4871	AAGAACGACAATGGAACCGC	
666	LEU2 +5038	ACACCAGCAAACATTCCAGC	
667	LEU2 +5715	ACAGTCCCTACGTCAAACCC	
668	LEU2 + 6521	TGGACAGCACGAATCCTTCA	
669	LEU2 + 7346	TGAAGGATTCGTGCTGTCCA	
702	pCLB2_fwd	tcgtcatatgaccctgttcttgacggtc	
703	pCLB2_rev	gaacttgagaagcgtaatctggaacgtc	
704	RAD51_fwd	agattacgcttctcaagttcaagaacaac	
705	RAD51_rev	cgtcgacctgcagcgtacgactactcgtcttcttctctg	
706	RAD51(-pDMC1)_fwd	agattacgcttctcaagttcaagaacaac	
707	RAD51(-pDMC1)_rev	gtgtgatccccatatgacgataacaaattagtag	

708	Degron_fwd	tcgtcatatggggatcacacatggtatg	
709	Degron_rev	gaacttgagaagcgtaatctggaacgtc	
710	PCR (-pCLB2)_fwd	ttgaacaaatatgtccttaattaacatcttttac	
711	PCR (-pCLB2)_rev	ttacgattaacatatgacgataacaaattagtag	
712	pDMC1_fwd	tcgtcatatgttaatcgtaaggaaaaataaaataatagtg	
713	pDMC1_rev	ttaaggacatatttgttcaaatgctttcc	
718	FWD primer RAD51 amplification	tagtcacgtcggtagccaga	
719	REV primer RAD51 amplification	ttcagggtatgcaccaggag	
720	ADE2 crRNA1_F	AATTGTAGAGACTATCCACAgtttt	
721	ADE2 crRNA1_R	TGTGGATAGTCTCTACAATTgatca	
722	ADE2 crRNA2_F	CTGCTCATAGAACTCCACATgtttt	
723	ADE2 crRNA2_R	ATGTGGAGTTCTATGAGCAGgatca	
724	ADE2 crRNA3_F	AATGTTCTATTTAGAAACAGgtttt	
725	ADE2 crRNA3_R	CTGTTTCTAAATAGAACATTgatca	
726	ADE2 crRNA4_F	GTATGGCGGAATGTGAACAAgtttt	
727	ADE2 crRNA4_R	TTGTTCACATTCCGCCATACgatca	
728	RecA FWD	taatttgttatcgtcatatgATGGCTATCGACGAAAAC	
729	RecA REV	cgtcgacctgcagcgtacgaTTAAAAATCTTCGTTAGTTTCTG	
730	GibsonDegron (-Deg/ RAD)_fwd RecA	cgtcgacctgcagcgtacgaTTAAAAATCTTCGTTAGTTTCTG	

731	GibsonDegron (-Deg/ RAD)_rev RecA	CATATGACGATAACAAATTAGTAGGCCTTTAACAAATAAC	
732	GibsonDegron (-Deg/ RAD)_fwd Rad51	TCGTACGCTGCAGGTCGAC	
733	GibsonDegron (-Deg/ RAD)_rev Rad51	CATATGACGATAACAAATTAGTAGGCCTTTAACAAATAAC	
734	MouseRAD51_fwd	taatttgttatcgtcatatgATGGCTATGCAAATGCAGC	
735	MouseRAD51_rev	cgtcgacctgcagcgtacgaTCAGTCTTTGGCATCGCC	
768	PromoterCas9_fwd	catggataacattacccctggggcgacagtcacatcatgc	
769	PromoterCas9_rev	acaaaaggattctagatgcggcgggcagtgagcgcaac	
770	FWD pDMC1 screen	TTCCCTGGAAGCGCCATTTT	
771	REV pDMC1 screen	GCGAACACACATTCAGCCTC	
789	GibsonDegron(-Deg/ RAD)_fwd RadA	gcccgagtaaTCGTACGCTGCAGGTCGAC	
790	GibsonDegron(-Deg/ RAD)_rev RadA	cttctgccatCATATGACGATAACAAATTAGTAGGCCTTTAACAAATAAC	
791	RadA(Haloferax)_fwd	tcgtcatatgATGGCAGAAGACGACCTC	
792	RadA(Haloferax)_rev	cagcgtacgaTTACTCGGGCTTGAGACC	
793	Gibson Transformation FWD	ACCTCTGACACATGCAGCTC	
794	Gibson Transformation REV	ATAGGGAGACCGGCAGATCC	
795	Cas9/YTK Integration FWD	gggggctgatgagacgtggatggcggcgttagtatc	
796	Cas9/YTK Integration REV	ggggtgcttgagacgcgagtcagtgagcgaggaag	
937	Cas9 Nsi1_fwd	acaatcaactATGGATAAAAAGTATAGTATTGGTTTAG	
938	Cas9 Nsi1_rev	ctacagcattcaaatatgcaTCATGAGCATGATGATAATTATTAATTTC	
1014	RadA 6xHis 3xHA_fwd	taatttgttatcgtcatatgCATCATCATCATCATCATATCTTTTAC	
1015	RadA 6xHis 3xHA_rev	tcgaggtcgtcttctgccatTCACTGAGCAGCGTAATC	

1016	RadA tagged_fwd	ATGGCAGAAGACGACCTC	
1017	RadA tagged _rev	CATATGACGATAACAAATTAGTAGGC	
1018	RecA 6xHis 3xHA_fwd	taatttgttatcgtcatatgCATCATCATCATCATCATATCTTTTAC	
1019	RecA6xHis 3xHA_rev	ttgttttcgtcgatagccatTCACTGAGCAGCGTAATC	
1020	RecA tagged _fwd	ATGGCTATCGACGAAAAC	
1021	RecA tagged _rev	CATATGACGATAACAAATTAGTAG	
1022	mRad516xHis 3xHA_fwd	taatttgttatcgtcatatgCATCATCATCATCATCATATCTTTTAC	
1023	mRad516xHis 3xHA_rev	agctgcatttgcatagccatTCACTGAGCAGCGTAATC	
1024	mRad51 tagged _fwd	ATGGCTATGCAAATGCAG	
1025	mRad51 tagged _rev	CATATGACGATAACAAATTAGTAG	
1026	wt Rad51_fwd	TCTCAAGTTCAAGAACAAC	
1027	wt Rad51_rev	CATATGACGATAACAAATTAGTAG	
1028	6xHis 3xHA_fwd	taatttgttatcgtcatatgCATCATCATCATCATCATATCTTTTAC	
1029	6xHis 3xHA_rev	tgttgttcttgaacttgagaTCACTGAGCAGCGTAATC	

VII S. cerevisiae strains

YSG Number	Mating type	Selection marker	Genotype	Comments
1	a	ADE	ade8	Used to determine mating type
2	p	ADE	ade8	
3	a		ho::LYS2, lys2, ura3, arg4-nsp, leu2::hisG, his4X::LEU2, nuc1::LEU2	
4	p		ho::LYS2, lys2, ura3, arg4-nsp, leu2::hisG, his4X::LEU2, nuc1::LEU2	
5	a/p		ho::LYS2/', lys2/', ura3/', arg4-nsp/', leu2::hisG/', his4X::LEU2/', nuc1::LEU2/'	Diploid of 3 and 4

13	a	URA, Hygromycin	ho::LYS2, lys2, ura3, arg4-nsp, leu2::hisG, his4X::LEU2, nuc1::LEU2, rad51Δ::hisG-URA3-hisG, dmc1Δ::HphMX,	*rad51 dmc1*
	p	URA, Hygromycin	ho::LYS2, lys2, ura3, arg4-nsp, leu2::hisG, his4X::LEU2, nuc1::LEU2, rad51Δ::hisG-URA3-hisG, dmc1Δ::HphMX,	
15	p	Kanamycin	ho::LYS2, lys2, ura3, arg4-nsp, leu2::hisG, his4X::LEU2, nuc1::LEU2, p^{CLB2}-3HA-MEC1::KanMX	
	a	Hygromycin	ho::LYS2, lys2, ura3, arg4-nsp, leu2::hisG, his4X::LEU2, nuc1::LEU2, P^{CLB2}::3xHA::RAD51::HphMX	RAD51 under the control of the CLB2 promoter
	p	Hygromycin	ho::LYS2, lys2, ura3, arg4-nsp, leu2::hisG, his4X::LEU2, nuc1::LEU2, p^{CLB2}::3xHA::RAD51::HphMX	
	a/p	Hygromycin	ho::LYS2/', lys2/', ura3/', arg4-nsp/', leu2::hisG/', his4X::LEU2/', nuc1::LEU2/', p^{CLB2}::3xHA::RAD51::HphMX/'	Diploids of RAD51 under the CLB2 promoter
	a/p	Hygromycin	ho::LYS2/', lys2/', ura3/', arg4-nsp/', leu2::hisG/', his4X::LEU2/', nuc1::LEU2/', p^{CLB2}::3xHA::RAD51::HphMX/'	
	a/p	Hygromycin	ho::LYS2/', lys2/', ura3/', arg4-nsp/', leu2::hisG/', his4X::LEU2/', nuc1::LEU2/', p^{CLB2}::3xHA::RAD51::HphMX/'	
	a	Hygromycin	ho::LYS2, lys2, ura3, arg4-nsp, leu2::hisG, his4X::LEU2, nuc1::LEU2, p^{DMC1}::3xHA::RAD51::HphMX	RAD51 under the control of the DMC1 promoter
	p	Hygromycin	ho::LYS2, lys2, ura3, arg4-nsp, leu2::hisG, his4X::LEU2, nuc1::LEU2, p^{DMC1}::3xHA::RAD51::HphMX	
	a/p	Hygromycin	ho::LYS2/', lys2/', ura3/', arg4-nsp/', leu2::hisG/', his4X::LEU2/', nuc1::LEU2/', p^{DMC1}::3xHA::RAD51::HphMX/'	Diploids of RAD51 under the DMC1 promoter
	a/p	Hygromycin	ho::LYS2/', lys2/', ura3/', arg4-nsp/', leu2::hisG/', his4X::LEU2/', nuc1::LEU2/', p^{DMC1}::3xHA::RAD51::HphMX/'	
	a/p	Hygromycin	ho::LYS2/', lys2/', ura3/', arg4-nsp/', leu2::hisG/', his4X::LEU2/', nuc1::LEU2/', p^{DMC1}::3xHA::RAD51::HphMX/'	
	a	Hygromycin	ho::LYS2, lys2, ura3, arg4-nsp, leu2::hisG, his4X::LEU2, nuc1::LEU2, P^{RAD51}::Degron::3xHA::RAD51::HphMX	RAD51 with a bidirectional Degron at it's N terminus
	p	Hygromycin	ho::LYS2, lys2, ura3, arg4-nsp, leu2::hisG, his4X::LEU2, nuc1::LEU2, P^{RAD51}::Degron::3xHA::RAD51::HphMX	

	a/p	Hygromycin	ho::LYS2/', lys2/', ura3/', arg4-nsp/', leu2::hisG/', his4X::LEU2/', nuc1::LEU2/', P^{RAD51}::Degron::3xHA::RAD51::HphMX/'	Diploids of RAD51 with a bidirectional Degron at it's N terminus
	a/p	Hygromycin	ho::LYS2/', lys2/', ura3/', arg4-nsp/', leu2::hisG/', his4X::LEU2/', nuc1::LEU2/', P^{RAD51}::Degron::3xHA::RAD51::HphMX/'	
	a/p	Hygromycin	ho::LYS2/', lys2/', ura3/', arg4-nsp/', leu2::hisG/', his4X::LEU2/', nuc1::LEU2/', P^{RAD51}::Degron::3xHA::RAD51::HphMX/'	
	a	ADE	ho::LYS2, lys2, ura3:: P^{IME2}::3XHA::TEV::URA3, arg4-nsp, leu2::hisG, his4X::LEU2, nuc1::LEU1	TEV protease under the IME2 promoter
	p	ADE	ho::LYS2, lys2, ura3:: P^{IME2}::3XHA::TEV::URA3, arg4-nsp, leu2::hisG, his4X::LEU2, nuc1::LEU2	
	a	ADE	ho::LYS2, lys2, ura3:: P^{ADH1}::3XHA::TEV::URA3, arg4-nsp, leu2::hisG, his4X::LEU2, nuc1::LEU2	TEV protease under the ADH1 promoter
	p	ADE	ho::LYS2, lys2, ura3:: P^{ADH1}::3XHA::TEV::URA3, arg4-nsp, leu2::hisG, his4X::LEU2, nuc1::LEU3	
	p	ADE, Hygromycin	ho::LYS2, lys2, ura3:: P^{IME2}::3XHA::TEV::URA3, arg4-nsp, leu2::hisG, his4X::LEU2, nuc1::LEU2, P^{RAD51}::Degron::3xHA::RAD51::HphMX	RAD51 with a bidirectional Degron at it's N terminus and the TEV protease under the IME2 promoter
	a	ADE, Hygromycin	ho::LYS2, lys2, ura3:: P^{ADH1}::3XHA::TEV::URA3, arg4-nsp, leu2::hisG, his4X::LEU2, nuc1::LEU2, P^{RAD51}::Degron::3xHA::RAD51::HphMX	RAD51 with a bidirectional Degron at it's N terminus and the TEV
	p	ADE, Hygromycin	ho::LYS2, lys2, ura3:: P^{ADH1}::3XHA::TEV::URA3, arg4-nsp, leu2::hisG, his4X::LEU2, nuc1::LEU2, P^{RAD51}::Degron::3xHA::RAD51::HphMX	

				protease under the ADH1 promoter
	a	URA	ho::LYS2, lys2, ura3, arg4-nsp, leu2::hisG, his4X::LEU2, nuc1::LEU2, rad51Δ::hisG-URA3-hisG,	*rad51*
	p	URA	ho::LYS2, lys2, ura3, arg4-nsp, leu2::hisG, his4X::LEU2, nuc1::LEU2, rad51Δ::hisG-URA3-hisG,	
	a		ho::LYS2, lys2, ura3, arg4-nsp, leu2::hisG, his4X::LEU2, nuc1::LEU2, P^{RAD51}::3xHA::RAD51::HphMX	Tagged RAD51
	p		ho::LYS2, lys2, ura3, arg4-nsp, leu2::hisG, his4X::LEU2, nuc1::LEU2, P^{RAD51}::3xHA::RAD51::HphMX	
	a/p		ho::LYS2/', lys2/', ura3/', arg4-nsp/', leu2::hisG/', his4X::LEU2/', nuc1::LEU2/', P^{RAD51}::3xHA::RAD51::HphMX/'	Tagged RAD51 Diploid
	a/p		ho::LYS2/', lys2/', ura3/', arg4-nsp/', leu2::hisG/', his4X::LEU2/', nuc1::LEU2/', P^{RAD51}::3xHA::RAD51::HphMX/'	

VIII E. coli strains

Strain	Genotype	Comments
DH5α	*fhuA2::IS2* Δ(*mmuP-mhpD*)*169* Δ*phoA8 glnX44* ϕ80d[Δ*lacZ58*(*M15*)] *rfbD1 gyrA96 luxS11 recA1 endA1 rph*^{WT} *thiE1 hsdR17*	NEB Chemically competent cells[87]

Chapter 3 Results

I Detection of Ectopic Mutants

During Meiosis, recombination between non-allelic loci, or ectopic recombination, can result in the formation of either acentric or dicentric chromosomes. Previous work from the Gray lab, using a *S. cerevisiae* strain which contains the *HIS4::LEU2* and *leu2::hisG* hotspots, have identified several common ectopic chromosomes generated during meiosis (Figure 1).

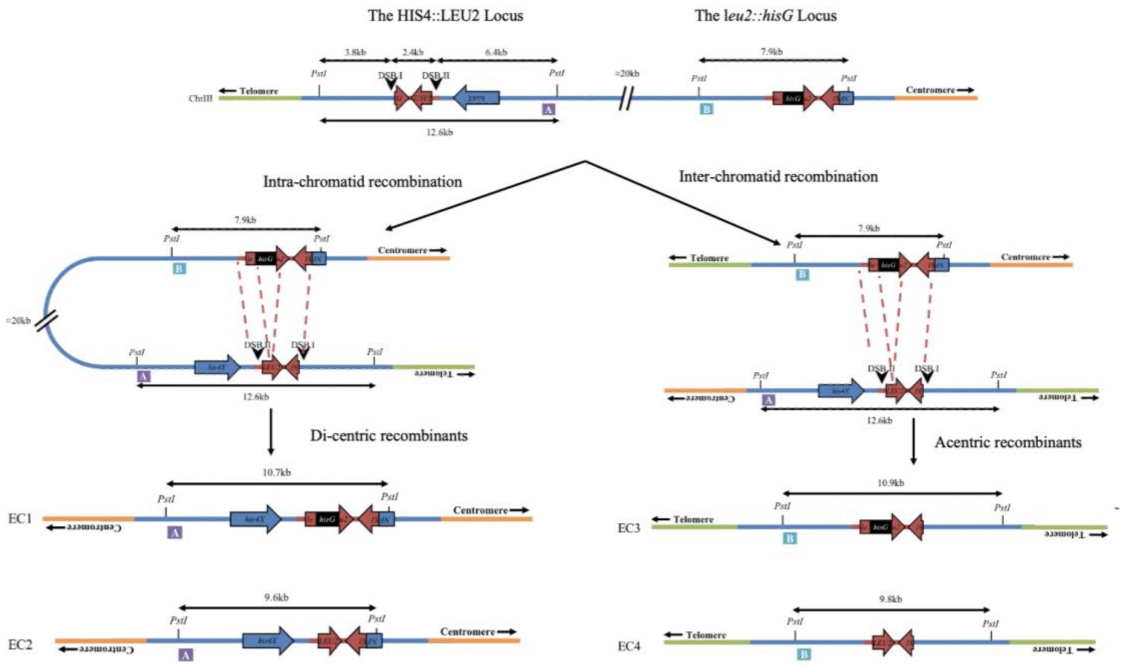

Figure 1 Ectopic recombination between the *HIS4::LEU2* and *leu2::hisG* loci. Both the *HIS4::LEU2* and *leu2::hisG* loci are recombinational hotspots. Recombination between these hotspots can produce both Acentric and Di-centric molecules, depending on the recombination partner. These can then be probed for by Southern blotting. Adapted from unpublished data from S. Gray.

However, alongside the expected chromosomal rearrangements, novel ectopic recombinants were also seen (Figure 2). There are two key issues preventing the identification and sequencing of these novel recombinants.

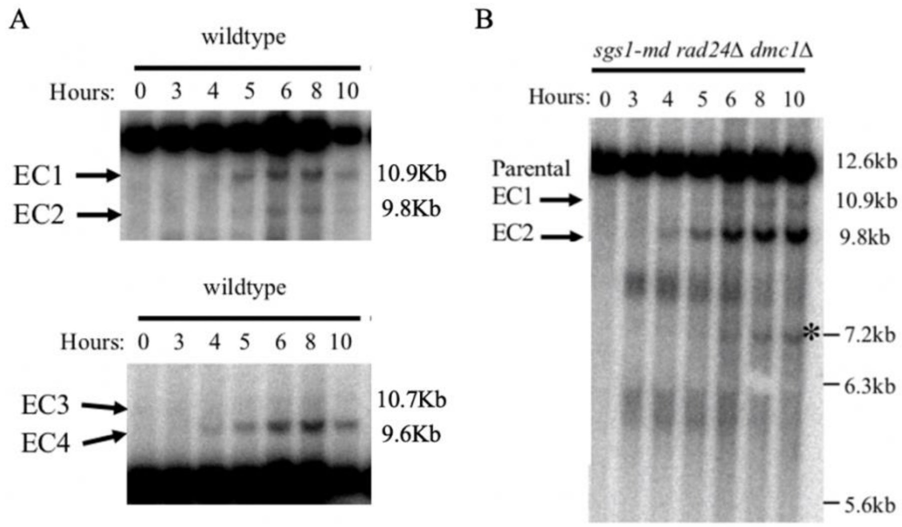

Figure 2 Ectopic recombinants produced from recombination events between the *HIS4::LEU2* and *leu2::hisG* loci, detected by Southern blotting after gDNA preparations were digested by PstI. A) Expected ectopic recombinants present in a wildtype background. EC1 and EC2 are dicentric recombinant chromosomes, generated by Intra-chromatid ectopic recombination. EC3 and EC4 are acentric recombinant chromosomes generated by Interchromatid ectopic recombination. B) A novel recombinant was detected at 7.2 Kb in the *sgs1-md rad24Δ dmc1Δ* mutant background. Figure adapted from unpublished data from S. Gray.

Firstly, when attempting to identify the novel recombinant in Figure 2, only one recombination partner is known, as it must be complementary to the probe, as it is detectable by Southern blot. The second problem is that novel recombinants may form at a frequency that it too low to be detectable by Southern blot.

In order to both identify the unknown partner locus of the novel recombinant appearing on the Southern blot and to identify previously undetected novel recombinants, a Cas9 sequencing tool based on Fusion Detection from Gene Enrichment (FUDGE)[88] was modified to target the *HIS4::LEU2* locus. FUDGE was originally developed to identify Fusion genes, as the name suggests, however the principle can also be applied to recombinant molecules. Using gRNAs to target Cas9 to catalyse DSBs close to the recombination hotspot, then annealing sequencing adaptors and sequencing across the break point (Figure 3).

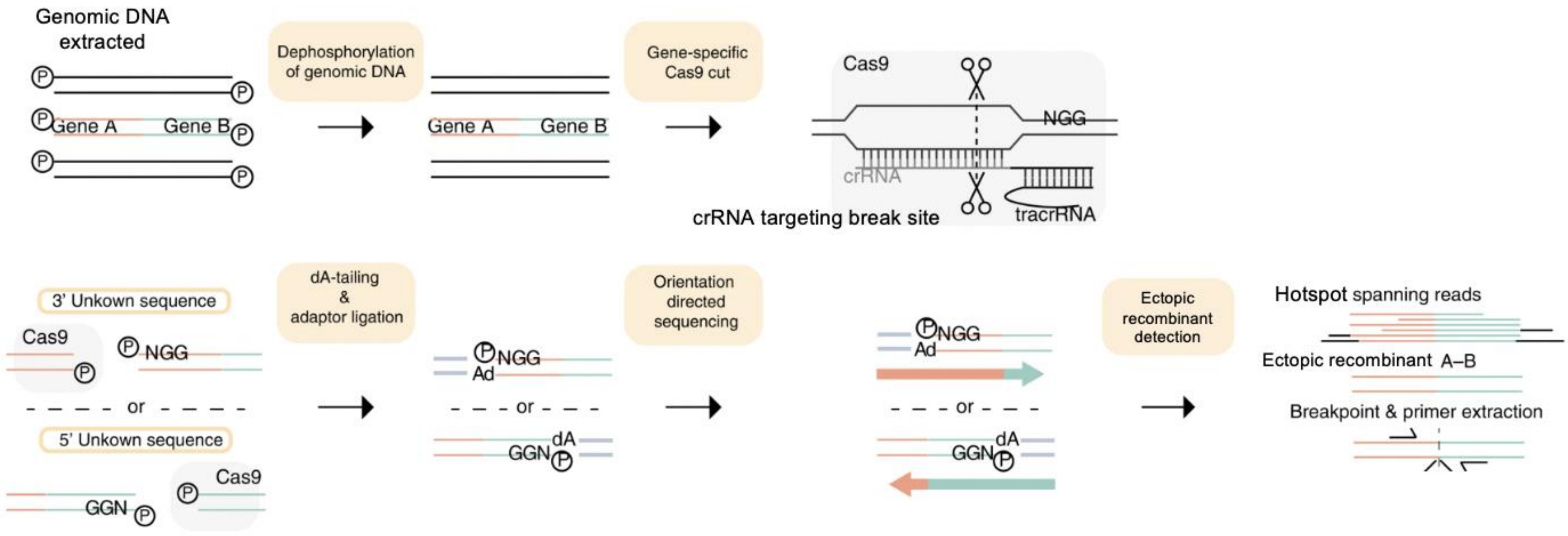

Figure 3 Workflow adapting FUDGE to target and sequence ectopic recombinants at known crossover hotspots. Genomic DNA is extracted and Cas9 used *in vitro* to induce DSBs within hotspot. Sequencing adaptors are then ligated onto the break site and sequencing is undertaken to identify the other side of the ectopic recombinant. Figure adapted from [88]

i Designing and Testing Cas9 strategy

(1) Amplification of the test fragment

To test the cleavage efficiency of the Cas9 assay, primers were designed to amplify a 6Kb fragment of Chromosome 3, which could be used as a cleavage substrate. The cleavage could then be assayed by running the cleavage reaction on an Agarose gel and quantitating the cleavage products relative to the ladder. Internal primers were also designed, in the instance that the 6Kb fragment could not be amplified due to its size. Primers were designed using the NCBI primer designer, which gave information on possible secondary structures and annealing temperatures. The primers were then validated using BLAST, to ensure the sequence did not occur elsewhere in the genome. crRNAs to cut within the fragment were also designed using CHOPCHOP[89], which gave information on possible off-target effects[89]. Using the crRNA binding sites, the expected fragments for each cleavage sites could be calculated. The Chromosome 3 fragment was amplified using a wildtype (YSG3) genomic DNA (gDNA) preparation, a fragment of 6646bp was expected but was unsuccessful. The PCR was re-attempted at a lower annealing temperature but was also unsuccessful. Therefore, to remove the possibility of sheared DNA the PCR amplification was reattempted with several gDNA preparations from different *S. cerevisiae* strains, and the primers were also re-diluted. This amplification was successful, Figure 4. The gDNA prep used as a template in reaction 3 was taken forward and re-amplified in octuplet, Figure 4, to provide enough DNA substrate for gel quantification of the Cas9 cleavage reaction.

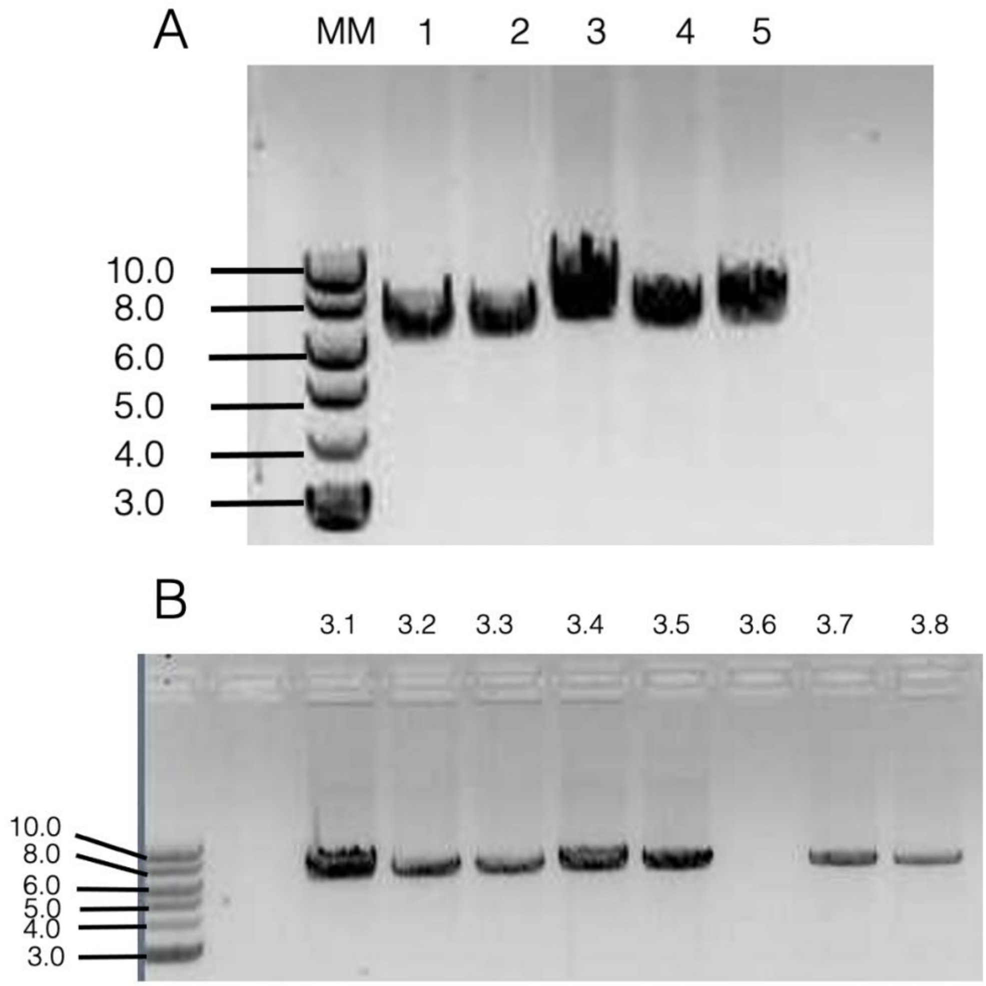

Figure 4 A Reattempting amplification of the 6646bp fragment of Chromosome 3 required for Cas9/gRNA activity assay using five different *S. cerevisiae* gDNA preps. DNA used in each reaction; 1= YSG3A/10. 2= YSG3A/100. 3= YSG3B/10. 4= YSG15/10. 5= YSG3S/10. Products of the PCR amplification separated by gel electrophoresis. MM= molecular marker (NEB 1kb ladder). **B Amplification of Reaction 3 in octuplet to generate the 6646bp fragment to assay gRNA specificity and Cas9 activity.** All reactions except 3.6 were successful. The samples, excluding 3.6 were pooled.

The reactions, excluding 3.6, were then pooled and cleaned up. The sample was diluted to several concentrations, and run on an agarose gel. The brightness of the bands was quantitated using Fiji to determine the threshold of DNA concentrations for cleavage quantification using the gel image from the Cas9 cleavage assay. To ensure accurate quantification, care was taken to avoid saturation of the gel image (Figure 5).

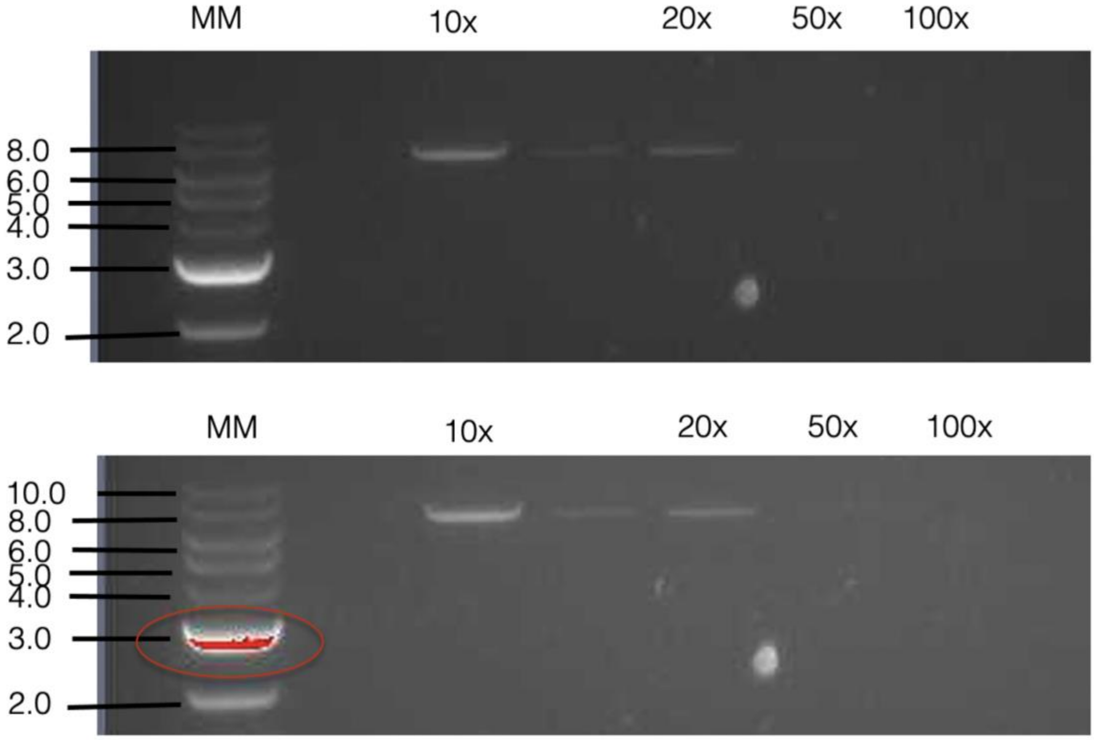

Figure 5 Several dilutions (stated in figure) of the 6kb fragment were run on an agarose gel for quantification. Top: Unsaturated gel allows for quantification of the bands using Fiji. Bottom: Red pixels identify saturated areas of the band. Exposure decreased and gel re-imaged. Bands expected: 6646 bp

The PCR was then re-attempted in quadruplicate generate enough substrate to perform the Cas9 cleavage assay, cleaned up and pooled (Figure 6).

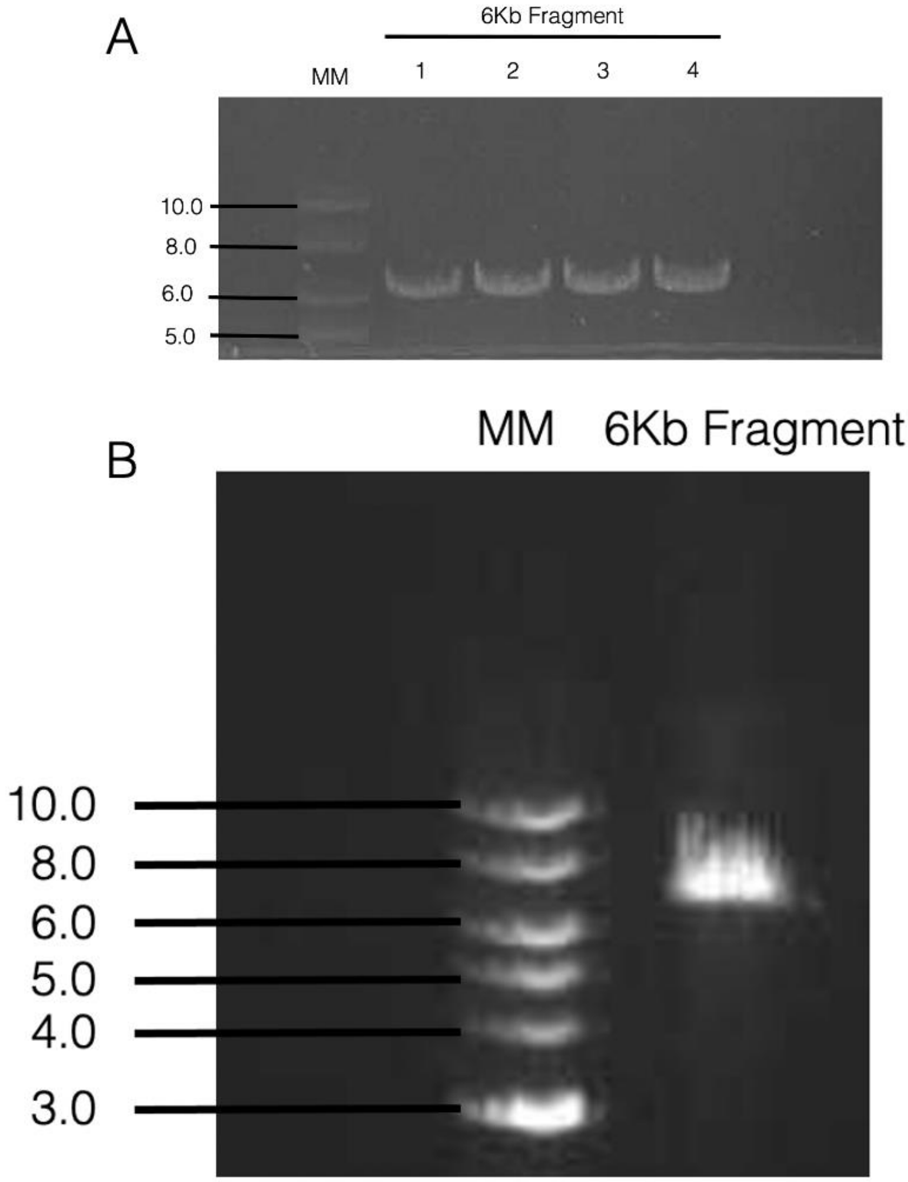

Figure 6 A Re-amplification of 6kb fragment of Chromosome 3 in quadruplicate. Fragments expected: 6646bp. The samples were then pooled to generate adequate target DNA for the cleavage assay. Fragment size: 6646bp **B Determining the DNA can be seen clearly on the gel to allow cleavage quantification.** 5μl of the sample was loaded onto the gel, as this was the volume that would be added to the Cas9 cleavage reaction. Band expected 6646 bp.

(2) Cas9 Cleavage assay

The gRNA was generated by annealing the individual crRNAs, which targeted different break sites, with the common tracrRNA. Once annealed, the gRNA was incubated with the Cas9 enzyme allow the formation of the Cas9/ gRNA complex. The substrate DNA was then added. The cleavage reaction was unsuccessful (Figure 7).

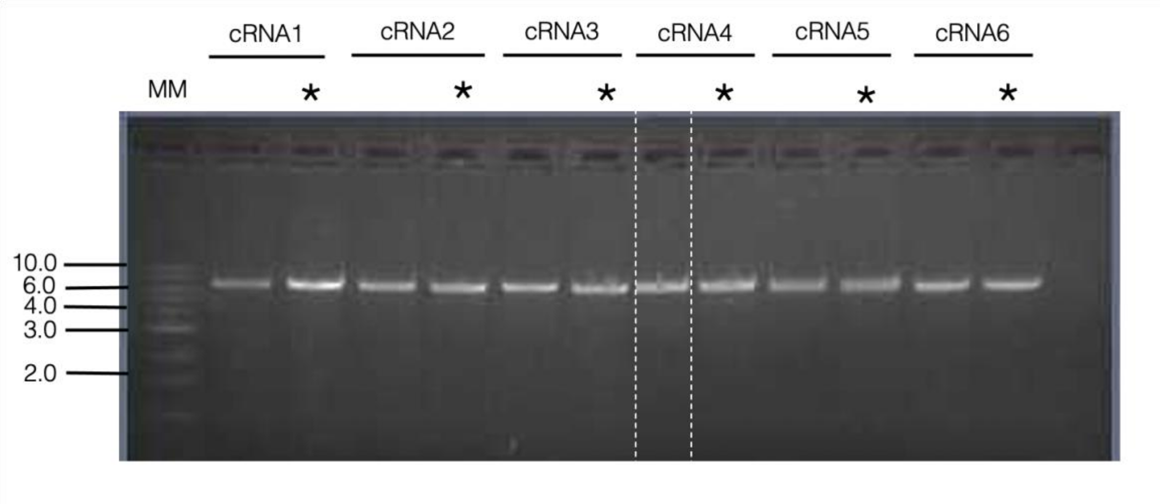

Figure 7 Gel demonstrating fragments before and after Cas9 cleavage reaction. * Indicates lanes loaded with mixture post 1 hour incubation at 37°C. Dashed lines indicate exclusion of poorly loaded lanes. The cleavage reaction was unsuccessful. Un-cleaved fragment: 6646 bp.

To reattempt the cleavage assay, the gRNAs were re-made, in this instance cooling the mixture inside the heat block to allow more gradual cooling and therefore, better annealing. The gRNAs were then run on a 2% Agarose gel, to determine whether annealing had been successful. It appeared that only one of the gRNAs from the re-annealed group was successful (Figure 8), however this cannot be stated definitively, as the ladder used was not adequate when determining the size of smaller DNA fragments. It was expected that the correctly annealed gRNAs would migrate at around 100bp[90, 91], however, the smallest fragment of the ladder used was 500bp.

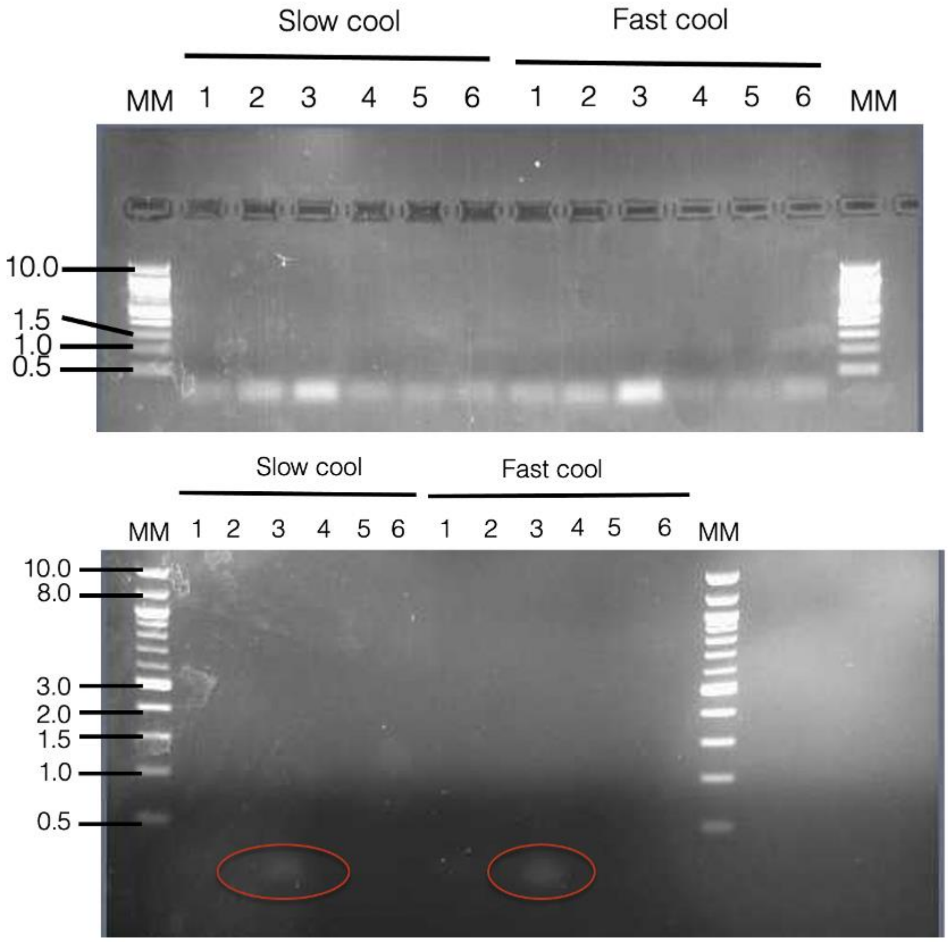

Figure 8 gRNAs run on a 2% agarose gel to determine whether they have annealed together. Top: gel run for 20 mins. Bottom: gel run for 40 mins. It appears the only gRNA annealed in both the fast and slow cool groups was gRNA 3.

Another 6Kb fragment was generated by PCR (Figure 9) and diluted. However, neither the dilutions nor the undiluted sample could clearly be seen on the gel. The PCR clean-up was then nanodropped to determine the DNA concentration, and it was found to be low. The low concentration of substrate DNA along with difficulty annealing the gRNAs led to the project being abandoned due to time constraints, to focus on the other projects.

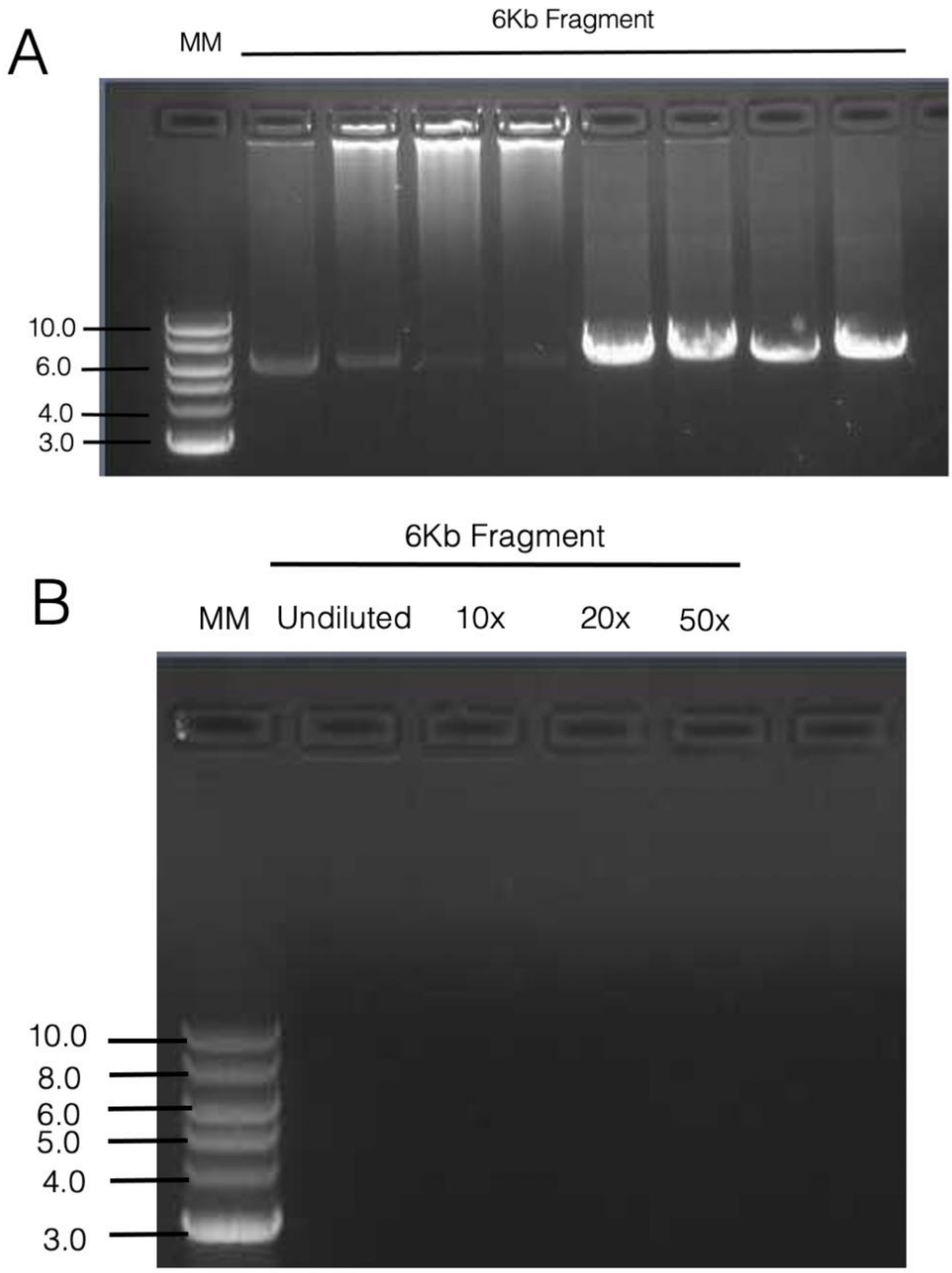

Figure 9 A Re-amplification of 6Kb fragment. The four successful reactions were pooled and cleaned up to provide substrate DNA for the cleavage assay. Fragment expected: 6646 bp. **B Dilutions run to allow quantification in preparation for the cleavage assay.** 10μl of several dilutions of the 6Kb fragment was loaded onto the gel to determine which dilution could be seen clearly to enable cleavage quantification, however none of the dilutions can be seen. Fragment expected: 6646 bp

II Altering Rad51 Expression

S. cerevisiae has been established as a model system for studying many cellular processes, due to its similarity to higher Eukaryotes and the ease of culturing. As a result, hundreds of reporter strains have been established, to study a range of biomolecular processes, from crossover formation to cellular aging. Alongside these tools, the Yeast Deletion, or YKO collection has also been developed. The YKO represented the only complete deletion collection for any organism and contains strains with a different ORF in the *S. cerevisiae* genome replaced by a Kanamycin (KanMX1) cassette[92]. However, the issue with this collection, is while it is a useful tool for *S. cerevisiae* genetic manipulation, if a specific reporter strain is required for the experiment, individual gene deletion cassettes must be amplified and transformed into the desired reporter strain from the YKO. This is a time-consuming process, and may require several rounds of transformations and screening, if several genes are to be altered.

This aim of this project was to create a selection of strains which could be used to generate deletion mutants in any desired reporter strain through the introduction of DSBs by Cas9, using gRNAs targeted to the desired genes. However, as discussed above, due to HR being the preferred DSB repair in *S. cerevisiae*, and the low error rate of break repair by HR, in order to generate deleterious mutations, it would be preferable if the breaks generated by Cas9 were repaired by NHEJ. To force the cell to repair DSBs induced by Cas9 by NHEJ, as opposed to HR, the expression pattern of *RAD51* was altered. Theoretically, if the recombinase was not present, the cell would not be able to repair by HR, as the key step of HR, strand invasion, could not be catalysed. However, as the Gray lab are interested in meiosis, it was vital that Rad51 was still present during this process, as *rad51* mutants demonstrate decreased spore viability. Therefore, *RAD51* was placed under the control of P^{DMC1}, as this would ensure the recombinase was present for meiosis. Another method of altering *RAD51* expression, which could be used when not focussed on meiosis, is placing *RAD51* under the control of the *CLB2* promoter, which is required for the G2/M transition. This ensures Rad51 is present for mitosis, so theoretically, the cells should not have an increased sensitivity to DNA damaging agents and should not be prone to chromosomal instability, while still having periods in the cell cycle where HR is impaired, and therefore mutations via DSBs generated by Cas9 can be induced.

Another system used to alter the expression of *RAD51* was the bidirectional degron system. A degron is a destabilising sequence of amino acids that can be inserted into a genetic sequence and, when exposed, induces degradation of the protein it is within. When one of 12 destabilising amino acids is exposed at the N terminus of the protein, it signals for the addition of poly-ubiquitin chains and proteasomal degradation[93]. A bidirectional degron was selected, which contains a dormant N terminal degron, used in the Tobacco Etch Virus (TEV) protease induced protein instability (TIPI) system[94], and a C- terminal degron from mouse Ornithine

Decarboxylase, which induces proteolysis through a Ubiquitin independent pathway. Both the N and C terminal degrons have been found to be effective in *S. cerevisiae* [95]. This bidirectional degron, uses the N terminal Degron as a ‘cap’ keeping the C terminal degron inactive until cleavage by the TEV protease exposes both degrons, triggering degradation of the protein, whether the degron is inserted internally or at either the N or C terminus of the protein.

i Generating the P^{CLB2}*-RAD51* plasmid

Gibson assembly was used to create plasmids to alter the expression of Rad51 by placing the *RAD51* gene under two different promoters: P^{CLB2}, to ensure Rad51 was present during mitosis but not meiosis, and P^{DMC1}, to ensure Rad51 was present during meiosis, and a bi-directional Degron. In order to replace the sequence at the *RAD51* locus, 1kb of both the upstream and downstream sequences of the *RAD51* gene were inserted into the plasmid. Once the transformation cassette was generated from the plasmid and transformed into *S. cerevisiae*, the DNA ends and the regions of homology to the *RAD51* locus should trigger a recombination event between the introduced transformation cassette, and the chromosome[96]. This should result in the endogenous sequence of *RAD51* being replaced by that of the transformation cassette, placing *RAD51* under a different promoter or a degron, altering the expression of *RAD51*.

The plasmid pSG70 was used as a backbone for the Gibson assembly. The plasmid was extracted from overnight *E. coli* cultures in quadruplicate.

Plasmid preparation 1 was taken forward and digested in a reaction volume of 20μl, at 37°C overnight, using HindIII and ClaI, producing two fragments, one containing the Hygromycin cassette and the other containing the Bacterial origin of Replication (OriC) and the Bacterial selection marker, Ampicillin resistance (Figure 1).

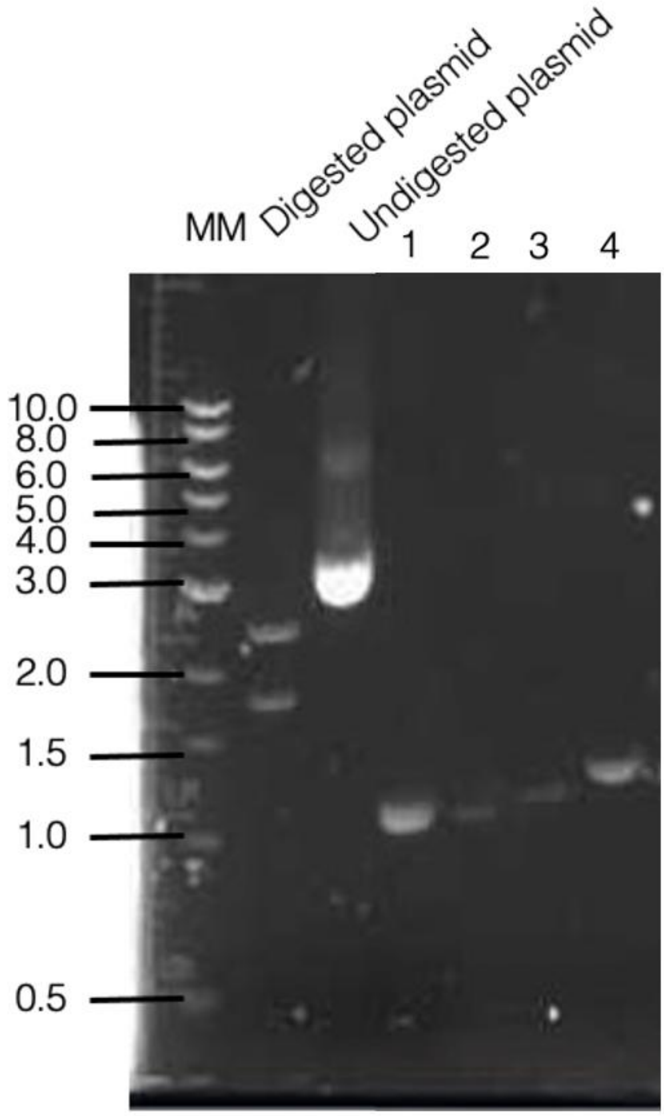

Figure 1 Digestion of pSG70 and Amplification of fragments for the *P^{CLB2}*-*RAD51* Gibson assembly. MM= molecular marker (NEB 1kb ladder). Digested plasmid is digestion of pSG70 by HindIII and ClaI, the fragments expected: Hyg resistance casette at 1787 bp and OriC and the Ampicillin selection marker at 2432 bp. Undigested plasmid was used as positive control, incubated alongside digestion at 37°C, fragment expected at 4225bp, as well as bands due to the nicked plasmid. PCR Fragments expected: 1= *RAD51* upstream fragment is 1000bp. 2= *RAD51* downstream fragment at 1000bp. 3= *P^{CLB2}* at 1110bp, 4 = *RAD51* at 1200bp.

The remaining fragments required for the *P^{CLB2}*- *RAD51* assembly were generated by PCR. The P^{CLB2} - 3XHA fragment was generated from a gDNA preparation of YSG15, while the *RAD51* gene, upstream, and downstream fragments were amplified from a gDNA preparation of wildtype (YSG3). The PCRs of the fragments were then run on a 0.7% agarose gel to confirm PCR amplification (Figure 1).

Once the product was confirmed, the PCR mixtures were cleaned up and the DNA concentration and purity were quantitated. The pmols were then calculated. The fragments and the digested plasmid were used to generate the *P^CLB2^* plasmid by Gibson assembly. The correct assembly of the plasmid was confirmed using PCR amplification, and run on a 0.7% agarose gel, shown in Figure 2.

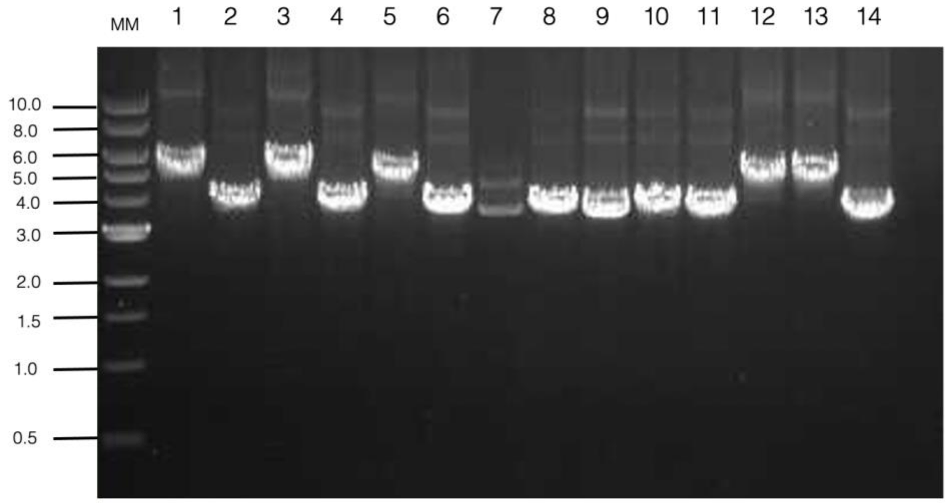

Figure 2 PCR amplification of the colonies selected from the P^{CLB2}- *RAD51* Gibson assembly, which was used to transform chemically competent *E. coli cells*. Fragment size expected: 6,138 bp. The extra larger bands seen are due to plasmid supercoiling. Assemblies 1,3,5, 12 and 13 were taken forward.

ii Generating the P^{DMC1}- *RAD51* plasmid

The correct P^{CLB2} - *RAD51* assemblies, were then selected and used to generate the backbone for both *the* P^{DMC1}-*RAD51* and *Degron- RAD51* assemblies. The backbone fragment contained the upstream, downstream and *3x HA- RAD51* sequences, but excluded the P^{CLB2} fragment. The backbone was PCR amplified from the correct assemblies, the PCR mixtures were then run on a 0.7% agarose gel, Figure 3.

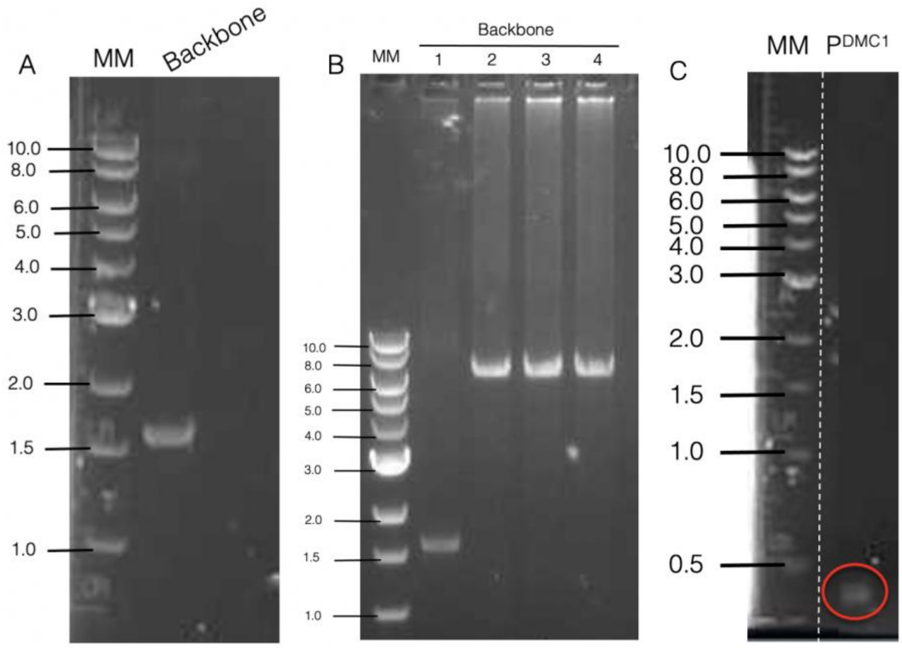

Figure 3 A Unsuccessful initial amplification of the Backbone for the *P^DMC1^-RAD51* plasmid. Fragment expected: 7551 bp. The fragment was amplified from the successful *P^CLB2^-RAD51* assembly 1 (Figure 38). The PCR was unsuccessful and was re-attempted. B **Generation of the backbone fragment of the *P^DMC1^* Gibson assembly.** The four remaining successful assemblies of the *P^CLB2^-RAD51* plasmid were used as the template for the *P^DMC1^-RAD51* plasmid backbone fragment. Expected fragment size of 7.5kb. Reaction 2 was taken forward and used to assemble the *P^DMC1^-RAD51* plasmid. **C Generation of the P^DMC1^ fragment for the *P^DMC1^-RAD51* Gibson assembly.** Fragment expected: 340 bp. Dashed line indicates where lanes have been omitted from the gel.

The *P^DMC1^* fragment was generated by PCR from a gDNA prep of YSG3 (Figure 3), this fragment and backbone amplification reaction were taken forward and cleaned up, and then used to generate *P^DMC1^-RAD51*, by Gibson assembly. This was then transformed into *E. coli* and screened, Figure 4. After several unsuccessful PCR attempts, the plasmids were screened by amplification of *P^DMC1^*, reaction 12 was taken forward and used to generate the backbone fragment of the *Degron-RAD51* Gibson assembly, Figure 5.

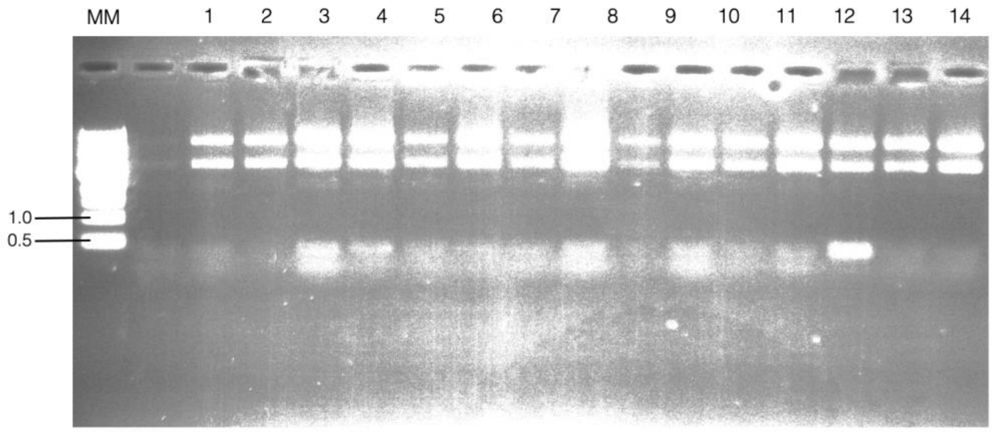

Figure 4 Screening the P^{DMC1}- *RAD51* Gibson assemblies for successful insertion of the P^{DMC1} fragment. The P^{DMC1} fragment amplified by PCR, only plasmid 12 appears to be successful and was taken forward to use as template for the Degron-*RAD51* plasmid. Fragment expected: 360 bp.

iii Generating the degron- *RAD51* plasmid

Assembly 12 (Figure 4) was taken forward and used as a template for the backbone fragment of the degron- *RAD51* assembly. The degron fragment was also generated by PCR, from a gDNA block, Figure 5.

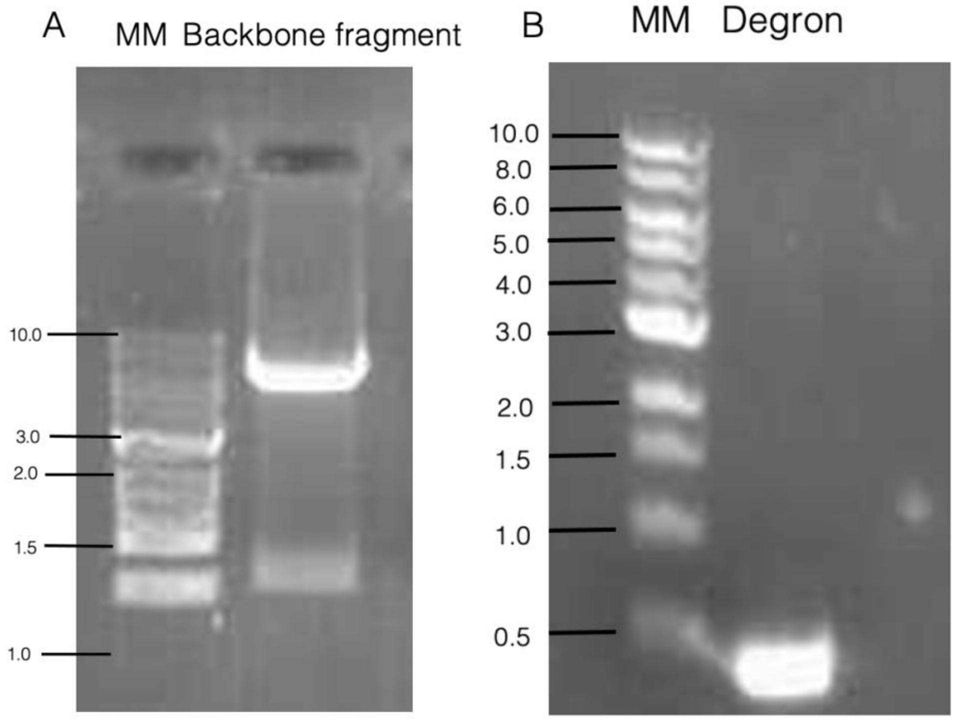

Figure 5 A Generation of the backbone fragment, which forms the backbone for the Degron-*RAD51* assembly, generated from P^{DMC1}-*RAD51* plasmid 12. The fragment length expected was 7420bp. **B Re-attempted amplification at a lower**

annealing temperature of the Degron fragment from a gBlock. Fragment expected: 483 bp. The PCR was successful, and the fragment was taken forward to assemble the Degron- *RAD51* plasmid.

The fragments, once generated, were cleaned up using the PCR cleanup protocol and nanodropped to determine the concentrations. The fragments were then assembled using Gibson assembly and the plasmid was transformed into chemically competent *E. coli* cells.

iv Transformation into *S. cerevisiae*

Once the plasmids were generated, the transformation cassette was then generated by PCR amplification (Figure 6). This was then used to transform both mating types of the wildtype *S. cerevisiae* strains (YSG3 and 4) using the protocol detailed above.

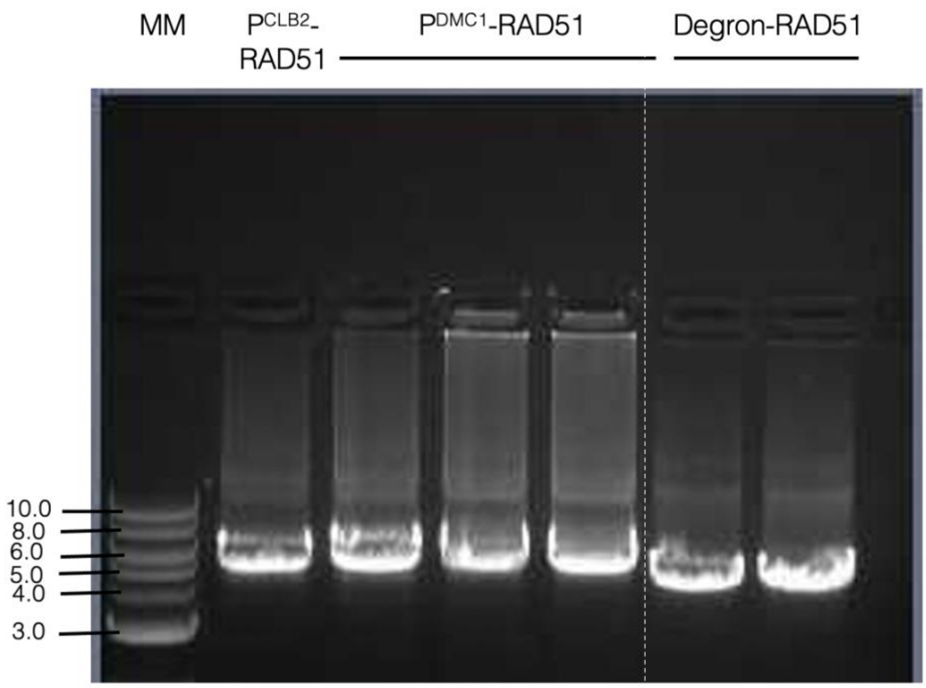

Figure 6 Generation of the transformation cassette. The plasmids were amplified, excluding the bacterial selection marker and Origin (OriC). Dashed line indicates where lanes have been omitted from the gel. Fragments expected: P^{CLB2} - *RAD51*: 6098 bp, P^{DMC1} - *RAD51*: 5419 bp, degron- *RAD51*: 5471 bp

To confirm the transformation and ensure the cassette had been recombined at the correct locus, primers were designed to bind to the sequence of the chromosome outside the transformation cassette and amplify through the cassette, wildtype was used as a control (Figure 7).

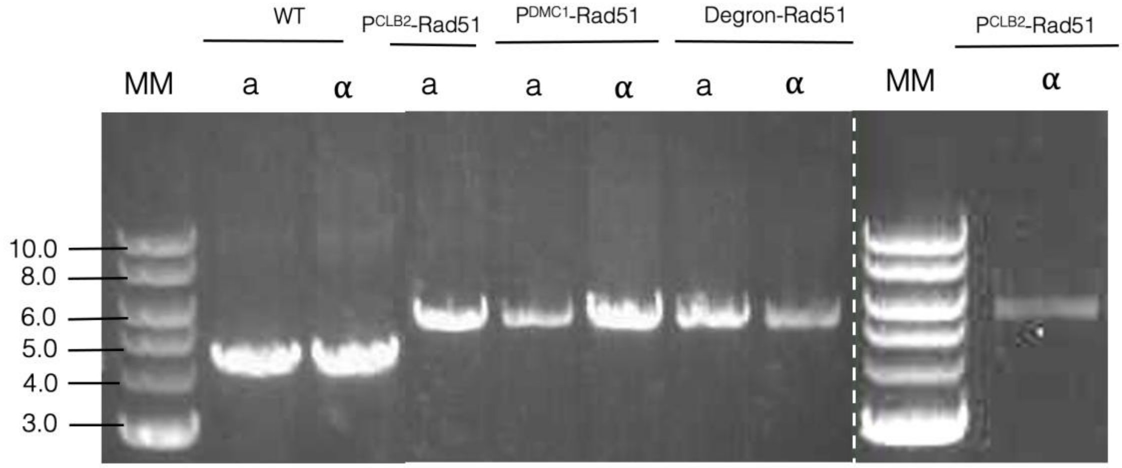

Figure 7 Confirmation of transformation. The primers bound outside the transformation cassette to determine whether the cassette had inserted at the correct locus. Fragments expected: Wildtype: 4205 bp, P^{CLB2} - *RAD51*: 7107 bp, P^{DMC1} - *RAD51*: 6422 bp Degron- *RAD51*: 6474 bp. Dashed lines indicate amalgamation of different gels.

v Sporulation Efficiency of strains

Once the strains generated were validated, their sporulation was assayed, to determine whether the altered expression of Rad51 had any impact on meiosis (Figure 8).

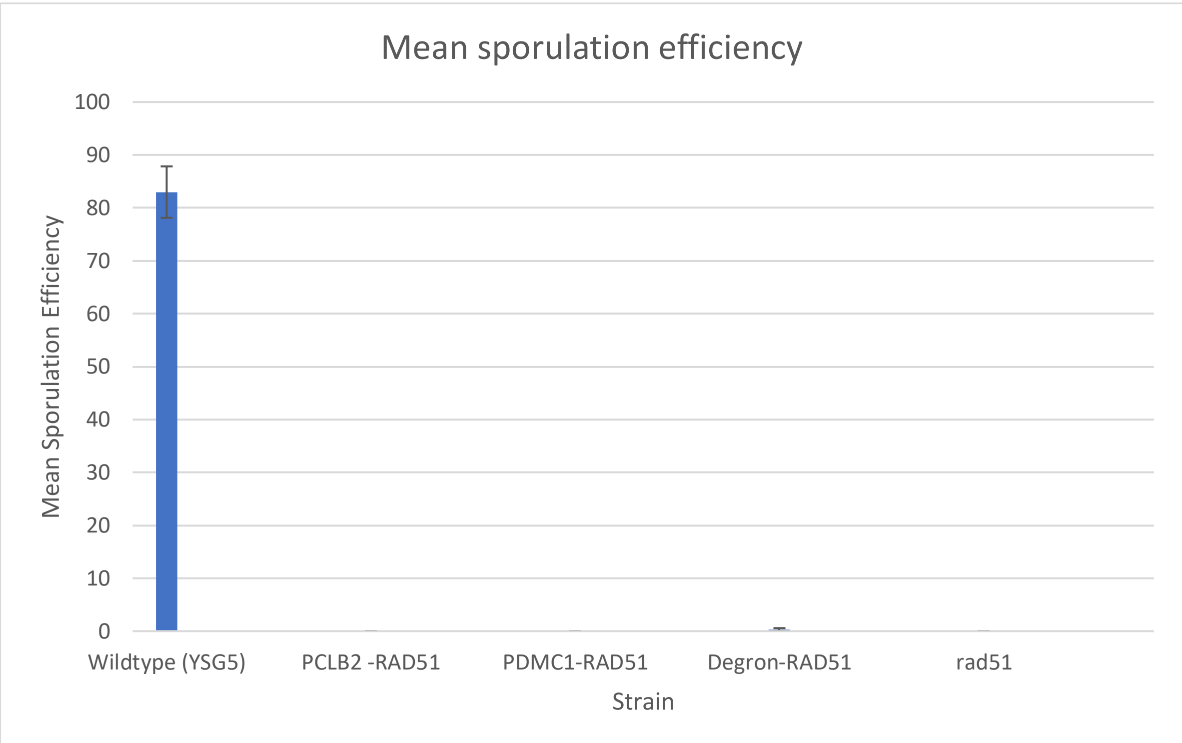

Figure 8 Mean sporulation efficiencies of the altered *RAD51* expression strains compared to Wildtype and *rad51* strains. Cultures were sporulated for at least 72

hours in KAc. Mean Sporulation Efficiency was calculated by counting a minimum of 200 cells in each sample and averaging 3 independent repeat strains. (Error bars represent Standard Deviation: Wildtype= 9.731, P^{CLB2}- *RAD51* = 0.00, P^{DMC1} - *RAD51*= 0.00, Degron- *RAD51*= 0.540 and *rad51* = 0.000)

Due to the lack of sporulation seen, it was hoped that Fluorescence Activated Cell sorting (FACs) could be used to demonstrate that the strains created were in fact diploid, and that the defect in sporulation seen is due to the arrest of meiosis rather than an inability to proceed through meiosis, due to being haploid. However, due to time constraints this was not pursued. A simple mating test, using a known haploid strain could also have been used, if any sporulation occurred following mating, the strains would in fact, be haploid, which would explain the lack of sporulation seen during the sporulation assay.

vi Generating the 6xHis 3xHA tagged-*RAD51* strain

In order to confirm the altered expression of Rad51 in the strains created and compare the effect of the different promoter on the expression patterns by Western blotting, a tagged wildtype Rad51 strain was required. This strain was created using the backbone of the degron-*RAD51* strain, so the 6xHis 3HA- *RAD51* would be under the control of the endogenous promoter. The 6xHis 3xHA fragment was amplified from pSG11 (Figure 9).

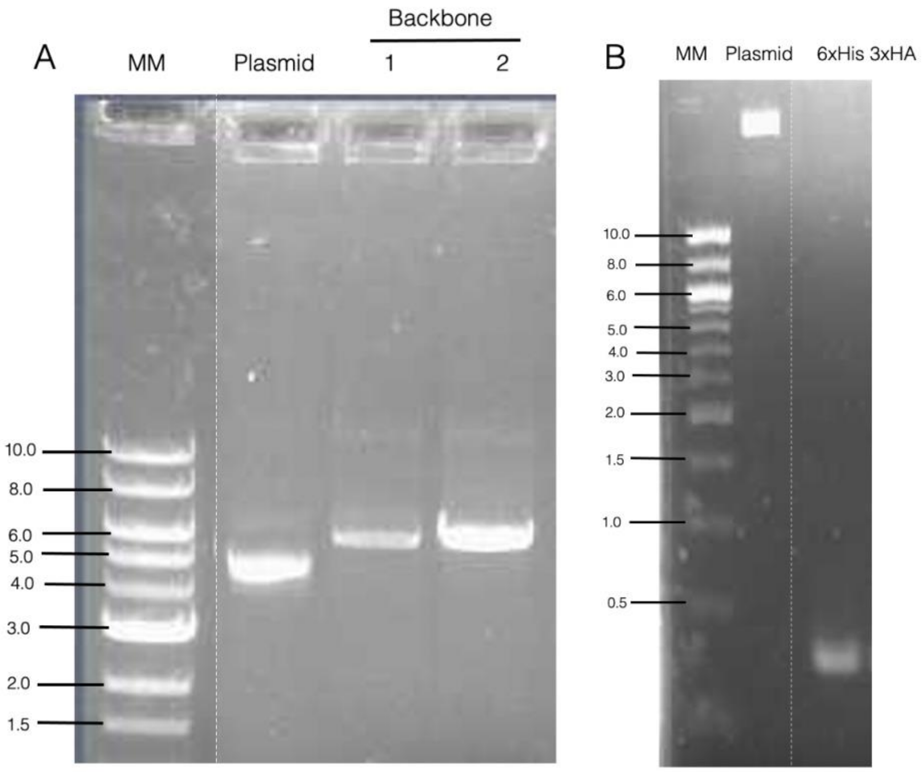

Figure 9 A Generating the 6xHis 3xHA fragment for the tagged- *RAD51* plasmid assembly. Fragment amplified from pSG11. Fragment expected: 163 bp. Dashed line indicates where lanes have been omitted from the gel. **B Backbone fragment for the**

generation of the 6xHis 3xHA tagged-*RAD51* plasmid. Fragment generated from the degron-*RAD51* plasmid. Fragment expected: 7420 bp. Dashed line indicates where lanes have been omitted from the gel**.**

The amplification of the backbone and insert fragments were successful (Figure 9). These were then ligated by Gibson assembly. The plasmid assemblies were then screened by generation of the transformation cassette, using the degron-*RAD51* plasmid as a control (Figure 10).

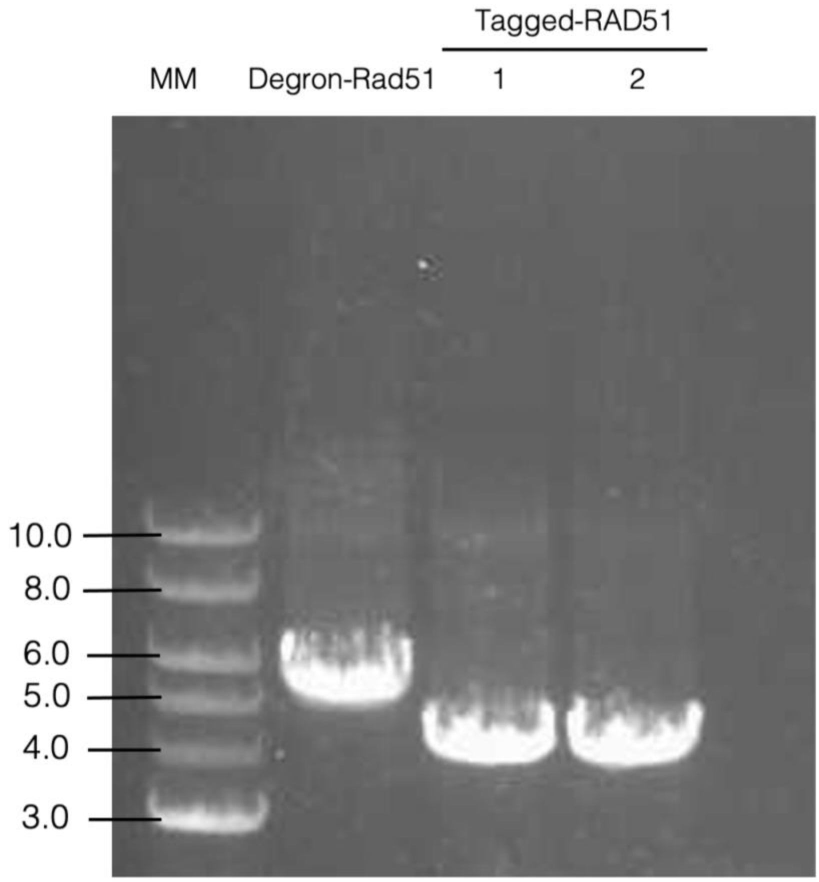

Figure 10 Validation of the tagged- *RAD51* plasmid assembly, using the degron- *RAD51* assembly as a control. Fragments expected: degron-*RAD51* 5785 bp, tagged *RAD51*: 5452 bp**.**

The cassette was then used to transform YSG3 and 4. The successful colonies were screened (Figure 11).

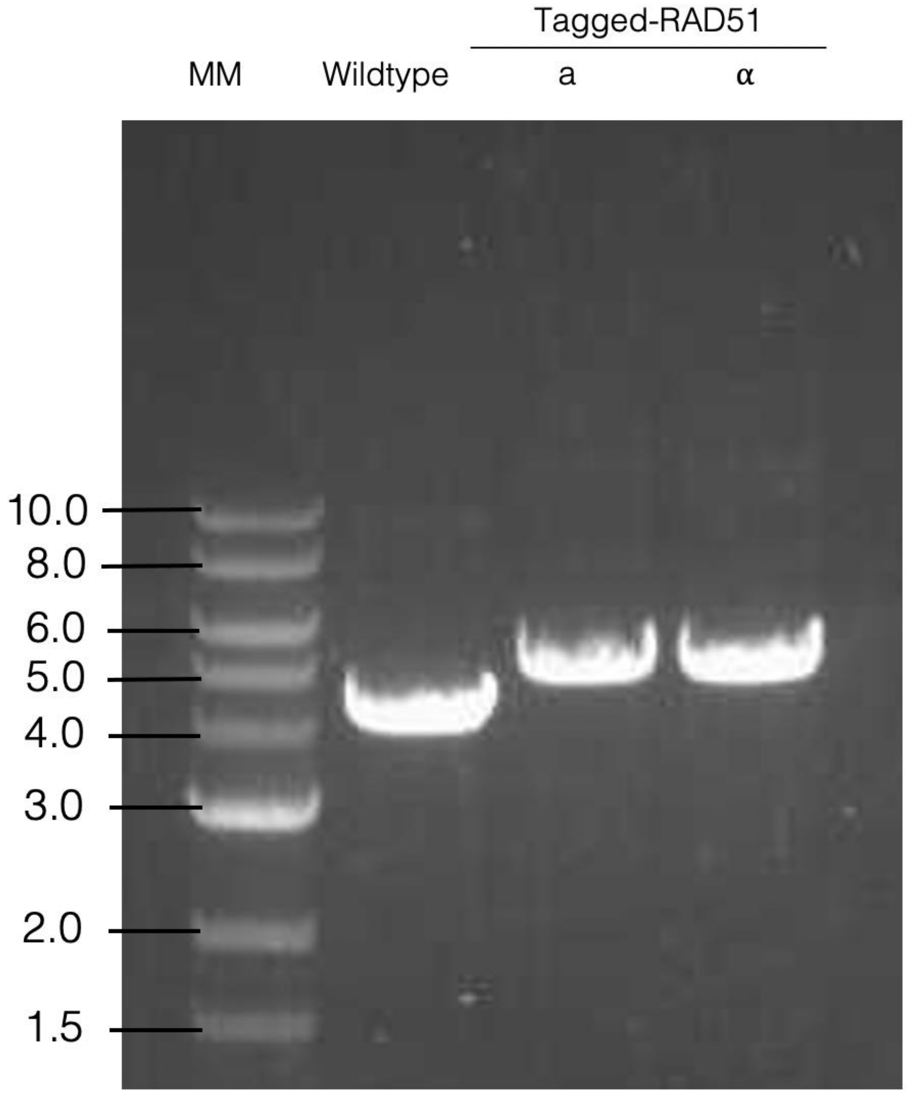

Figure 11 Validation of the transformation. Primers designed to anneal outside the transformation cassette to ensure the cassette has integrated at the correct locus. Fragments expected: Tagged- *RAD51*: 6428 bp, Wildtype: 4205 bp.

The tagged- *RAD51* strain was then used as a control during the meiotic time course. Ideally, the sporulation efficiency of the tagged- *RAD51* diploids would have been assayed, however due to time constraints this was not undertaken, it would be expected that the tagged- *RAD51* strains exhibit a similar sporulation efficiency to wildtype, as the 6xHis 3xHA tag should not affect the function of Rad51. A growth assay was undertaken of both mating types of the tagged- *RAD51* strain to verify that it grew similarly to wildtype and if it could be used as a positive control during the meiotic time course and Western blot (Figure 12). It was expected that the tagged- *RAD51* strain should grow comparably to wildtype, as similarly to sporulation efficiency, the 6xHis 3xHA tag should not affect Rad51 function.

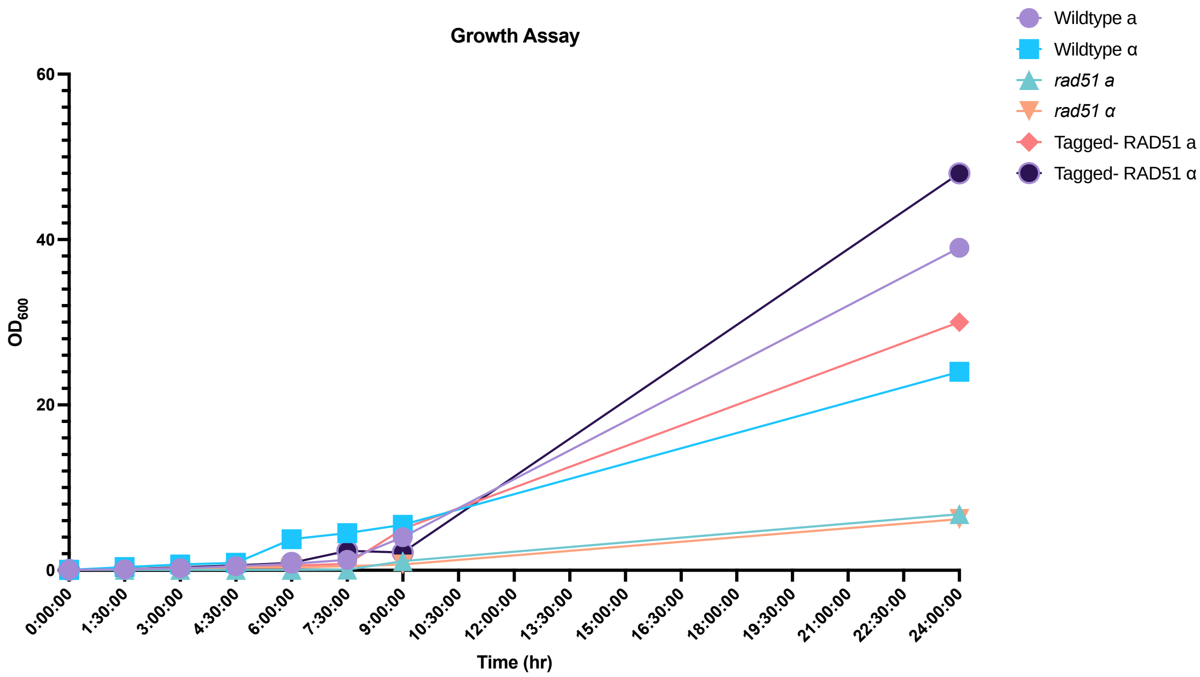

Figure 12 Growth assay of Tagged- *RAD51* strain, with wildtype and *rad51* used as positive and negative controls, respectively. The strains were grown in YPD with spectrophotometer measurements taken every 90 minutes. Both the a and α strains were measured to determine whether there were any unexpected mating type specific effects. Figure generated using GraphPad Prism.

vii Meiotic time course

A meiotic time course and Western blot were carried out, to compare the expression of Rad51 in the wildtype, tagged- *RAD51* strain, to the strains with altered Rad51 expression; *P^{CLB2}-RAD51, P^{DMC}1-RAD51* and degron- *RAD51*. The wildtype diploid (YSG5) during vegetative growth was also used as a control for total protein content. It was expected that Rad51 would not be present in meiosis in the *P^{CLB2}* strain, as Clb2 is a mitotic cyclin required for mitotic entry and is not expressed in meiosis. While, it may be present in the cell, prior to inoculation into nutrient depleted media, it was expected that the protein levels of Rad51 under the *CLB2* promoter would decrease due to the degradation of existing proteins in the cell during pre-meiotic S phase, and due to the lack of active expression during meiosis. This would generate the 'meiotic depleted' phenotype desired and explains the decreased sporulation efficiency when compared to wildtype seen above. A western blot would also show if there was a difference in Rad51 expression between the *P^{DMC1}- RAD51* and the wildtype expression of the tagged- *RAD51* strain. If a difference in Rad51 expression was identified, this may explain the low sporulation phenotype. The degron- *RAD51* strain, without the TEV system should express Rad51 at a similar level as the wildtype tagged- *RAD51* strain, as, without the cleavage and exposure of the bidirectional degron, Rad51 should not be targeted for degradation.
However, when the meiotic time course was undertaken, the pellets were too small to be prepared for western blot. The only strain that could be prepared was the tagged- *RAD51* strain. However, when the gel was initially activated and imaged, the gel had to be imaged for over one minute, suggesting that the protein levels within

the samples were very low. It was decided that the protein levels were too low for it to be worthwhile to proceed with the western blot. In order to further evaluate the strains as useful tools in the lab and determine why the pellets were so small, a growth assay was carried out, to compare the growth of the altered Rad51 expression strains to wildtype and *rad51* strains.

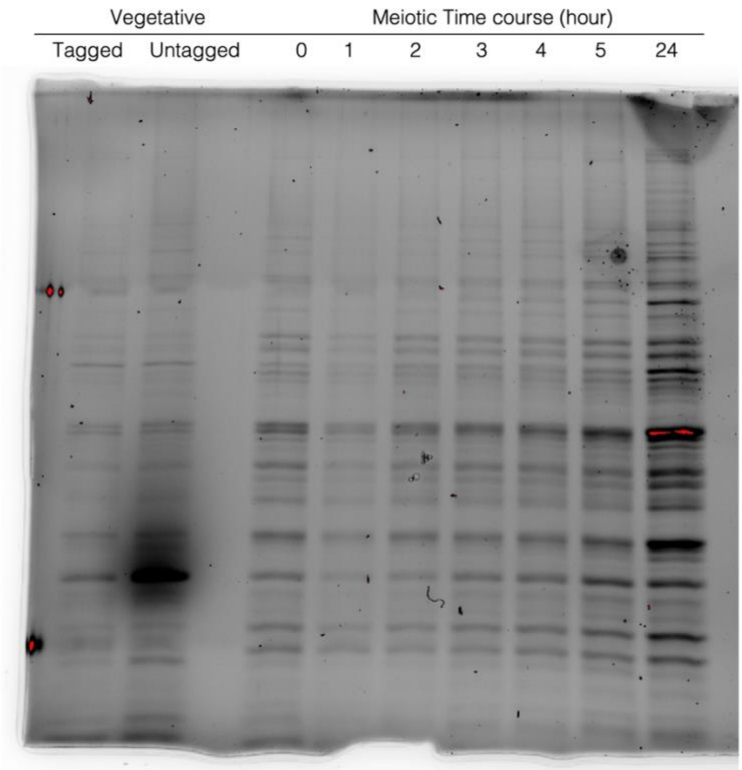

Figure 13 SDS- PAGE gel of protein samples of the tagged- RAD51 strain, generated during a meiotic time course illustrating total protein content of the cell. The gel was activated and imaged for over one minute. Later time points were omitted due to inadequate sample. The ladder was not included, as it would reach saturation before the protein samples. Red pixels identify saturated areas of the band.

viii Growth assay

The strains were grown, and regular OD_{600} measurements were taken (Figure 14).

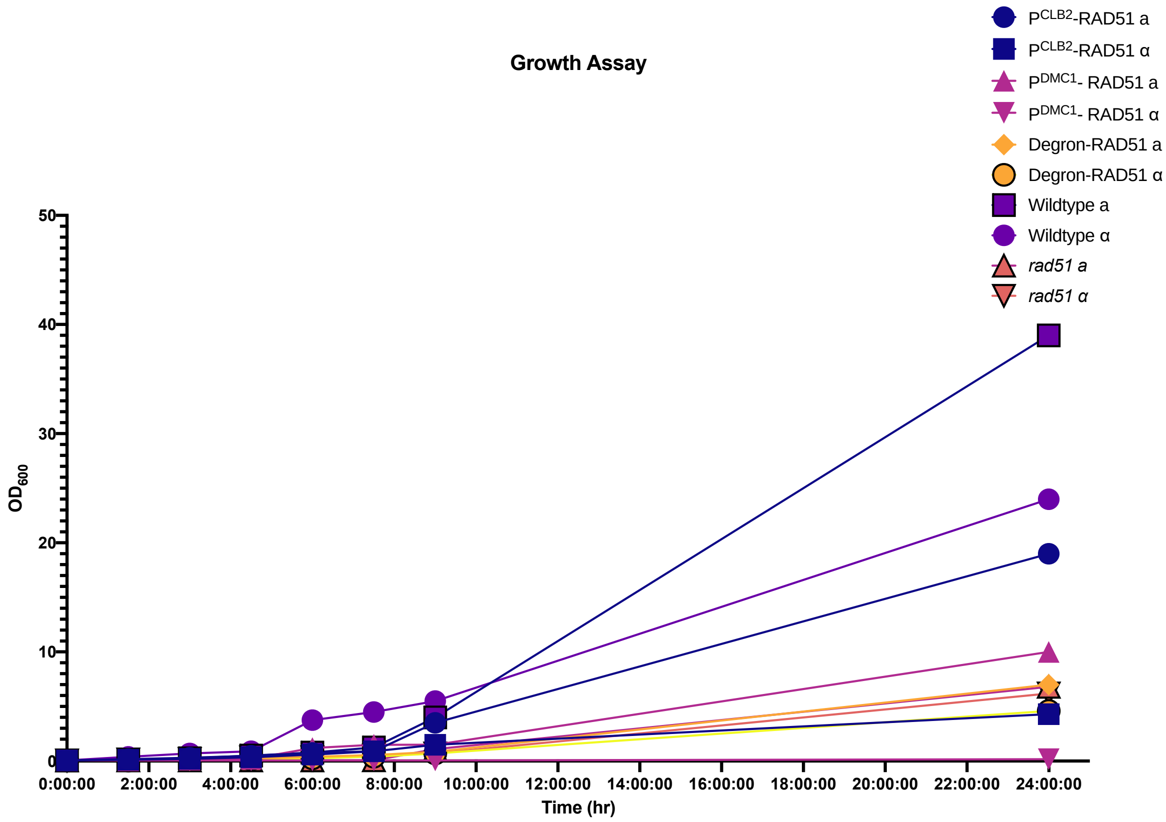

Figure 14 Growth assay of the strains with altered Rad51 expression. The strains were grown in YPD with spectrophotometer measurements taken every 90 minutes. Both the a and α strains were assayed to determine whether there were any unexpected mating type specific growth effects. Figure generated using GraphPad Prism.

While a large difference between the growth of the a and α wildtype strains was observed, it does appear that the *P^CLB2^-RAD51* a strain grows similarly to wildtype, as Rad51 should be present during mitosis. While both the *P^DMC1^- RAD51* and degron- *RAD51* strains exhibit a growth rate more similar to the *rad51* strain as expected. However, the *P^DMC1^- RAD51* a mating type does appear to be an anomaly, as the OD_{600} remained at the initial OD_{600} of 0.05, suggesting that either the cells are very slow growing, and had not yet reached the lag phase or that the initial OD_{600} measurement had been incorrect and in fact very few cells had been inoculated into the new media. However, because the growth assay was carried out manually, it was not possible to determine whether this phenotype resulted from experimental error or was characteristic of this strain.

ix Insertion of the TEV cassette

Plasmids containing the Tobacco Etch Virus (TEV) protease under the control of several promoters had previously been generated by the Gray lab. The plasmids included the TEV cassette, which contains the TEV protease under the control of a promoter of choice, and the *URA3* gene, therefore, when transformed into *S.*

cerevisiae the cassette inserts at the *URA3* locus. The promoter, TEV and *URA3* are flanked by Not1 cleavage sites, allowing generation of the cassette by Not1 digest, Figure 15. The TEV protease is cleaves the degron cap, exposing the degron, and causing the protein the degron is attached to be targeted for degradation. The TEV was placed under the control of either *P^ADH1^* or *P^IME2^*, *P^CUP1^* was also considered, however due to time constraints it was excluded.

The initial transformation was unsuccessful, so the plasmids were re-digested, and the transformation was reattempted with just *P^IME2^-TEV* and *P^ADH1^- TEV* as it was hoped that the efficacy of TEV knockdown could be assayed during either vegetative growth or meiosis, as this is the research focus of the Gray lab.

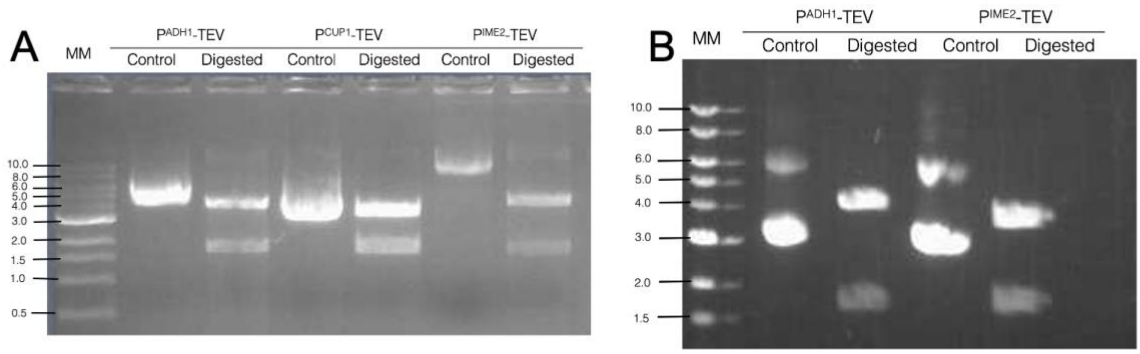

Figure 15 A Not1 digest of the plasmids containing the TEV protease under the control of either *P^ADH1^*, *P^CUP1^* or *P^IME2^*. The Not1 digest was used to generate the transformation cassette. Fragments expected 4432 bp and 1754 bp. **B Re-digestion of *P^ADH1^-TEV* and *P^IME2^-TEV* with Not1.** Fragments expected: transformation cassette at 4432 bp and bacterial origin and selection marker at 1754 bp.

The digest was successful, and the cassettes were used to transform both YSG3 and 4 and both mating types of the degron- *RAD51* strain. However the transformation was only successful into YSG3 and 4. These strains were then mated with the opposite mating type of the degron-*RAD51* strain and sporulated. The spores were dissected, and replica plated. Spores that were both URA+ and Hygromycin resistant were selected. These colonies were then screened (Figure 16).

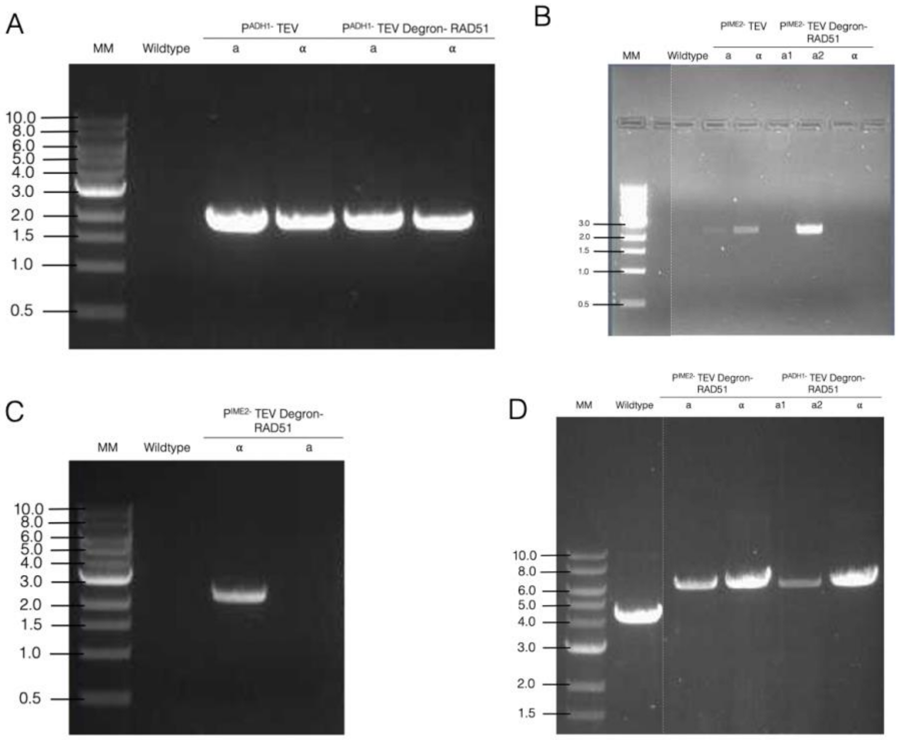

Figure 16 A-C Screening for the insertion of the TEV cassette, using primers previously designed by Gray lab. Primers annealed inside the cassette, so no fragment was expected if wildtype. Fragment expected in either *P^{ADH1}-TEV* or *P^{ADH1}-TEV*: 1990 bp. **D Screening for the degron fragment in the TEV, degron strains.** Primers designed to anneal outside the transformation cassette to ensure the cassette has integrated at the correct locus. Fragment expected: Wildtype: 4205 bp, TEV, Degron strains: 6474 bp. Dashed line indicates where lanes have been omitted from the gel.

x The Degron system

Once the TEV cassette was transformed into YSG3, YSG 4 and both mating types of the degron- *RAD51* strain, a growth assay was carried out to determine whether the insertion of the TEV affected the growth. It was expected that both strains containing only the TEV cassette, either under the control of the *ADH1* or *IME2* promoter, would grow comparably to the wildtype strains, as the TEV system should not be active, and therefore should not impact the growth. If there is a reduction in growth, this would suggest that these are due to off-target effects of the TEV protease, however this has not been noted previously[97]. The degron-Rad51 strain should also grow comparably to a wildtype strain, for the same reason, as without the TEV, Rad51 should be expressed and active at the same levels as wildtype. However, as noted previously, the degron appears to impair Rad51 function, leading to a *rad51* phenotype. In addition, the strains with *P^{ADH1}-TEV*, degron- *RAD51* should grow similarly to a *rad51* strain, as any Rad51 produced should be targeted for degradation by the cleaving of the degron cap. Further, the *P^{IME2}-TEV*, degron-*RAD51,* had the degron not impaired Rad51 function, should have been expected to grow similarly to wildtype, as the degron cap should not be cleaved, as the TEV should only be expressed during meiosis.

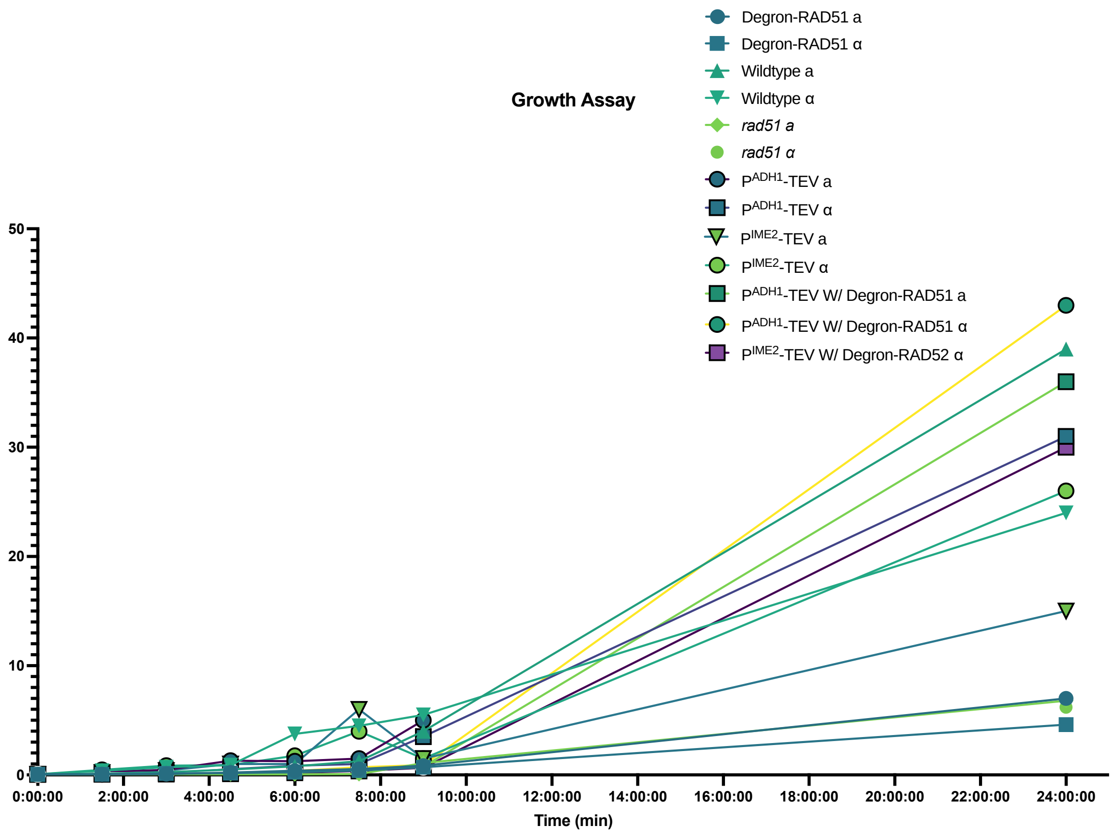

Figure 17 Growth assay of the TEV and degron strains. The strains were grown in YPD and both mating types were assayed. Wildtype and *rad51* strains were included as positive and negative controls. OD_{600} measurements were taken every 90 minutes, the 24th hour measurement of the a mating type *P^ADH1^-TEV* could not be carried out. *P^IME2^-TEV*, degron- *RAD51* mating type a could not be generated in time for the growth assay. Figure generated using GraphPad Prism.

As expected, once the growth assay was carried out, the degron-RAD51 strain grew poorly, possibly due to the degron disrupting the function of Rad51, while both mating types of the *P^ADH1^- TEV*, degron-*RAD51* grew similarly to wildtype strains. This either suggests that the TEV protease is not being expressed at adequate levels or is unable bind to its recognition site, and cleave the degron cap.

No repeats were carried out, therefore statistical analysis could not be done to determine whether the differences in growth rate are significant, and if the growth rates exhibited by these cultures are characteristic of the phenotype. Going forward, the growth assay should be carried out with multiple repeats to facilitate the exclusion of anomalous results, and characterisation of the growth phenotype of the strain.

Western blotting of protein preparations generated during either vegetative growth, for the *P^ADH1^-TEV*-degron-*RAD51* strains, or meiosis, for the *P^IME2^-TEV*-degron-*RAD51* strains, could also be carried out to determine the efficacy of degradation of the TEV degron system. It would be expected that during vegetative growth and

depending on the efficacy of degradation in the P^{ADH1}-*TEV*-degron-*RAD51* strains, there would be minimal Rad51 present in the cell, however the growth assay suggests this is not the case. While the degron-*RAD51*, P^{ADH1}-*TEV*, and P^{IME2}-*TEV* strains should have Rad51 levels comparable to wildtype, both during vegetative growth and meiosis. On the other hand, during meiosis, the P^{IME2}-*TEV*- degron-*RAD51* strains should have low levels of Rad51 but have wildtype levels of Rad51 during vegetative growth.
Determining the levels of Rad51 during meiosis would require the creation of diploids of both *the* P^{ADH1}-*TEV, degron-RAD51 and* P^{IME2}-*TEV, degron-RAD51* strains as well as the P^{ADH1}-*TEV* and P^{IME2}-*TEV* strains. The sporulation efficiency of these diploids should also be determined to allow complete characterisation of the phenotype. It would be expected that neither *the* P^{ADH1}-*TEV-degron-RAD51* and P^{IME2}-*TEV-degron-RAD51* strains will produce spores, as there should be minimal levels of Rad51 present in the cell, however this depends on the efficacy of knockdown.

xi Generation of the *ADE2* Disruption plasmid

The aim of generating the strains which altered the expression of *RAD51* was to alter the DSB repair pathway choice, biasing it towards NHEJ, instead of HR, which is favoured in *S. cerevisiae.* In order to assay the DSB repair pathway choice of the strains with altered expression of RAD51, the *ADE2* red/white colony was used. In *S. cerevisiae*, if either the *ADE1* or *ADE2* genes are mutated and the cells are plated on minimal adenine medium, this activates the adenine biosynthetic pathway. Without either the functional *ADE1*, N-Succinyl-5-Aminoimidazole-4-Carboxamide Ribotide Synthetase, or *ADE2*, which encodes Phosphoribosylaminoimidazole Carboxylase, an intermediate in the Adenine biosynthetic pathway, Phosphoribosylaminoimidazole, accumulates in the vacuole of the cells[97, 98]. The accumulation of this intermediate results in the colonies appearing a characteristic red colour, as opposed to the wildtype white colonies, hence this assay is known as the red/white colony assay.
Plasmids pSG19 and pSG201 were used to generate a vector for the disruption of *ADE2*. Cas9 was placed under the control of the constitutive *ADH1* promoter (P^{ADH1}). However the *ADE2* plasmid could not be constructed due to time constraints, the *ADE2* assay could be used to assay the extent of success in altering DSB pathway choice. It was expected that there would be a greater number of red colonies on each plate with the P^{DMC1} and the degron strain, once the TEV protease, under the control of P^{ADH1}, had been transformed into the strain. However, in the P^{CLB2} strain, the extent of deleterious mutations may be lower, as Rad51 will still be present.
In addition to the true positive colonies, there will also be false negative colonies, as Cas9 generates relatively clean breaks that are more likely to be repaired accurately by NHEJ. Another possible issue with the assay is that the colonies may not be entirely red or white, and the extent of either red or white would need to be quantitated. This could be achieved through spectrometry of the colonies.
The initial strategy was to generate two PCR fragments, using the Terminator and GFP from pSG201 and the Cas9 from pSG19, as pSG201 was constructed using

dCas9. The initial PCR amplification of the fragment failed, so it was re-attempted at a lower annealing temperature. When this also failed, the plasmid was linearised by digestion with NruI. The digested plasmid was then PCR amplified unsuccessfully hence, the strategy was changed.

New primers were designed to amplify the section of plasmid pSG19, which would be assembled with pSG201, digested with Nsi1, to remove the point mutations that generated dCas9. The fragments were generated, and the plasmid was digested (Figures 18). The fragments were assembled by Gibson assembly and transformed into chemically competent *E. coli* cells. Individual colonies were selected and to verify the correct construction of the plasmid, it was digested with BstXI and NsiI, along with the original plasmid (Figure 18).

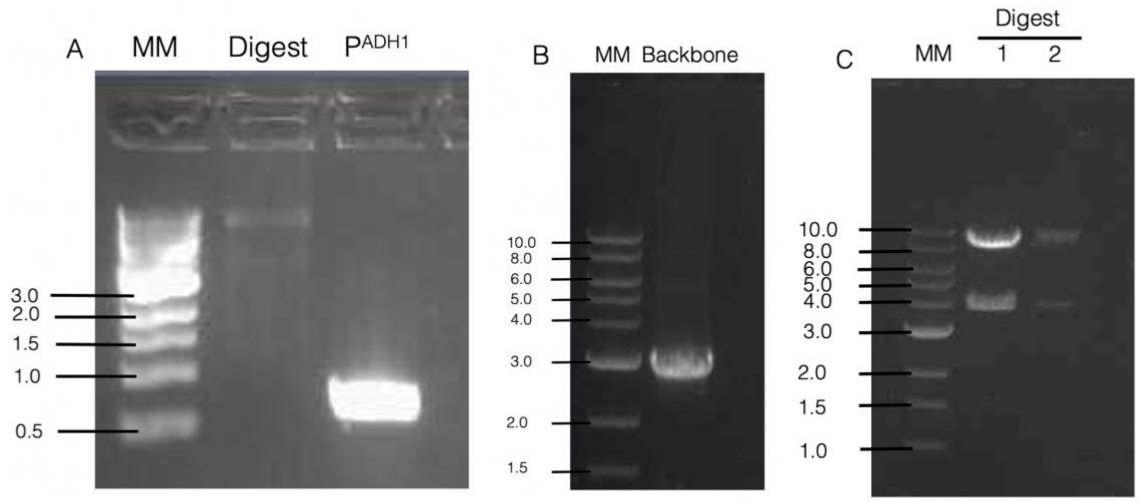

Figure 18 Generation of the P^{ADH1}-Cas9 vector A PCR amplification of the *P^{ADH1}* fragment and restriction digest of Nsi1, to generate fragments for the *P^{ADH1}-Cas9* plasmid for *ADE2* disruption. *P^{ADH1}* =705 bp, Digest was expected to produce two fragments 7897 bp and 3692 bp. **B PCR amplification of pSG19 (pBRA66) fragment of Cas9 up to the Nsi1 restriction site, in order to bypass the mutations inactivating the Cas9 in pSG201.** Fragment expected: 2965 bp. **C Digest of pSG 202 with Nsi1 and BstXI to generate part of the backbone for the *ADE2* disruption plasmid.** Fragments expected: 7897 bp and 3692 bp.

Once verified, the plasmid was then amplified using primers containing BsmBI restriction sites, to allow integration into pYTK096 (pSG 319)(Figure 20). pSG319 was also digested with BsmBI. However, due to difficulties digesting using BsmBI, due to the overactivity of BsmBI, this delayed the project. The plasmid was then generated by Gibson assembly and digested with Not1 to screen the plasmid assembly. However, the fragments were not those expected and due to time constraints, the plasmid could not be generated further. However, had the assembly been correct, the plasmid would then have been digested using Bpl1 and then dephosphorylated, to allow the insertion of the gRNAs targeting *ADE2* into the gRNA scaffold. The gRNAs were annealed together, using equimolar quantities of the single stranded sense and antisense sequences. The annealed gRNAs would then be treated with a kinase to allow ligation to the dephosphorylated vector. The DNA fragments would then be ligated using T4 DNA ligase and used to transform chemically competent *E. coli*. Digestion with BplI would have resulted in the loss of the GFP and allowed the insertion of the gRNA, therefore white colonies would be selected and screened by digestion with SalI and BasI. The correct assemblies could then be digested with NotI to generate the transformation cassette. This could then be used to transform P^{CLB2}- *RAD51*, P^{DMC1}- *RAD51* and degron-*RAD51* strains. These strains could then be screened and assayed for DSB repair pathway choice.

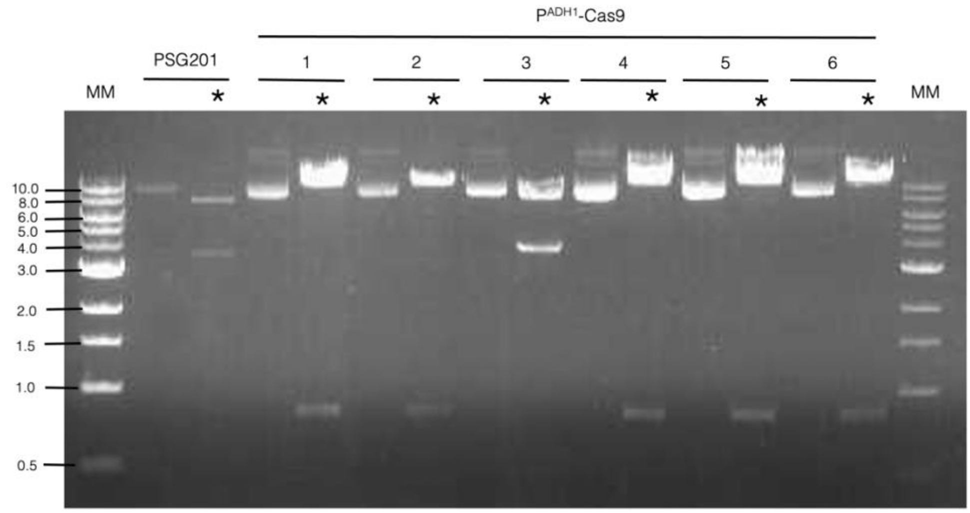

Figure 19 Screening restriction digest with BstXI and Nsi1 to determine correct construction of *ADE2* disruption vector. If successfully assembled, fragments expected: 821 bp and 10742 bp. pSG201 fragments 7897 bp and 3705 bp. Also seen, supercoiled, nicked and linearised plasmid.

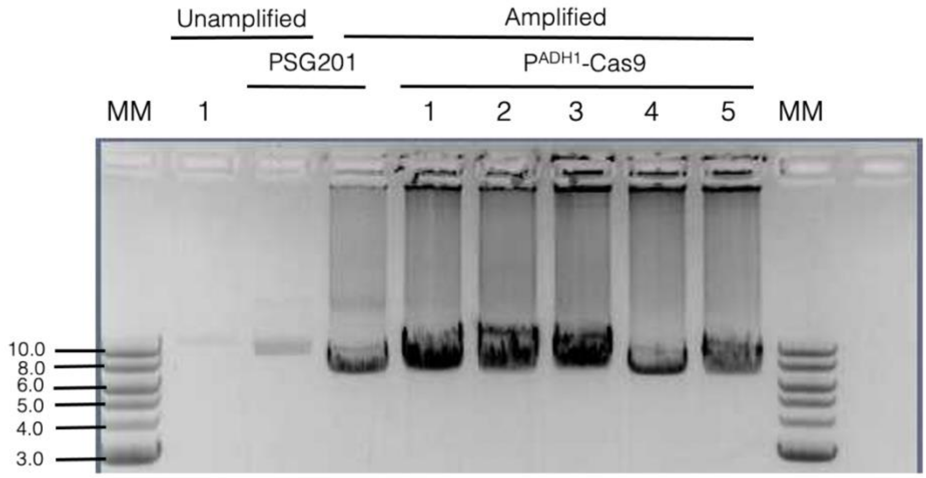

Figure 20 The *P*^{ADH1}- Cas9 constructs amplified with primers containing a Bsmb1 cut site for insertion into pSG319. Fragment expected: 7219 bp

III Determining the extent of RecA homolog compensation

Rad51 and Dmc1 belong to a larger family of RecA homologs, these proteins share a central RecA-like fold, which allows them to catalyse the strand invasion and D loop formation steps of HR. Previous experiments have determined that, while Rad51 is required for Dmc1 nucleation, RecA does not adversely affect the nucleation of Dmc1, suggesting it is a species specific interaction that enables the formation of Dmc1 filaments on ssDNA[74]. While studies have shown that mRad51 is able to partially compensate for Rad51 during MMS treatment, however, was shown to compensate when expressed from the *GAL1* promoter. However, partial compensation suggests mRad51 is able to catalyse strand exchange, which requires interaction with Rad51 binding partners, suggesting the structure of some binding domains may be conserved. By replacing Rad51 with the RecA homologs of higher Eukaryotes and Archaea, under the control of the endogenous promoter, it was hoped that the interactions required between Rad51, and its binding partners could be better elucidated. To visualise the sequence conservation between the RecA homologs studied, the sequences were aligned using the NCBI BLAST tool, highlighting key conserved residues shared by the homologs (Figure 1).

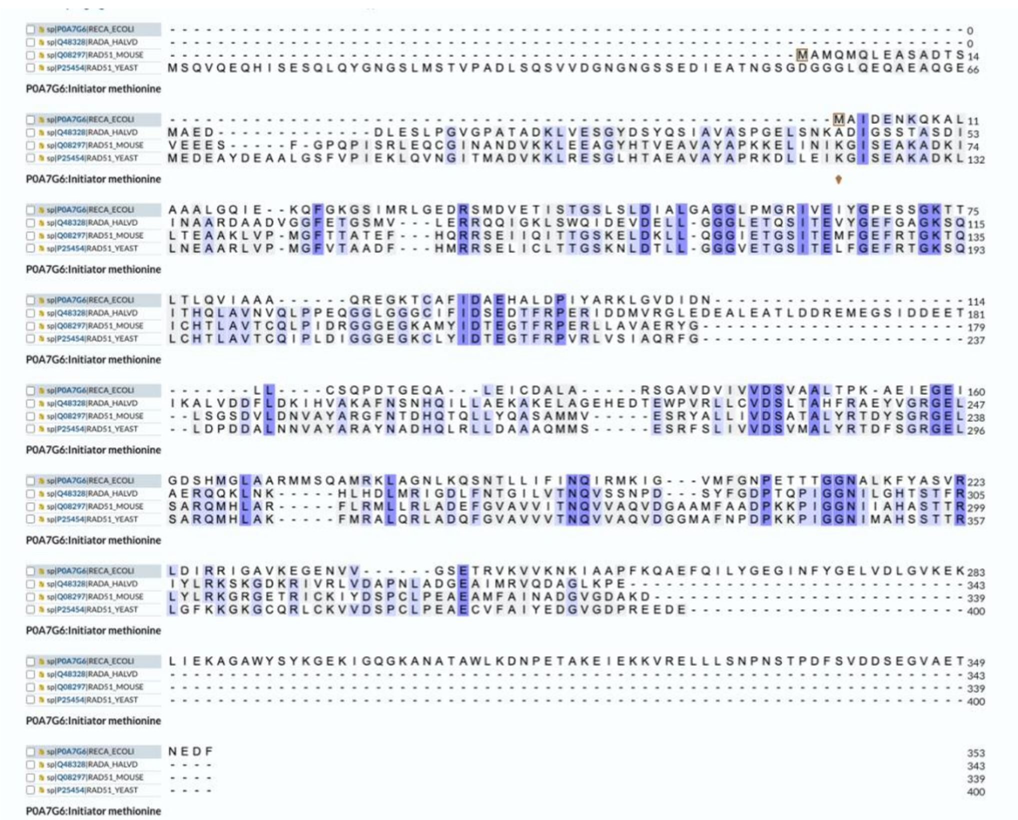

Figure 1 Alignment of nucleotide sequences of (from top) RecA from *E. coli*, RadA from *H. volcanii*, Rad51 from *M. musculus* and *RAD51* from *S. cerevisiae*, aligned using NCBI BLAST. Demonstrating how the Eukaryotic Rad51 sequences

have the greatest similarity to each other and the Archaeal RadA. Figure generated by author using NCBI BLAST.

i Replacing *RAD51* with RecA homologs

To determine the extent of compensation between RecA homologs, the RAD51 gene sequence was replaced with the sequence of either RecA from *E. coli*, RadA from *Haloferax volcanii* or Rad51 from *Mus musculus* (mRAD51). These constructs used the same backbone as the degron- *RAD51* plasmid to allow the replacement of the *RAD51* locus with the desired RecA homolog. Therefore, as the backbone was already generated, the assemblies could be generated in parallel, as opposed to sequentially.

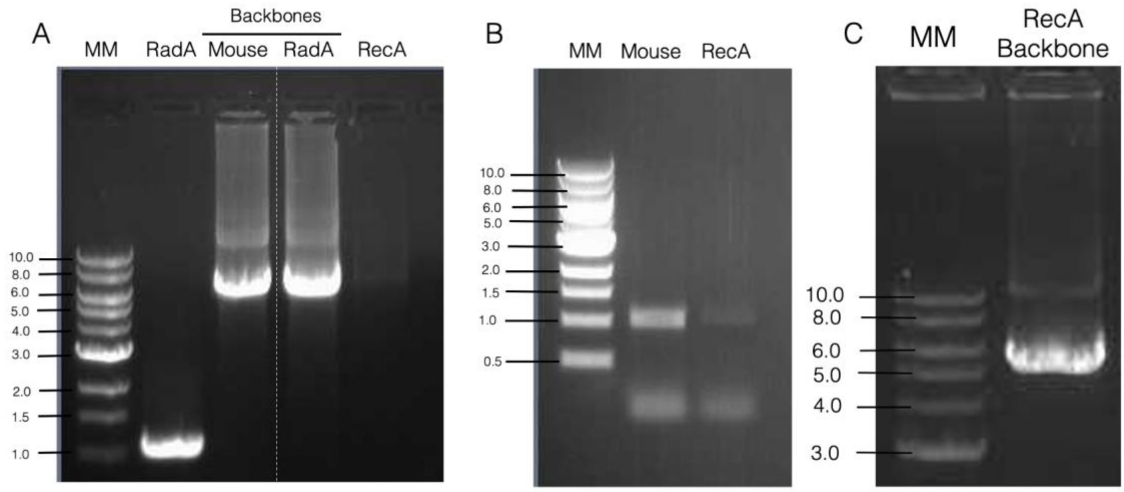

Figure 2 A The backbones and inserts for the Rad51 replacement assemblies were generated by PCR. The RadA fragment was generated from a gDNA preparation of *H. volcanii* (kindly donated by the Allers lab) and RecA was generated by colony PCR. The backbones were generated from the degron- *RAD51* plasmid. Fragments expected: RadA: 1052 bp, RadA backbone: 6240, Mouse backbone: 6220 bp, RecA: 1102 bp. **B Fragments for the RecA homologs Gibson assembly generated by PCR.** Mouse Rad51 was generated from a gDNA prep, RecA fragment was generated by colony PCR. Fragments expected: RecA: 1102 bp, Mouse Rad51: 1060 bp. **C RecA plasmid backbone generated by PCR from the degron- *RAD51* plasmid.** Fragment expected: 6220 bp.

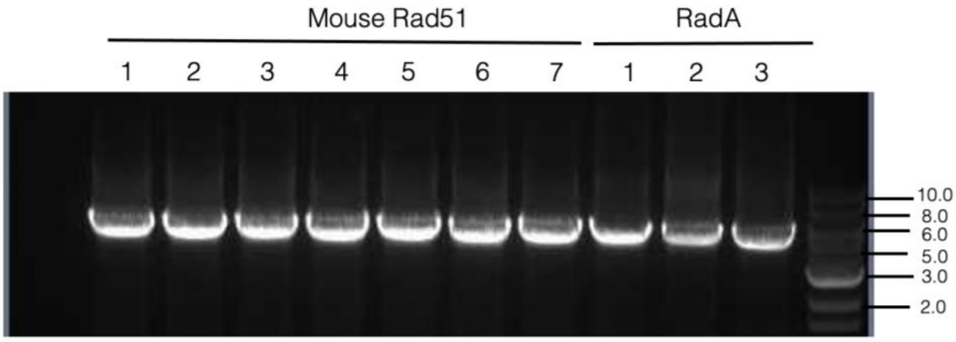

Figure 3 Screening of the RadA and mouse Rad51 plasmid assemblies. Fragments expected: Mouse Rad51: 5122 bp, RadA: 5134 bp, if fragments had not been inserted (degron- *RAD51* plasmid), fragment expected: 5785 bp.

The respective backbones were generated from the degron -*RAD51* plasmid and the RecA homologs were amplified from gDNA preps of each organism (Figure 2). The PCR mixtures were then run on an agarose gel, once amplification had been confirmed, the PCR reactions were cleaned up. The fragments were then nanodropped to determine the DNA concentration and the plasmids were assembled by Gibson assembly. The mRad51 and RadA plasmids were then screened (Figure 3) and the transformation cassette was generated (Figure 4). For the RecA plasmid, due to time constraints, the generation of the transformation cassette was also used as a screening reaction. The transformation cassettes were then used to transform YSG3 and 4. The successful transformants were then gDNA prepped and screened (Figure 5).

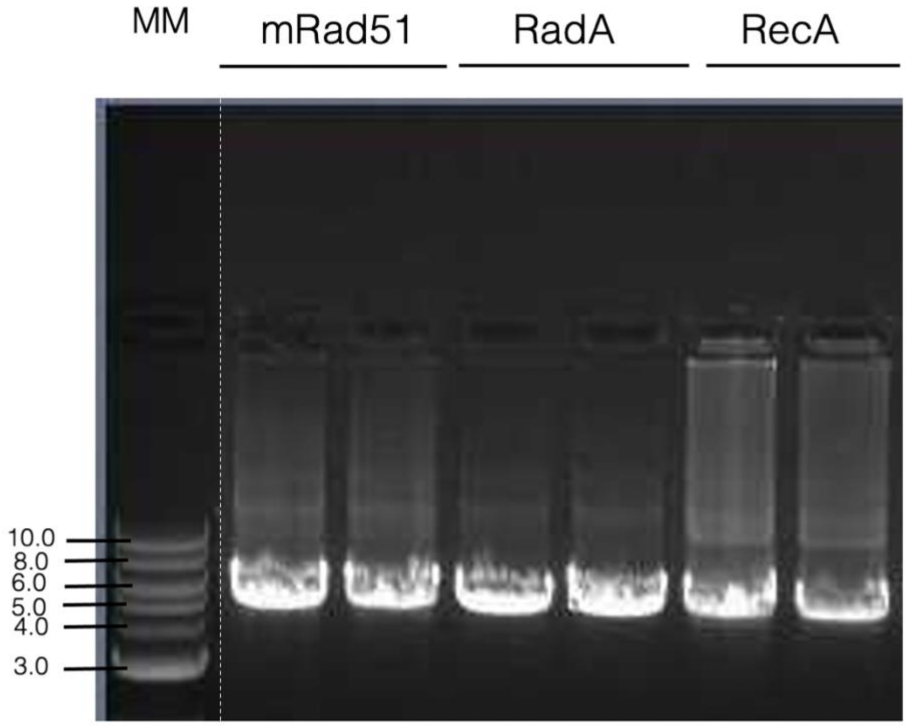

Figure 4 Generation of transformation cassette of *RAD51* replacement strains by PCR. Fragments expected: Mouse Rad51: 5122 bp, RadA: 5134 bp, RecA: 5164 bp.

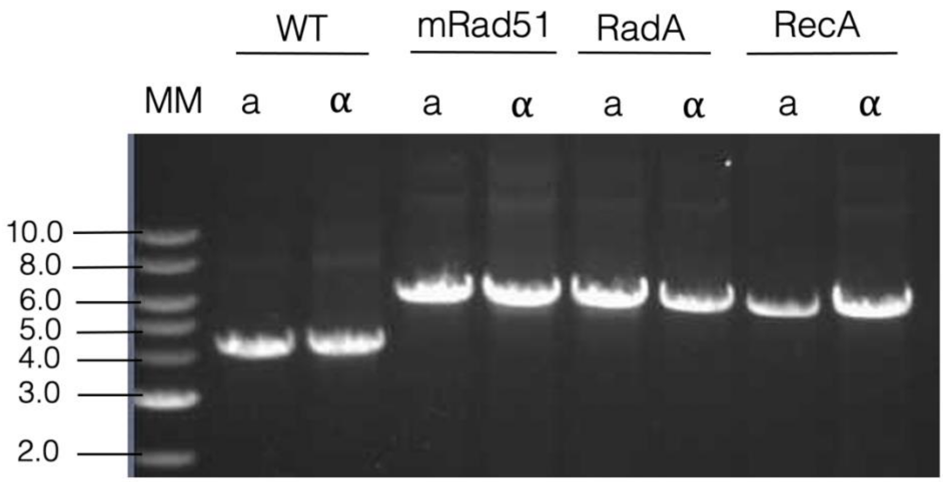

Figure 5 Confirmation of transformation of the *RAD51* replacement transformation cassettes into wildtype strains YSG3 and 4. Primers annealed to outside the insertion of the transformation cassette. Fragments expected: WT (wildtype): 4205 bp. Mouse Rad51: 5811 bp, RadA: 5823 bp and RecA: 5853 bp.

ii Sporulation efficiency

RecA has been shown to not negatively affect the polymerisation of Dmc1, however it does not perform the same function as Rad51, in supporting the nucleation of Dmc1 filaments, suggesting the interactions are species specific. To determine whether the RecA and mRad51 could act similarly or compensate for Rad51 by interacting with Dmc1, and stimulate filaments formation along ssDNA, the phenotypes of the RecA and mRad51 replacement strains were compared to the *rad51* and the *rad51dmc1* strains.

The sporulation efficiency was determined by counting at least 200 cells in each sample and mean sporulation efficiency was calculated by averaging 3 independent repeat strains (Figure 6). RadA was able to partially compensate during meiosis, to determine spore viability, spores were dissected and grown up to determine whether they were viable, and counted (Figure 7).

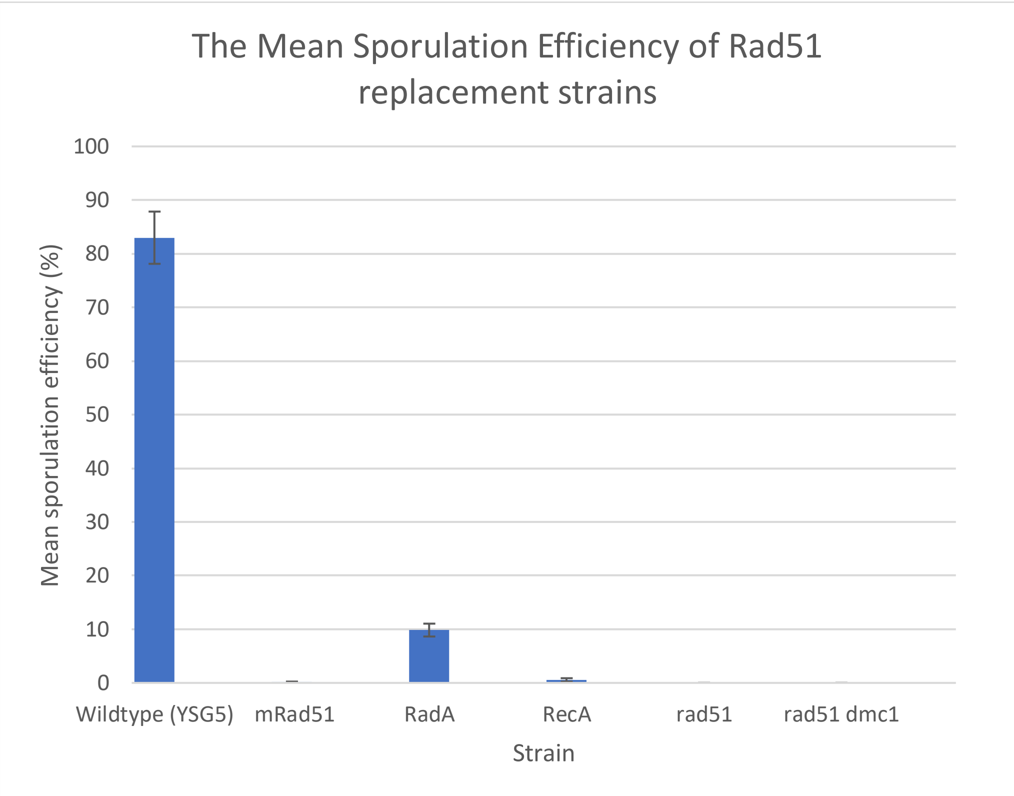

Figure 6 Graph comparing sporulation efficiencies of mRad51, RadA and RecA with the wildtype diploid strain YSG5 along with *rad51* and *rad51 dmc1*. (Error bars represent Standard Deviation: WT= 9.731, mRad51=0.228, RadA =2.395, RecA=0.629, *rad51* and *rad51dmc1*= 0.000) Mean Sporulation Efficiency was calculated by counting at least 200 cells in each sample and averaging 3 independent repeat strains. Sporulated for 72 hours.

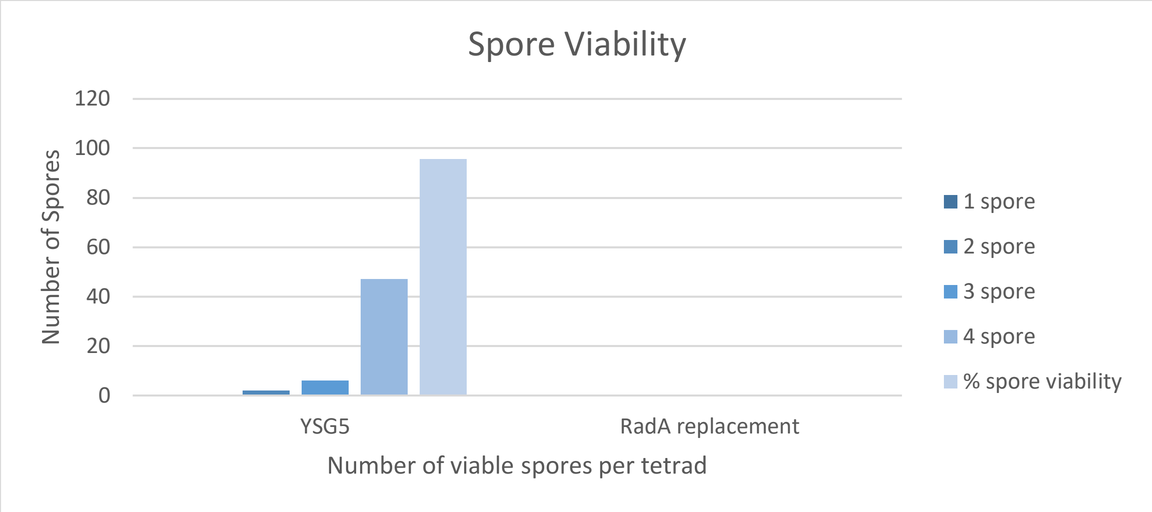

Figure 7 Spore viability of the RadA replacement strain, compared to wildtype. From the wildtype strain 220 spores were dissected, while from the RadA strain only 112 spores were dissected and grown up. The breakdown of the spore viability of each tetrad was noted as well as the total viable spores, which was used to calculate the percentage spore viability.

Due to time constraints, it was not possible to dissect 200 spores, and given more the time, all 200 spores should have been dissected for completeness, and to allow comparison with other mutant phenotypes, such as the *rad51* and *rad51dmc1*.

Chapter 4 Discussion

I Detection of Ectopic Mutants

The aim of this project was to adapt the fusion gene detection tool, FUDGE, to allow detection and sequencing of a novel ectopic recombinant previously identified by the Gray lab from the recombination hotspot *HIS4::LEU2 leu2::hisG*. Once successful, this tool could be used to detect other recombinants, which cannot be directly probed for. However, when testing the activity of Cas9 using a fragment of Chromosome 3 containing the *HIS4::LEU2 leu2::hisG* hotspot, the Cas9 cleavage was unsuccessful. One possible reason for the initial Cas9 cleavage reaction was unsuccessful could be due to the failure of the formation of the gRNA-Cas9 complexes, as it was clear that the substrate DNA was present. This could either be due to the failure of gRNA annealing or gRNA- Cas9 binding. The tracrRNAs and crRNAs were purchased from IDT, and then annealed, while the Cas9 was purchased from NEB, whose system utilises a single gRNA, as opposed to an annealed tracrRNA and crRNA. One solution may be to purchase the Cas9 from IDT, which has been optimised to function with the two RNA system, as opposed to a single gRNA. It may also be possible that the Cas9 protein or either the tracrRNA or crRNA has degraded. The annealed tracrRNA and crRNA were previously run on a gel to determine annealing, however conclusions could not be drawn from this gel as the ladder used was too large, and the higher agarose concentration meant the gel should have been made from and run in a Tris-borate EDTA (TBE) buffer, which is better suited for separating small DNA fragments. If the crRNA and tracrRNA were found to be degraded, new samples should be ordered, however, if the RNAs are not degraded, but annealing is still unsuccessful it may be more suitable to use a single gRNA, and the NEB Cas9. RNA annealing can also be determined using a gel electrophoresis. There are several options which could be altered to create a functional assay, and once created it would be a useful tool to allow the identification of recombinants that cannot otherwise be detected by Southern blotting. This would enable the cataloguing of other non-allelic loci within the genome, and how different mutant backgrounds alter the locus choice during ectopic recombination.

II Altering Rad51 expression

The aim of creating these strains was to generate strains that had altered expression patterns of Rad51 to allow for easier Cas9 editing in *S. cerevisiae.* Rad51 was placed under promoters that would ensure it was either not present in vegetatively growing cells, P^{DMC1}, or not present during G1 and early S phase, P^{CLB2}. Rad51 was also placed under the control of a bidirectional degron to allow inducible degradation, depending on the promoter the TEV was placed under. By removing the recombinase, it was anticipated that this would prevent the repair of the DSBs created by Cas9 by HR, as the key step of HR, strand invasion, cannot be catalysed. By forcing the cells to repair break by NHEJ there is a greater likelihood of the formation of deleterious mutations caused by indels at the break site. The repair pathway choice was assayed through the disruption of *ADE2*, which if disrupted, results in red colonies. A plasmid containing Cas9 and gRNAs targeting *ADE2* was generated. If the break pathway choice was altered, the plasmids used to generate the P^{DMC1}-*RAD51*, P^{CLB2}-*RAD51* and degron- *RAD51* strains could be used to transform reporter strains, along with Cas9 and a gRNA library targeting the gene(s) of interest, allowing mutations to be easily made in the reporter strains. When used to transform any reporter strain required, these plasmids could enable the targeting and mutating of multiple genes or entire pathways. However, in order for these strains to be useful in the lab, they must grow comparably to wildtype and have a similar sporulation efficiency, so that, when used in conjunction with other reporter strains, the altered expression of *RAD51* does not act as a confounding variable.

To determine whether the strains exhibit a wildtype phenotype, outside of DSB repair pathway choice, the sporulation efficiency and growth of the strains was assayed. Although it was expected that *RAD51* under the control of P^{CLB2} would be unable to sporulate as *CLB2* is not expressed during meiosis, it has been shown that proteins controlled by P^{CLB2} have some expression during early meiosis[99]. Rad51 is not the primary recombinase during meiosis, as its strand exchange activity is not required, therefore, lower Rad51 expression may be adequate to drive the cell through meiosis[100, 101]. On the other hand, the P^{DMC1}- *RAD51* strain was expected to have a sporulation efficiency comparable to wildtype. One possible explanation for the lack of sporulation, in the P^{DMC1}- *RAD51* strain, is that placing Rad51 under P^{DMC1} may lead to Rad51 competing with Dmc1 for binding at DSBs. As in wildtype Rad51 strand exchange activity is inhibited during meiosis by Hed1. Increased Rad51 expression, if there is inadequate Hed1 inhibition, may alter the inter- sister: inter-homolog ratio, disrupting the formation of chiasmata during meiosis and preventing the progression of sporulation, resulting in a low sporulation efficiency [69]. The degron -*RAD51* strain was expected to behave as a wildtype, however, the addition of the bidirectional degron appears to be hampering the function of Rad51. Another possibility is that the strains are not diploid, so FACs or a mating test, with a known haploid strain, could be used to ensure that all the strains contained two copies of the genome.

A western blot was undertaken using protein samples collected during a meiotic time course to determine the expression levels of Rad51, however due to small pellet sizes, resulting in inadequate sample, it could not be completed. To determine whether the small pellets were due to a slow growth phenotype, a growth assay was carried out, using wildtype and *rad51* strains as controls. It was expected that the P^{CLB2}-*RAD51* strain would grow similarly to wildtype, as Rad51 would be present during vegetative growth to repair any DSBs, while the P^{DMC1}-*RAD51* strain would grow similarly to the *rad51* strain, as Rad51 would not be present outside of meiosis. Theoretically the degron- *RAD51* strain should grow similarly to the wildtype strain, as, without the TEV insertion, Rad51 should be expressed comparably to wildtype. However, the lack of sporulation of the degron- *RAD51* strain suggested that the function of Rad51 was affected by the addition of the degron. Therefore, while Rad51 may be present at similar levels to a wildtype strain, it may be unable to act in DSB repair, and therefore the strain may grow similarly to a *rad51* strain.
Ideally, the growth assay would have been repeated using a shaking spectrophotometer, as this would have adequate space for repeats and would enable overnight measurements. Consistent measurement would allow better identification of the lag, log, and stationary growth phases, and therefore, a clear growth curve could be plotted for each strain. Three repeats of each strain would be measured, allowing the calculation of the mean growth and standard deviation, and statistical analysis could be carried out to determine whether the differences in growth seen were statistically significant, and, therefore due to the altered expression of *RAD51*, or natural variation between colonies. Repeats would also allow the identification and elimination of anomalous results, such as the P^{DMC1}-*RAD51* a mating type. However, the assay was carried out manually, due to time constraints, a calibration curve, comparing the growth of wildtype strains in standard growth conditions and the shaking spectrophotometer could not be carried out. Therefore, the shaking spectrophotometer could not be used for the growth assay as, SK1 is known for flocculation at higher cell densities. Flocculation occurs when the cells begin to clump, resulting in a non-uniform solution [102] which may result in inaccurate readings when grown in the smaller volumes of the shaking spectrophotmeter[103]. Once the calibration has been performed and if flocculation is not evident, the growth assay could be carried out using the shaking spectrophotometer.

To determine whether the lack of sporulation and slow growth phenotypes seen in the P^{CLB2}-*RAD51*, P^{DMC1}- *RAD51* and degron-*RAD51* strain were due to an altered Rad51 expression, the Western blot would be carried out, however due to the slower growth phenotypes seen during the growth assay, a larger volume of cells should be inoculated into the sporulation media. Vegetative samples should also be compared to determine Rad51 expression during vegetative growth.
Due to their lack of sporulation and their slow growth phenotypes, the P^{CLB2}-*RAD51* and P^{DMC1}-*RAD51* strategies are not suitable for use alongside reporter strains in the lab, as the altered phenotype would be difficult to distinguish from any results

measured. To make strains with which favour NHEJ over HR, Rad51 may not have been the correct protein to target, as after resection has occurred, without a recombinase present, only SSA, which is Rad51 independent, can act to repair the break[54]. While SSA is deleterious, it also requires repeats which may not be present at every locus targeted for mutation. However, without carrying out the *ADE2* disruption assay to determine whether the DSB repair pathway choice has been altered, it cannot be definitively stated if, altering Rad51 alters DSB repair pathway and results in a higher likelihood of mutations. Possible alternative targets to force the cells to repair DSBs by NHEJ during vegetative growth, could include the proteins which act in resection, such as the nucleases Sae2, which is already inhibited during G1, and Exo1. Placing the nucleases under meiotic specific controls would limit resection to meiosis and therefore, hopefully forcing breaks to be repaired by NHEJ, without altering meiosis and sporulation. In these strains, a decreased growth phenotype may be observed, however this is preferable to a lack of sporulation, as growth phenotypes can be compensated for, i.e., by increasing culturing times.

i Evaluating the TEV Degron system

The degron, even when not cleaved, appears to disrupt the function of Rad51, preventing the repair of DSBs by HR. This means the strain is unsuitable for use in the laboratory as, for the inducible knockdown of Rad51 to be useful, the strain must behave as a wildtype when the degron cap is intact. The degron was placed at the N terminus of the protein, as it was thought that if the degron was placed at the C terminus, it may disrupt the intrinsically disordered region at the C terminal containing the two DNA binding loops L1 and L2, therefore, potentially disrupting the function of Rad51. However, when placed at the N terminal, the degron may affect the polymerisation of the recombinase, by altering the position of the phenylalanine residue which is inserted into the cleft of the adjacent monomer[56]. This may account for the lack of sporulation seen in the degron strains, as Rad51 is required for Dmc1 nucleation prior to filament formation.

However, had the bidirectional degron not impacted the function of Rad51, it would have been possible to place both the TEV and the Cas9 targeting the desired gene under the same inducible promoter, therefore inducing both the expression of Cas9 and the degradation of Rad51 during the same interval. This would have allowed Cas9 to catalyse break formation, without the presence of Rad51, forcing the cell to repair the DSBs generated by Cas9 via NHEJ. On the other hand, this does not mean the degron system cannot be used to selectively degrade other proteins. Ideally, prior to using the degron system the protein of interest, with the degron attached, should be modelled to determine any obvious alterations to the folding of the protein, and the phenotype of the degron fusion protein should be fully characterised to identify any unintended effects of the addition of the degron. The degron system has been shown to effectively trigger protein degradation[95], however without a Western blot to quantitate the extent and speed of Rad51 degradation once the degron has been cleaved, the efficacy of the degron system in these strains cannot be fully evaluated.

In summary, neither of the three plasmids generated are suitable for use alongside reporter strains, as the phenotype exhibited when the plasmids are transformed into wildtype strains is not comparable to wildtype, and will therefore act as a confounding variable during experiments using either, these strains or reporter strains, with these constructs transformed in. However, selecting a different protein target, such as one of the nucleases involved in initial end resection may be a more suitable target for altering pathway choice. It would be worthwhile reattempting the generation of these strains, as with the correct target they would be useful for generating deletion mutants, while decreasing the time required. On the other hand, while the degron system was not suitable for use with Rad51, it has potential to be a useful tool when attached to other proteins, provided care is taken to ensure that the degron does not alter the function of the protein it has been attached to. Without carrying out assays to determine the efficacy of degradation induced by degron cleavage it cannot be determined how useful the degron system may be, however, other studies have shown that it can induce rapid degradation of other proteins in *S. cerevisiae*. The degron system has the potential to be a useful tool in the field, as inducible degradation of a targeted protein has several uses, especially in understanding the regulation of the cell cycle, however, care must be taken to ensure the results seen are purely due to the degradation of the protein and not because of altered protein function due to the degron tag.

III Determining the extent of compensation between RecA homologs

Due to their essential function, RecA homologs show a high level of conservation, especially in the key CAD domain, which is required for catalysis. However, the structure of the other protein binding and interaction domains are less well understood. It was hoped that by comparing the extent of compensation during meiosis, where Rad51 is only required for Dmc1 filament formation, and vegetative DSB repair, where Rad51 catalyses the homology search and strand invasion, a better understanding of how Rad51 interacts with other proteins could be gained. From this data, it is evident, that while RecA and mRad51 are unable to compensate for scRad51 during meiosis, having a sporulation efficiency similar to that of the *rad51* strain, RadA appears to be able to partially compensate for scRad51 during sporulation. As the RadA strain exhibits an intermediate phenotype when compared with the wildtype strain, not complete sporulation rescue. While RecA appeared to have very low sporulation efficiency with very few tetrads seen, this is more likely due to the fact that Rad51 is not essential for Meiosis rather than compensation by the recombinase, as *rad51* strains do complete sporulation. However, the sporulation efficiency for the *rad51* strain is lower than expected, having previously been reported at approximately 39%[68]. The lower than expected *rad51* sporulation may suggest inadequate time was given for sporulation. Also, because of the lack of sporulation in the *rad51* strain it is difficult to say if the RecA homologs are affecting sporulation more than *rad51* or if the strains would eventually sporulate if given more time, as the negative control does not fall where expected. To confirm the expression and compare the protein abundance with wildtype, creation of strains in which the RecA homolog is tagged with a 6xHis 3xHA tag were also attempted. However, these were not completed in time. Generating these strains and Western blotting meiotic time course protein preparations would not only confirm that the RecA homologs were present, but that they were also being expressed at comparable levels to wildtype, demonstrating that the low sporulation phenotype is not due to an absence of protein, but because the homologs cannot compensate for scRad51. The possible compensation of RadA for Rad51 during meiosis could provide more insight into the mechanism and protein interactions of Rad51 during meiosis. It was expected that the RadA mutant would display reduced spore viability, compared to wildtype, however the complete lack of viable spores suggests that the DNA breaks generated during meiosis have not been adequately repaired. To further examine this phenotype, a yeast two hybrid assay could be used to identify whether RadA and, possibly the other Rad51 homologs are able to interact with key Rad51 binding partners such as Rad52 and Rad54 to determine the extent of DNA repair possible by the homologs. The yeast two hybrid system, and mutagenesis of key residues within either Rad51 or the other RecA homologs could also be used to identify key binding domains, and further elucidate how to structure of Rad51 mediates protein interactions. However, it is possible that the RadA from *H. volcanii* has not folded properly when expressed in *S. cerevisiae* due to the drastically decreased salt content within the *S. cerevisiae* cell, compared to *H. volcanii*[104]. Therefore, other archaeal RadA proteins, such as *M. voltae,* should also be tested to determine whether they can compensate for Rad51, or whether this is due to the incorrect folding of the *H.volcanii* RadA protein.

To further determine the extent to which RecA homologs are able to compensate for Rad51, an MMS survival assay could be used to determine the extent of compensation, when Rad51 is the sole recombinase involved. mRad51 has been demonstrated to partially compensate for a *rad51* allele during MMS treatment in both the *rad51-1* and the *rad51* strains[105], however it was expressed from the *GAL1* promoter. Recapitulating these results with mRad51 expressed chromosomally under the endogenous promoter would determine whether mRad51 can compensate during DSB repair outside of meiosis, and, by comparing the structures of the two homologs, what protein interactions are required to mediate this process.

Overall, the partial compensation by RadA for Rad51 during meiosis was unexpected, but with further analysis of the interaction domains of the two homologs, could provide some interesting insight into the binding domains of the RecA homologs, and which binding partners are essential for DSB repair, either during meiosis, or in the case of MMS treatment, during vegetative growth.

Acknowledgments

Firstly, I would like to give special thanks to my supervisors Dr Gray and Prof Allers for allowing me to undertake a project in his lab and for supporting me over the course of my MRes. I would also like to thank the members of D119 for creating an enjoyable work environment and helping me develop as a scientist. I would also like to give thanks to my family for their continuous support, especially Lily.
I would also like to thank Ben Blount for kindly sharing his synthetic dropout mix at the eleventh hour, and the Allers lab for providing *Haloferax* gDNA samples.

Chapter 5 Bibliography

[1] Marston, A. L., and Amon, A. (2004) Meiosis: cell-cycle controls shuffle and deal, *Nature Reviews Molecular Cell Biology 5*, 983-997.

[2] Thacker, D., Lam, I., Knop, M., and Keeney, S. (2011) Exploiting spore-autonomous fluorescent protein expression to quantify meiotic chromosome behaviors in Saccharomyces cerevisiae, *Genetics 189*, 423-439.

[3] Pâques, F., and Haber, J. E. (1999) Multiple Pathways of Recombination Induced by Double-Strand Breaks in <i>Saccharomyces cerevisiae</i>, *Microbiology and Molecular Biology Reviews 63*, 349-404.

[4] Mitchell, A. P., and Bowdish, K. S. (1992) Selection for early meiotic mutants in yeast, *Genetics 131*, 65-72.

[5] Nachman, I., Regev, A., and Ramanathan, S. (2007) Dissecting Timing Variability in Yeast Meiosis, *Cell 131*, 544-556.

[6] Kim, K. P., Weiner, B. M., Zhang, L., Jordan, A., Dekker, J., and Kleckner, N. (2010) Sister cohesion and structural axis components mediate homolog bias of meiotic recombination, *Cell 143*, 924-937.

[7] Shonn, M. A., McCarroll, R., and Murray, A. W. (2002) Spo13 protects meiotic cohesin at centromeres in meiosis I, *Genes Dev 16*, 1659-1671.

[8] Lee, B. H., Amon, A., and Prinz, S. (2002) Spo13 regulates cohesin cleavage, *Genes Dev 16*, 1672-1681.

[9] Peoples, T. L., Dean, E., Gonzalez, O., Lambourne, L., and Burgess, S. M. (2002) Close, stable homolog juxtaposition during meiosis in budding yeast is dependent on meiotic recombination, occurs independently of synapsis, and is distinct from DSB-independent pairing contacts, *Genes Dev 16*, 1682-1695.

[10] Hong, S., Joo, J. H., Yun, H., and Kim, K. (2019) The nature of meiotic chromosome dynamics and recombination in budding yeast, *Journal of Microbiology 57*, 221-231.

[11] Chan, Y. L., Zhang, A., Weissman, B. P., and Bishop, D. K. (2019) RPA resolves conflicting activities of accessory proteins during reconstitution of Dmc1-mediated meiotic recombination, *Nucleic Acids Res 47*, 747-761.

[12] Borde, V., and de Massy, B. (2013) Programmed induction of DNA double strand breaks during meiosis: setting up communication between DNA and the chromosome structure, *Current Opinion in Genetics & Development 23*, 147-155.

[13] Neale, M. J., Pan, J., and Keeney, S. (2005) Endonucleolytic processing of covalent protein-linked DNA double-strand breaks, *Nature 436*, 1053-1057.

[14] Bishop, D. K., Park, D., Xu, L., and Kleckner, N. (1992) DMC1: A meiosis-specific yeast homolog of E. coli recA required for recombination, synaptonemal complex formation, and cell cycle progression, *Cell 69*, 439-456.

[15] Shinohara, A., Gasior, S., Ogawa, T., Kleckner, N., and Bishop, D. K. (1997) Saccharomyces cerevisiae recA homologues RAD51 and DMC1 have both distinct and overlapping roles in meiotic recombination, *Genes to Cells 2*, 615-629.

[16] Liu, Y., Gaines, W. A., Callender, T., Busygina, V., Oke, A., Sung, P., Fung, J. C., and Hollingsworth, N. M. (2014) Down-Regulation of Rad51 Activity during Meiosis in Yeast Prevents Competition with Dmc1 for Repair of Double-Strand Breaks, *PLOS Genetics 10*, e1004005.

[17] Alexeev, A., Mazin, A., and Kowalczykowski, S. C. (2003) Rad54 protein possesses chromatin-remodeling activity stimulated by the Rad51–ssDNA nucleoprotein filament, *Nature Structural & Molecular Biology 10*, 182-186.
[18] Mehta, A., and Haber, J. E. (2014) Sources of DNA double-strand breaks and models of recombinational DNA repair, *Cold Spring Harb Perspect Biol 6*, a016428.
[19] Boulton, S. J., and Jackson, S. P. (1996) Saccharomyces cerevisiae Ku70 potentiates illegitimate DNA double-strand break repair and serves as a barrier to error-prone DNA repair pathways, *EMBO J 15*, 5093-5103.
[20] Moynahan, M. E., and Jasin, M. (2010) Mitotic homologous recombination maintains genomic stability and suppresses tumorigenesis, *Nat Rev Mol Cell Biol 11*, 196-207.
[21] Sun, Y., McCorvie, T. J., Yates, L. A., and Zhang, X. (2020) Structural basis of homologous recombination, *Cellular and Molecular Life Sciences 77*, 3-18.
[22] Sung, P., Krejci, L., Van Komen, S., and Sehorn, M. G. (2003) Rad51 Recombinase and Recombination Mediators *, *Journal of Biological Chemistry 278*, 42729-42732.
[23] Demogines, A., East, A. M., Lee, J. H., Grossman, S. R., Sabeti, P. C., Paull, T. T., and Sawyer, S. L. (2010) Ancient and recent adaptive evolution of primate non-homologous end joining genes, *PLoS Genet 6*, e1001169.
[24] Daley, J. M., Palmbos, P. L., Wu, D., and Wilson, T. E. (2005) Nonhomologous end joining in yeast, *Annu Rev Genet 39*, 431-451.
[25] Unal, E., Arbel-Eden, A., Sattler, U., Shroff, R., Lichten, M., Haber, J. E., and Koshland, D. (2004) DNA damage response pathway uses histone modification to assemble a double-strand break-specific cohesin domain, *Mol Cell 16*, 991-1002.
[26] Rouse, J., and Jackson, S. P. (2002) Interfaces Between the Detection, Signaling, and Repair of DNA Damage, *Science 297*, 547-551.
[27] Jung, K. W., Lee, Y., Huh, E. Y., Lee, S. C., Lim, S., and Bahn, Y. S. (2019) Rad53- and Chk1-Dependent DNA Damage Response Pathways Cooperatively Promote Fungal Pathogenesis and Modulate Antifungal Drug Susceptibility, *mBio 10*.
[28] Frank-Vaillant, M., and Marcand, S. (2001) NHEJ regulation by mating type is exercised through a novel protein, Lif2p, essential to the ligase IV pathway, *Genes Dev 15*, 3005-3012.
[29] Haber, J. E. (1998) MATING-TYPE GENE SWITCHING IN SACCHAROMYCES CEREVISIAE, *Annual Review of Genetics 32*, 561-599.
[30] Karathanasis, E., and Wilson, T. E. (2002) Enhancement of Saccharomyces cerevisiae end-joining efficiency by cell growth stage but not by impairment of recombination, *Genetics 161*, 1015-1027.
[31] Valencia, M., Bentele, M., Vaze, M. B., Herrmann, G., Kraus, E., Lee, S. E., Schär, P., and Haber, J. E. (2001) NEJ1 controls non-homologous end joining in Saccharomyces cerevisiae, *Nature 414*, 666-669.
[32] Enserink, J. M., and Kolodner, R. D. (2010) An overview of Cdk1-controlled targets and processes, *Cell Division 5*, 11.
[33] Gobbini, E., Cesena, D., Galbiati, A., Lockhart, A., and Longhese, M. P. (2013) Interplays between ATM/Tel1 and ATR/Mec1 in sensing and signaling DNA double-strand breaks, *DNA Repair 12*, 791-799.
[34] Eckert-Boulet, N., Rothstein, R., and Lisby, M. (2011) Cell biology of homologous recombination in yeast, *Methods Mol Biol 745*, 523-536.

[35] Kowalczykowski, S. C. (2015) An Overview of the Molecular Mechanisms of Recombinational DNA Repair, *Cold Spring Harb Perspect Biol 7*.
[36] Sung, P., Trujillo, K. M., and Van Komen, S. (2000) Recombination factors of Saccharomyces cerevisiae, *Mutation Research/Fundamental and Molecular Mechanisms of Mutagenesis 451*, 257-275.
[37] Miyazaki, T., Bressan, D. A., Shinohara, M., Haber, J. E., and Shinohara, A. (2004) In vivo assembly and disassembly of Rad51 and Rad52 complexes during double-strand break repair, *EMBO J 23*, 939-949.
[38] Ogawa, T., Shinohara, A., and Ikeya, T. (1995) A species-specific interaction of Rad51 and Rad52 proteins in eukaryotes, *Advances in Biophysics 31*, 93-100.
[39] Bugreev, D. V., Pezza, R. J., Mazina, O. M., Voloshin, O. N., Camerini-Otero, R. D., and Mazin, A. V. (2011) The resistance of DMC1 D-loops to dissociation may account for the DMC1 requirement in meiosis, *Nature Structural & Molecular Biology 18*, 56-60.
[40] Miura, T., Yamana, Y., Usui, T., Ogawa, H. I., Yamamoto, M. T., and Kusano, K. (2012) Homologous recombination via synthesis-dependent strand annealing in yeast requires the Irc20 and Srs2 DNA helicases, *Genetics 191*, 65-78.
[41] Kramara, J., Osia, B., and Malkova, A. (2018) Break-Induced Replication: The Where, The Why, and The How, *Trends Genet 34*, 518-531.
[42] Åström, S. U., Okamura, S. M., and Rine, J. (1999) Yeast cell-type regulation of DNA repair, *Nature 397*, 310-310.
[43] Shrivastav, M., De Haro, L. P., and Nickoloff, J. A. (2008) Regulation of DNA double-strand break repair pathway choice, *Cell Research 18*, 134-147.
[44] Kowalczykowski, S. C. (2015) An Overview of the Molecular Mechanisms of Recombinational DNA Repair, *Cold Spring Harbor Perspectives in Biology 7*.
[45] Chapman, J. R., Taylor, Martin R. G., and Boulton, Simon J. (2012) Playing the End Game: DNA Double-Strand Break Repair Pathway Choice, *Molecular Cell 47*, 497-510.
[46] Walker, J. R., Corpina, R. A., and Goldberg, J. (2001) Structure of the Ku heterodimer bound to DNA and its implications for double-strand break repair, *Nature 412*, 607-614.
[47] Hefferin, M. L., and Tomkinson, A. E. (2005) Mechanism of DNA double-strand break repair by non-homologous end joining, *DNA Repair 4*, 639-648.
[48] Mathiasen, D. P., and Lisby, M. (2014) Cell cycle regulation of homologous recombination in Saccharomyces cerevisiae, *FEMS Microbiology Reviews 38*, 172-184.
[49] Gao, S., Honey, S., Futcher, B., and Grollman, A. P. (2016) The non-homologous end-joining pathway of S. cerevisiae works effectively in G1-phase cells, and religates cognate ends correctly and non-randomly, *DNA Repair (Amst) 42*, 1-10.
[50] Kegel, A., Sjöstrand, J. O. O., and Åström, S. U. (2001) Nej1p, a cell type-specific regulator of nonhomologous end joining in yeast, *Current Biology 11*, 1611-1617.
[51] Lee, C.-D., and Wang, T.-F. (2009) The N-terminal domain of Escherichia coli RecA have multiple functions in promoting homologous recombination, *Journal of Biomedical Science 16*, 37.
[52] Ye, J., Osborne, A. R., Groll, M., and Rapoport, T. A. (2004) RecA-like motor ATPases—lessons from structures, *Biochimica et Biophysica Acta (BBA) - Bioenergetics 1659*, 1-18.

[53] Lin, Z., Kong, H., Nei, M., and Ma, H. (2006) Origins and evolution of the <i>recA</i>/<i>RAD51</i> gene family: Evidence for ancient gene duplication and endosymbiotic gene transfer, *Proceedings of the National Academy of Sciences 103*, 10328-10333.
[54] Heyer, W. D. (2007) Biochemistry of eukaryotic homologous recombination, *Top Curr Genet 17*, 95-133.
[55] Kowalczykowski, S. C., and Eggleston, A. K. (1994) Homologous pairing and DNA strand-exchange proteins, *Annual review of biochemistry 63*, 991-1043.
[56] Short, J. M., Liu, Y., Chen, S., Soni, N., Madhusudhan, M. S., Shivji, M. K., and Venkitaraman, A. R. (2016) High-resolution structure of the presynaptic RAD51 filament on single-stranded DNA by electron cryo-microscopy, *Nucleic Acids Res 44*, 9017-9030.
[57] Lee, J. Y., Terakawa, T., Qi, Z., Steinfeld, J. B., Redding, S., Kwon, Y., Gaines, W. A., Zhao, W., Sung, P., and Greene, E. C. (2015) DNA RECOMBINATION. Base triplet stepping by the Rad51/RecA family of recombinases, *Science 349*, 977-981.
[58] Kurumizaka, H., Aihara, H., Ikawa, S., Kashima, T., Bazemore, L. R., Kawasaki, K., Sarai, A., Radding, C. M., and Shibata, T. (1996) A Possible Role of the C-terminal Domain of the RecA Protein: A GATEWAY MODEL FOR DOUBLE-STRANDED DNA BINDING *, *Journal of Biological Chemistry 271*, 33515-33524.
[59] Bianco, P. R., Tracy, R. B., and Kowalczykowski, S. C. (1998) DNA strand exchange proteins: a biochemical and physical comparison, *Front Biosci 3*, D570-603.
[60] Yu, X., Jacobs, S. A., West, S. C., Ogawa, T., and Egelman, E. H. (2001) Domain structure and dynamics in the helical filaments formed by RecA and Rad51 on DNA, *Proceedings of the National Academy of Sciences 98*, 8419-8424.
[61] Nicholls, A., Bharadwaj, R., and Honig, B. (1993) GRASP: graphical representation and analysis of surface properties, *Biophys. J 64*, A166-A166.
[62] Aihara, H., Ito, Y., Kurumizaka, H., Terada, T., Yokoyama, S., and Shibata, T. (1997) An interaction between a specified surface of the C-terminal domain of RecA protein and double-stranded DNA for homologous pairing11Edited by A. R. Fersht, *Journal of Molecular Biology 274*, 213-221.
[63] Rao, B. J., Chiu, S., Bazemore, L. R., Reddy, G., and Radding, C. M. (1995) How specific is the first recognition step of homologous recombination?, *Trends in Biochemical Sciences 20*, 109-113.
[64] Conway, A. B., Lynch, T. W., Zhang, Y., Fortin, G. S., Fung, C. W., Symington, L. S., and Rice, P. A. (2004) Crystal structure of a Rad51 filament, *Nature Structural & Molecular Biology 11*, 791-796.
[65] Shinohara, A., Ogawa, H., Matsuda, Y., Ushio, N., Ikeo, K., and Ogawa, T. (1993) Cloning of human, mouse and fission yeast recombination genes homologous to RAD51 and recA, *Nature Genetics 4*, 239-243.
[66] Tsubouchi, H., and Roeder, G. S. (2006) Budding yeast Hed1 down-regulates the mitotic recombination machinery when meiotic recombination is impaired, *Genes Dev 20*, 1766-1775.
[67] Bishop, D. K., Park, D., Xu, L., and Kleckner, N. (1992) DMC1: a meiosis-specific yeast homolog of E. coli recA required for recombination, synaptonemal complex formation, and cell cycle progression, *Cell 69*, 439-456.

[68] Dresser, M. E., Ewing, D. J., Conrad, M. N., Dominguez, A. M., Barstead, R., Jiang, H., and Kodadek, T. (1997) DMC1 Functions in a Saccharomyces cerevisiae Meiotic Pathway That Is Largely Independent of the RAD51 Pathway, *Genetics 147*, 533-544.
[69] Liu, Y., Gaines, W. A., Callender, T., Busygina, V., Oke, A., Sung, P., Fung, J. C., and Hollingsworth, N. M. (2014) Down-regulation of Rad51 activity during meiosis in yeast prevents competition with Dmc1 for repair of double-strand breaks, *PLoS Genet 10*, e1004005.
[70] Luo, S.-C., Yeh, H.-Y., Lan, W.-H., Wu, Y.-M., Yang, C.-H., Chang, H.-Y., Su, G.-C., Lee, C.-Y., Wu, W.-J., Li, H.-W., Ho, M.-C., Chi, P., and Tsai, M.-D. (2021) Identification of fidelity-governing factors in human recombinases DMC1 and RAD51 from cryo-EM structures, *Nature Communications 12*, 115.
[71] Brown, M. S., Grubb, J., Zhang, A., Rust, M. J., and Bishop, D. K. (2015) Small Rad51 and Dmc1 Complexes Often Co-occupy Both Ends of a Meiotic DNA Double Strand Break, *PLoS Genet 11*, e1005653.
[72] Hinch, A. G., Becker, P. W., Li, T., Moralli, D., Zhang, G., Bycroft, C., Green, C., Keeney, S., Shi, Q., Davies, B., and Donnelly, P. (2020) The Configuration of RPA, RAD51, and DMC1 Binding in Meiosis Reveals the Nature of Critical Recombination Intermediates, *Mol Cell 79*, 689-701.e610.
[73] Cloud, V., Chan, Y.-L., Grubb, J., Budke, B., and Bishop, D. K. (2012) Rad51 Is an Accessory Factor for Dmc1-Mediated Joint Molecule Formation During Meiosis, *Science 337*, 1222-1225.
[74] Lan, W.-H., Lin, S.-Y., Kao, C.-Y., Chang, W.-H., Yeh, H.-Y., Chang, H.-Y., Chi, P., and Li, H.-W. (2020) Rad51 facilitates filament assembly of meiosis-specific Dmc1 recombinase, *Proceedings of the National Academy of Sciences 117*, 11257-11264.
[75] Lee, M.-H., Leng, C.-H., Chang, Y.-C., Chou, C.-C., Chen, Y.-K., Hsu, F.-F., Chang, C.-S., Wang, A. H. J., and Wang, T.-F. (2004) Self-polymerization of archaeal RadA protein into long and fine helical filaments, *Biochemical and Biophysical Research Communications 323*, 845-851.
[76] Shi, W.-X., and Larson, R. G. (2005) Atomic Force Microscopic Study of Aggregation of RecA-DNA Nucleoprotein Filaments into Left-Handed Supercoiled Bundles, *Nano Letters 5*, 2476-2481.
[77] Wiktor, J., Gynnå, A. H., Leroy, P., Larsson, J., Coceano, G., Testa, I., and Elf, J. (2021) RecA finds homologous DNA by reduced dimensionality search, *Nature 597*, 426-429.
[78] Žgur-Bertok, D. (2013) DNA damage repair and bacterial pathogens, *PLoS Pathog 9*, e1003711-e1003711.
[79] Dudáš, A., Marková, E., Vlasáková, D., Kolman, A., Bartošová, Z., Brozmanová, J., and Chovanec, M. (2003) The Escherichia coli RecA protein complements recombination defective phenotype of the Saccharomyces cerevisiae rad52 mutant cells, *Yeast 20*, 389-396.
[80] Wu, Y., He, Y., Moya, I. A., Qian, X., and Luo, Y. (2004) Crystal Structure of Archaeal Recombinase RadA: A Snapshot of Its Extended Conformation, *Molecular Cell 15*, 423-435.
[81] Sandler, S. J., Satin, L. H., Samra, H. S., and Clark, A. J. (1996) recA-like genes from three archaean species with putative protein products similar to Rad51 and Dmc1 proteins of the yeast Saccharomyces cerevisiae, *Nucleic Acids Res 24*, 2125-2132.

[82] Chen, L.-T., Ko, T.-P., Chang, Y.-W., Lin, K.-A., Wang, A. H. J., and Wang, T.-F. (2007) Structural and Functional Analyses of Five Conserved Positively Charged Residues in the L1 and N-Terminal DNA Binding Motifs of Archaeal RadA Protein, *PLOS ONE 2*, e858.
[83] Nidhi, S., Anand, U., Oleksak, P., Tripathi, P., Lal, J. A., Thomas, G., Kuca, K., and Tripathi, V. (2021) Novel CRISPR-Cas Systems: An Updated Review of the Current Achievements, Applications, and Future Research Perspectives, *Int J Mol Sci 22*.
[84] Adli, M. (2018) The CRISPR tool kit for genome editing and beyond, *Nature Communications 9*, 1911.
[85] Jinek, M., East, A., Cheng, A., Lin, S., Ma, E., and Doudna, J. (2013) RNA-programmed genome editing in human cells, *Elife 2*, e00471.
[86] Agatep, R., Kirkpatrick, R. D., Parchaliuk, D. L., Woods, R. A., and Gietz, R. D. (1998) Transformation of Saccharomyces cerevisiae by the lithium acetate/single-stranded carrier DNA/polyethylene glycol protocol, *Technical Tips Online 3*, 133-137.
[87] Anton, B. P., and Raleigh, E. A. (2016) Complete Genome Sequence of NEB 5-alpha, a Derivative of Escherichia coli K-12 DH5α, *Genome Announc 4*.
[88] Stangl, C., de Blank, S., Renkens, I., Westera, L., Verbeek, T., Valle-Inclan, J. E., González, R. C., Henssen, A. G., van Roosmalen, M. J., Stam, R. W., Voest, E. E., Kloosterman, W. P., van Haaften, G., and Monroe, G. R. (2020) Partner independent fusion gene detection by multiplexed CRISPR-Cas9 enrichment and long read nanopore sequencing, *Nature Communications 11*, 2861.
[89] Montague, T. G., Cruz, J. M., Gagnon, J. A., Church, G. M., and Valen, E. (2014) CHOPCHOP: a CRISPR/Cas9 and TALEN web tool for genome editing, *Nucleic Acids Res 42*, W401-407.
[90] Hernandez-Huertas, L., Kushawah, G., Díaz-Moscoso, A., Laura, T.-G., Moreno-Sánchez, I., Pescador, G., Bazzini, A., and Moreno-Mateos, M. (2022) Optimized CRISPR-RfxCas13d system for RNA targeting in zebrafish embryos, *STAR Protocols 3*, 101058.
[91] Varshney, G., Carrington, B., Pei, W., Bishop, K., Chen, Z., Fan, C., Xu, L., Jones, M., LaFave, M., Ledin, J., Sood, R., and Burgess, S. (2016) A high-throughput functional genomics workflow based on CRISPR/Cas9-mediated targeted mutagenesis in zebrafish, *Nat. Protocols 11*, 2357-2375.
[92] Giaever, G., and Nislow, C. (2014) The yeast deletion collection: a decade of functional genomics, *Genetics 197*, 451-465.
[93] Taxis, C., Stier, G., Spadaccini, R., and Knop, M. (2009) Efficient protein depletion by genetically controlled deprotection of a dormant N-degron, *Mol Syst Biol 5*, 267.
[94] Taxis, C., and Knop, M. (2012) TIPI: TEV protease-mediated induction of protein instability, *Methods Mol Biol 832*, 611-626.
[95] Jungbluth, M., Renicke, C., and Taxis, C. (2010) Targeted protein depletion in Saccharomyces cerevisiae by activation of a bidirectional degron, *BMC Syst Biol 4*, 176.
[96] Orr-Weaver, T. L., Szostak, J. W., and Rothstein, R. J. (1981) Yeast transformation: a model system for the study of recombination, *Proc Natl Acad Sci U S A 78*, 6354-6358.

[97] Renicke, C., Spadaccini, R., and Taxis, C. (2013) A Tobacco Etch Virus Protease with Increased Substrate Tolerance at the P1' position, *PLOS ONE 8*, e67915.
[98] Chaudhuri, B., Ingavale, S., and Bachhawat, A. K. (1997) apd1+, a gene required for red pigment formation in ade6 mutants of Schizosaccharomyces pombe, encodes an enzyme required for glutathione biosynthesis: a role for glutathione and a glutathione-conjugate pump, *Genetics 145*, 75-83.
[99] Lee, B. H., and Amon, A. (2003) Role of Polo-like Kinase <i>CDC5</i> in Programming Meiosis I Chromosome Segregation, *Science 300*, 482-486.
[100] Bishop, D. K. (2012) Rad51, the lead in mitotic recombinational DNA repair, plays a supporting role in budding yeast meiosis, *Cell Cycle 11*, 4105-4106.
[101] Chen, H., He, C., Wang, C., Wang, X., Ruan, F., Yan, J., Yin, P., Wang, Y., and Yan, S. (2021) RAD51 supports DMC1 by inhibiting the SMC5/6 complex during meiosis, *The Plant Cell 33*, 2869-2882.
[102] Verstrepen, K. J., Derdelinckx, G., Verachtert, H., and Delvaux, F. R. (2003) Yeast flocculation: what brewers should know, *Appl Microbiol Biotechnol 61*, 197-205.
[103] Williams, R. M., Primig, M., Washburn, B. K., Winzeler, E. A., Bellis, M., Sarrauste de Menthiere, C., Davis, R. W., and Esposito, R. E. (2002) The Ume6 regulon coordinates metabolic and meiotic gene expression in yeast, *Proc Natl Acad Sci U S A 99*, 13431-13436.
[104] Haque, R. U., Paradisi, F., and Allers, T. (2020) Haloferax volcanii for biotechnology applications: challenges, current state and perspectives, *Appl Microbiol Biotechnol 104*, 1371-1382.
[105] Morita, T., Yoshimura, Y., Yamamoto, A., Murata, K., Mori, M., Yamamoto, H., and Matsushiro, A. (1993) A mouse homolog of the Escherichia coli recA and Saccharomyces cerevisiae RAD51 genes, *Proceedings of the National Academy of Sciences 90*, 6577-6580.